PNWD-3808
Limited Distribution

Dynamic Pile Driving and Pile Driving Underwater Impulsive Sound

Thomas J. Carlson
Mark A. Weiland

Final Report

March 30, 2007

Prepared for Washington State Department of Transportation
Under Contract Y-8846, Task No. AB

Battelle
The Business of Innovation

LEGAL NOTICE

PNWD-3808
Limited Distribution

Dynamic Pile Driving and Pile Driving Underwater Impulsive Sound

Thomas J. Carlson
Mark A. Weiland

Final Report

March 30, 2007

Prepared for Washington State Department of Transportation
Under Contract Y-8846, Task No. AB

Battelle–Pacific Northwest Division
Richland, Washington 99352

TECHNICAL REPORT STANDARD TITLE PAGE

1. REPORT NO.	2. GOVERNMENT ACCESSION NO.	3. RECIPIENTS CATALOG NO
WA-RD 673.1	---	---

4. TITLE AND SUBTILLE

Dynamic Pile Driving and Pile Driving Underwater Impulsive Sound

5. REPORT DATE

March 30, 2007

6. PERFORMING ORGANIZATION CODE

---

7. AUTHOR(S)

Thomas J. Carlson and Mark A. Weiland

8. PERFORMING ORGANIZATION REPORT No.

PNWD-3808

9. PERFORMING ORGANIZATION NAME AND ADDRESS

Battelle-Pacific Northwest Division
PO Box 999
Richland WA 99352

10. WORK UNIT NO.

---

11. CONTRACT OR GRANT NO.

6, Task AB

12. CPONSORING AGENCY NAME AND ADDRESS

Washington State Department of Transportation
PO Box 47300
Olympia WA 98504-7300

13. TYPE OF REPORT AND PERIOD COVERED

Research report,

14. SPONSORING AGENCY CODE

---

15. SUPPLEMENTARY NOTES

This study was conducted in cooperation with the U.S. Department of Transportation, Federal Highway Administration.

16. ABSTRACT

Under contract to the Washington State Department of Transportation, Battelle, Pacific Northwest Division, conducted a re-analysis of dynamic pile driving and impulsive underwater sound data acquired at WA DOT construction projects (Hood Canal Bridge and Friday Harbor Ferry Terminal) to better understand the mechanisms of impulsive sound generation by pile driving in support of efforts to determine the effects of impulsive sound on fish health and behavior. Analysis focused on derivation of statistics from impulsive sound and dynamic pile driving data sets that permitted evaluation of the amount of variability in impulsive sound metrics that might be driven by variability in pile driving mechanics metrics. The energy required to drive a pile at various depths and substrates and an index of the sound energy produced during the pile drives were also compared.

These comparisons yielded the conclusion that most of the variability in impulsive sound during driving of a pile can be accounted for by changes the impact hammer operator makes to overcome resistance to increases in pile depth. Thus, it is the operation of an impact hammer in response to changes in substrate, not the substrate itself, that is responsible for changes in impulsive energy metrics during driving of a pile. A recommendation of the study is that any future data acquisition and analysis efforts to improve understanding of linkages between pile driving mechanics and impulsive sound or underwater sound monitoring activities in support of construction activities include hammer stroke data as a basic element of underwater sound data sets.

As an element of comparison of data sets to assess the relationship in variability between impulsive sound and pile driving mechanics, the importance of wetted pile length was evaluated. It appears, based on the data sets analyzed for this study, that the wetted length of the pile is not related to impulsive sound metrics such as peak pressure. The lack of relationship between impulsive sound metrics and wetted pile length probably results from the way sound is produced by the pile when it is deformed by a hammer impact. As a consequence, when evaluating the potential for sound generation during project planning it should be assumed that a pile with minimum wetting length may produce impulsive sound levels of the same magnitude as piles with significantly greater wetted length. Environmental factors not evaluated in this study will determine how the generated impulsive sounds propagate.

Analysis of the cumulative energy required to drive a pile and an index of the cumulative sound energy produced during driving of a pile revealed a relationship between the diameter of a steel shell pile and the amount of energy transferred to the pile at impact to obtain an incremental increase in pile depth and the amount of sound energy produced per incremental increase in pile depth. It appears, logically so, that the energy required to drive a pile an increment in depth and the sound produced during that process are directly related to pile diameter. This being the case, we recommend that sound mitigation measure development, such as bubble curtains, focus on piles 30 inches or larger in diameter. It is unlikely that sound mitigation measures that would result in reduction of energy transfer to a pile, which will be necessary to reduce sound production, will be acceptable economically for larger piles because of the rapid increase in energy per foot of drive with pile diameter.

17. KEY WORDS	18. DISTRIBUTION STATEMENT
Pile driving; underwater sound; impulsive sound; fish injury; bridge; ferry terminal;	---

19. SECURITY CLASSIF. (of this report)	20. SECURITY CLASSIF. (of this page)	21. NO. OF PAGES	22. PRICE
None	None	136	---

Executive Summary

Under contract to the Washington State Department of Transportation, Battelle, Pacific Northwest Division, conducted a reanalysis of dynamic pile driving and impulsive underwater sound data acquired at WA DOT construction projects. Impulsive underwater sound data obtained during monitoring of pile driving from Hood Canal Bridge construction and dynamic pile driving data acquired during construction activity at the Friday Harbor Ferry terminal were analyzed to improve our understanding of the linkage between the mechanics of pile driving and impulsive sound generated during pile driving.

Analysis focused on derivation of statistics from impulsive sound and dynamic pile driving data sets that permitted evaluation of the amount of variability in impulsive sound metrics that might be driven by variability in pile driving mechanics metrics. In addition to the variability in pile driving and impulsive sound metrics, the energy required to drive a pile and an index of the sound energy produced during the pile drive were compared.

Comparison of the measures of variability in impulsive sound metrics with that for metrics related to pile driving mechanics determined that most of the variability in impulsive sound during driving of a pile can be accounted for by changes the impact hammer operator makes to overcome resistance to increases in pile depth. This finding led to the conclusion that it is the operation of an impact hammer in response to changes in substrate, not the substrate itself that is responsible for changes in impulsive energy metrics during driving of a pile. A recommendation of the study is that any future data acquisition and analysis efforts to improve understanding of linkages between pile driving mechanics and impulsive sound or, underwater sound monitoring activities in support of construction activities, acquire hammer stroke data as a basic element of underwater sound data sets.

As an element of comparison of data sets to assess the relationship in variability between impulsive sound and pile driving mechanics, the importance of wetted pile length was evaluated. It appears, based on the data sets analyzed for this study, that the wetted length of the pile is not related to impulsive sound metrics such as peak pressure. The lack of relationship between impulsive sound metrics and wetted pile length probably results from the way sound is produced by the pile when it is deformed by a hammer impact. As a consequence, when evaluating the potential for sound generation during project planning it should be assumed that a pile with minimum wetting length may produce impulsive sound levels of the same magnitude as piles with significantly greater wetted length. Environmental factors not evaluated in this study will determine how the generated impulsive sounds propagate.

Analysis of the cumulative energy required to drive a pile and an index of the cumulative sound energy produced during driving of a pile revealed a relationship between the diameter of a steel shell pile and the amount of energy transferred to the pile at impact to obtain an incremental increase in pile depth and the amount of sound energy produced per incremental increase in pile depth. It appears, logically so, that the energy required to drive a pile an increment in depth and the sound produced during that process are directly related to pile diameter. This being the case, we recommend that sound mitigation measure development, such as bubble curtains, focus on piles 30 inches or larger in diameter. It is unlikely that sound mitigation measures that would result in reduction of energy transfer to a pile, which will be necessary to reduce sound production, will be acceptable economically for larger piles because of the rapid increase in energy per foot of drive with pile diameter.

Contents

Figures

Tables

1.0 Introduction

Impulsive underwater sound generated during pile driving has been identified as a potential source of injury and behavioral disruption to fish. In the Northwest, of particular importance are listed salmonids. The effect of sound on human health has been an issue for decades and has received a great deal of attention. With the possible exception of impulsive sound generated by explosions, the effect of sound on animals, and in particular on fish, has not been widely studied. Currently, efforts are being expended to better understand the mechanisms of impulsive sound generation by pile driving and to determine the effects of impulsive sound on fish health and behavior.

This study was undertaken by Battelle under contract with the Washington State Department of Transportation in support of pile driving activities conducted by the ferry system and other transportation construction activities that require driving piles in or near bodies of water. The focus of this effort was to perform analyses on existing dynamic pile driving and impulsive sound data provided by WA DOT to determine if measures routinely obtained during pile driving activities to assess the integrity of a pile and its performance as a foundation element could help explain some of the variability and other features observed in impulsive sound signals. This information will help WA DOT to better evaluate pile driving alternatives and mitigation measure to reduce the production of impulsive sound.

2.0 Methods

The effort described here was an analysis of existing data obtained in prior field studies for the purposes of investigating linkages between the mechanics of pile driving and the generation of impulsive sound by pile driving. Two types of data were required for analysis, dynamic pile driving data and impulsive underwater sound data. Several prior studies were considered as potential sources for the data.

When this project was first considered, a construction project was in the final planning stages that included driving many piles as part of maintenance and improvement activities at the Friday Harbor Ferry Terminal on San Juan Island. It was suggested that dynamic pile driving data could be acquired in conjunction with monitoring to concurrently acquire underwater impulsive sound data. The sound data acquired for this project and the conclusions drawn from it to evaluate the effectiveness of bubble curtain design and operation are given in Laughlin 2005.

Concurrent with the sound data described in Laughlin 2005, dynamic pile driving data were acquired for three piles. The piles and conditions for which dynamic pile driving data were acquired are shown in Table 2.1 below. Considerable effort was expended attempting to reformat this dynamic pile driving data, which consisted of output from single-axis accelerometers and strain gages attached to the monitored piles. It became obvious that these data could not readily be obtained in a form suitable for reduction and additional analysis. In addition, it also became obvious that the primary experimental objective to evaluate the effectiveness of bubble curtain design and operation for a sample of piles and pile driving hammers resulted in an experimental design that included variables within the period of record for individual piles that significantly confounded analysis of the relationship between the mechanics of pile driving and impulsive sound generation.

Consideration of other readily available pile driving impulsive sound and dynamic pile driving data sets resulted in selection of dynamic pile driving data for four piles driven during the Friday Harbor Ferry Terminal Restoration Project (Miner 2005a, 2005b) and extensive underwater impulsive sound data acquired during pile driving for the Hood Canal Bridge project (Carlson et al. 2005). Obviously these data sets are not directly linked because they were acquired for different projects. However, they do have features that make them suitable for re-analysis. The primary characteristic that makes them suitable is that data are available for individual piles over complete impact hammer pile driving events without introduction of variables in addition to those normally experienced during driving of a pile such as changes in substrate as the driven depth of the pile increases and changes in hammer operation.

Given the characteristics of the available data, the approach taken to address the project objective was to first separately analyze the dynamic pile driving and impulsive sound data sets. The results of analysis were then compared, both qualitatively and quantitatively, to identify features of pile-driving mechanics that appear to contribute to observed variability in underwater sound.

Table. 2.1. Piles and Bubble Curtain Operating Conditions for which Dynamic Pile Driving Data Were Available for the Friday Harbor Ferry Terminal Restoration Project

Date	Pile ID	Hammer Type	Event	Time
2/10/05	Pile #1 ("C")	Diesel	Start Hammer Bubble Curtain: OFF	3:20 PM
			Bubble Curtain: Lowest Ring @ ½ air flow	3:50 PM
			Bubble Curtain: Middle Ring ½@ air flow	3:56 PM
			Bubble Curtain: Top Ring @ ½ air flow	3:57 PM
			Bubble Curtain: Lowest Ring @ Full air flow	3:58 PM
			Bubble Curtain: Middle Ring @ Full air flow	3:59 PM
			Bubble Curtain: Top Ring @ Full air flow	4:01 PM
			Bubble Curtain: OFF	4:02 PM
2/11/05	Pile #2 ("A")	Air	Start Hammer Bubble Curtain: OFF	4.12 PM
			Bubble Curtain: Bottom Ring @ Full air flow	4:13 PM
			Bubble Curtain: All Rings @ Full air flow	4:19 PM
			Bubble Curtain: OFF	4:31 PM
2/12/05	Pile #3 ("B")	Hydraulic	Start Hammer Bubble Curtain: OFF	10:36 AM
			Bubble Curtain: Lowest Ring @ Full air flow	10:37 AM
			Bubble Curtain: All Rings @ Full air flow	10:39 AM
			Bubble Curtain: OFF	10:40 AM

3.0 Dynamic Pile Driving

Dynamic pile testing is routinely conducted during pile driving to measure the stress applied to a pile during driving, to evaluate the performance of the pile driving hammer, to protect the pile from damage, and to ensure that the pile when driven will support its design load. The data required for dynamic pile testing is acquired using accelerometers and strain gages attached to the upper part of the pile. These sensors provide data needed to estimate the energy transferred to the pile and the stress in the pile resulting from each blow. A number of different analytical approaches are used to estimate important parameters such as pile-bearing capacity and pile integrity.

In addition to the estimates of energy transferred to a pile each blow available from dynamic pile-driving analysis, other metrics of the pile-driving process are also very helpful in understanding pile-driving mechanics and their potential effect on underwater sound generation. These metrics include hammer stroke and the number of blows required to drive a pile a set distance such as a foot.

In the following subsections, the results of analysis of dynamic pile driving and other pile-driving data for four piles will be presented. When considered in total, the data for the four piles cover a range of pile-driving conditions sufficient to provide insight into variables affecting pile-driving mechanics and variability in impulsive sound production.

3.1 Pile 7

Pile 7 was a 24-in. outer-diameter open-end, vertical steel pipe pile with a wall thickness of 1.00 in. Pile 7 was approximately 105 ft long. This pile, like the others discussed in this report, was installed in three phases. In the first phase, the pile was placed and driven to a depth of approximately 20 ft in water approximately 35 ft deep with a vibratory hammer. In the second phase, it was driven to its set depth using an impact hammer. After a resting period of a couple of days, it was “proofed” to ensure its bearing capacity. The data for our analysis are from the second phase.

Impact pile driving of pile 7 was conducted using an ICE 120S open-end diesel impact hammer (see the hammer specification sheet in Appendix A). This hammer has a 12 kips ram, a nominal maximum stroke of 12.4 ft, and a maximum rated energy of 149 kips-ft. The data presented in Table 3.1 below as well as that for pile 8 to be discussed in the next section were abstracted from Miner 2005a. Pile 7 was driven on 2/23/05 at Friday Harbor.

Table 3.1. Dynamic Pile Driving and Related Data for Pile 7

Friday Harbor Bridge Seat Pile # 7, 24" OD Open End, Vertical Steel Pipe Pile, Wall Thickness 1", Driven 2/23/05								
End Blow #	Blows/ft	Pile Drive Depth in ft	Average Max Transferred Energy per Blow Kips-ft	SD Average Max Transferred Energy per Blow Kips-ft	Average Hammer Stroke in ft	SD Average Hammer Stroke in ft	Transferred Energy per ft of Pile Depth Kips-ft	Cumulative Energy to Drive Pile Kips-ft
1	0	55.0	0	0	0.00	0.00	0	0
22	21	56.0	47	4	7.86	0.07	987	987
47	25	57.0	50	1	7.90	0.08	1250	2237
70	23	58.0	53	4	8.42	0.49	1219	3456
90	20	59.0	56	1	8.85	0.11	1120	4576
109	19	60.0	49	16	7.96	2.24	931	5507
128	19	61.0	34	2	7.02	0.21	646	6153
170	84	61.5	46	7	8.12	0.60	3864	10017
Data from letter report for Dynamic Pile Measurements and CAPWAP Analyses from Robert Miner Dynamic Testing, Inc. to ACC West Coast (Hurlen) dated March 6, 2005								

In Table 3.1 above, the energy transferred to the pile from the hammer is estimated by integrating the product of the force applied by the hammer and the velocity of the pile over the duration of the blow impulse. The driving statistics are summarized for each foot the pile is driven (with the exception of the first and last lines in the table).

Figure 3.1 below shows the number of blows per foot of pile depth. For this pile and for the others reviewed in subsequent sections, it appears that pile driving contractors manage the time spent driving a pile by keeping the number of blows required to drive the pile a foot as consistent as possible. For pile 7 this was the case with the exception of the last half foot when the pile was approaching its set depth and bearing capacity. Over most of the course of driving this pile, the number of blows required to drive the pile a foot was near 25.

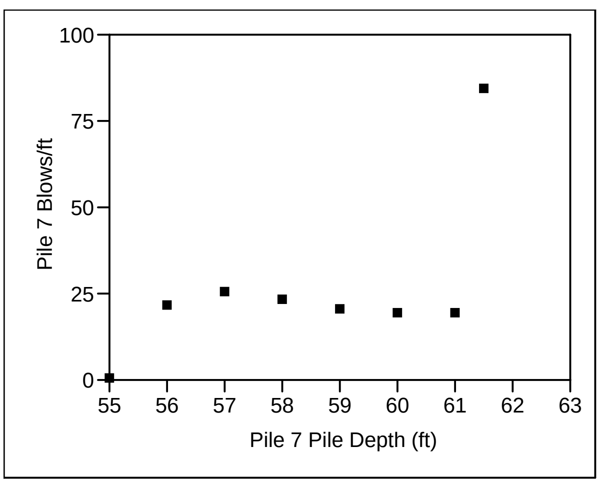

Figure 3.1. The Number of Hammer Blows per Foot of Pile Depth for Pile 7

Figure 3.2 shows the average length of the stroke of the impact hammer for each foot of pile drive depth. This data reveals the action taken by the pile driving contractor to maintain a pile driving schedule. As substrate characteristics and other factors change the resistance to penetration by the pile, the contractor appears to change impact hammer stroke to keep the number of blows, and thereby the time, required to drive the pile a foot as constant as possible. As the hammer stroke standard deviation data in Table 3.1 above show, the variability in hammer stroke within a foot of drive depth is typically very small, the exception in this data set being that for the 60-ft-depth increment.

The energy delivered to the top of the pile by the impact hammer is a function of the hammer stroke and the mass of the hammer ram. However, diesel hammers do not have exactly the same stroke from blow to blow at the same operating settings and the range of settings over which a hammer may be operated during driving of a pile can be quite variable. In addition, the amount of energy delivered to the top of the pile by the hammer is not all transferred to the pile. Therefore the most reliable measure of hammer performance is the estimate of transferred energy obtained by dynamic pile-driving analysis of data from accelerometers attached to a pile. For pile 7, the relationship between the average hammer stroke and the average amount of energy transferred to the pile per blow is shown in Figure 3.3.

A line was fit to the average transferred energy and stroke data. Analysis of the fit of this line is shown in Table 3.2 below. The regression was highly significant with the regression explaining about 88% of the variability in the data.

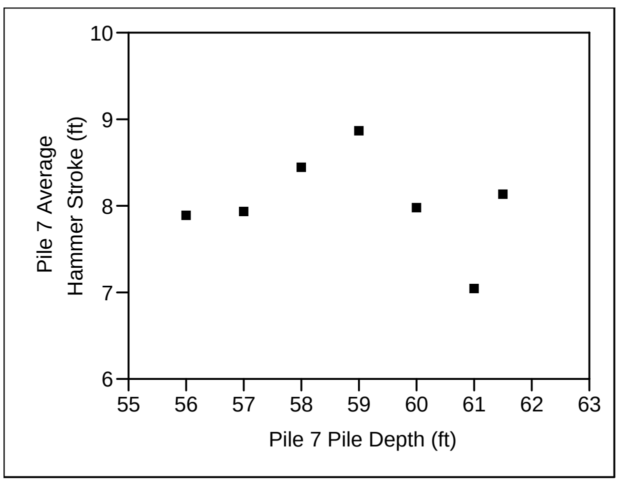

Figure 3.2. The Average Hammer Stroke for each Foot of Drive Depth for Pile 7

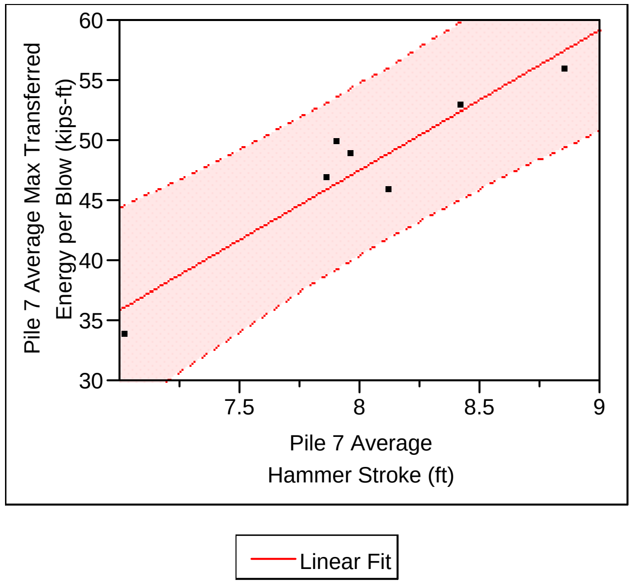

Figure 3.3: Linear Regression of Energy Transfer and Hammer Stroke during Driving of Pile 7. The shaded region is the 95% confidence interval for individual estimates of average maximum transferred energy per blow, given average hammer stroke.

Table 3.2. Statistics and Analysis for Regression of Energy Transfer and Impact Hammer Stroke for Pile 7

Linear Fit

Pile 7 Average Max Transferred Energy per Blow (kips-ft) = -46.12658 + 11.720756 Pile 7 Average Hammer Stroke (ft)

Summary of Fit

RSquare	0.886382
Rsquare Adj	0.863659
Root Mean Square Error	2.588475
Mean of Response	47.85714
Observations (or Sum Wgts)	7

Analysis of Variance

Source	DF	Sum of Squares	Mean Square	F Ratio
Model	1	261.35612	261.356	39.0072
Error	5	33.50102	6.700	Prob > F
C. Total	6	294.85714		0.0015

Parameter Estimates

Term	Estimate	Std Error	t Ratio	Prob>|t|
Intercept	-46.12658	15.07982	-3.06	0.0281
Pile 7 Average Hammer Stroke (ft)	11.720756	1.87665	6.25	0.0015

Because of the strong linear relationship between hammer stroke and the amount of energy transferred to the pile, the average maximum energy transferred per blow for each pile depth increment shows the same trend as that shown for hammer stroke in Figure 3.3 above. The range in average maximum transferred energy over the period required to drive pile 7 was 34 to 56 kips-ft. Figure 3.4 also provides some insight into how the apparent pile driving strategy by the contractor to keep the time to drive the pile a foot as constant as possible results in considerable variation in the amount of energy transferred to the pile and, most likely, in the amount of energy transferred from the pile into the water in the form of sound.

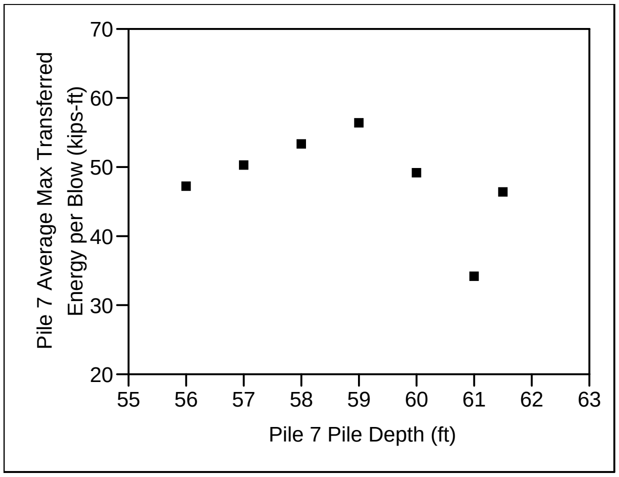

Figure 3.4. The Average Maximum Energy Transferred to Pile 7 per Hammer Blow by Pile Depth

The cumulative energy transferred to the pile during driving for pile 7 is estimated as the product of the number of blows and average maximum transferred energy per blow for each depth increment summed over the drive depth for the pile. This energy is shown in Figure 3.5 below. With the exception of the last half foot (when the pile was nearing its set depth and probably encountered very hard substrate) the rate of accumulation of energy for each successive foot is quite uniform. This is again the result of the contractor's pile driving strategy where changes in substrate are accommodated by changes in hammer stroke and, to a limited extent, by the number of blows to keep the time required to achieve each foot of pile depth fairly constant.

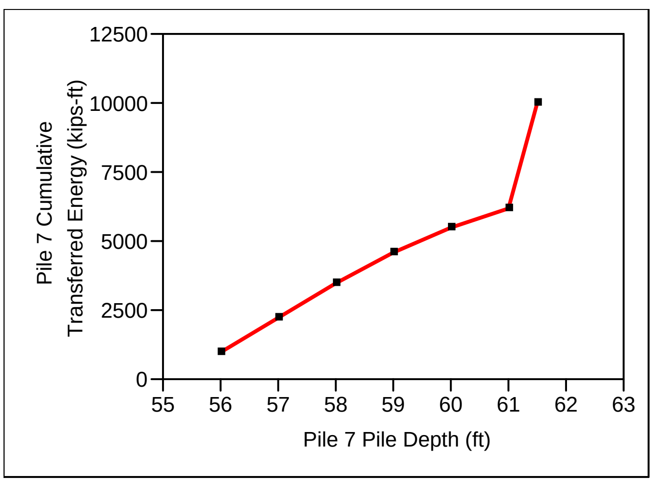

Figure 3.5. Cumulative Energy Transferred to Pile 7 over the Course of Driving the Pile to its Set Depth

3.2 Pile 8

Pile 8 was the same as pile 7, a 24-in. outer-diameter open-end, vertical steel pipe pile with a wall thickness of 1.00 in. Pile 8 was also approximately 105 ft long. As was the case for pile 7, pile 8 was set and driven to a depth of approximately 20 ft in approximately 30 ft of water using a vibratory hammer before impact pile driving began.

As was pile 7, pile 8 was driven using an ICE 120S open end diesel impact hammer. The data presented in Table 3.3 below were abstracted from Miner 2005a. Pile 8 was driven on 2/23/05 at Friday Harbor.

The drive depth of pile 8 was 17.8 ft, over twice the drive depth of pile 7, which was driven 6.5 ft.

Table 3.3. Dynamic Pile Driving and Related Data for Pile 8

Friday Harbor Bridge Seat Pile # 8, 24" OD Open End, Vertical Steel Pipe Pile, Wall Thickness 1", Driven 2/23/05								
End Blow #	Blows/ft	Pile Drive Depth in ft	Average Max Transferred Energy per Blow Kips-ft	SD Average Max Transferred Energy per Blow Kips-ft	Average Hammer Stroke in ft	SD Average Hammer Stroke in ft	Transferred Energy per ft of Pile Depth Kips-ft	Cumulative Energy to Drive Pile Kips-ft
1	0	50.0	0	0	0.00	0.00	0	0
10	10	51.0	38	6	6.93	0.47	380	380
21	10	52.0	38	6	6.93	0.47	380	760
32	10	53.0	38	6	6.93	0.47	380	1140
43	10	54.0	38	6	6.93	0.47	380	1520
56	13	55.0	42	2	7.48	0.06	546	2066
72	16	56.0	46	2	7.48	0.07	736	2802
88	16	57.0	47	1	7.51	0.06	752	3554
120	32	58.0	54	6	8.04	0.39	1728	5282
136	16	59.0	63	1	8.69	0.05	1008	6290
151	15	60.0	64	2	8.81	0.12	960	7250
166	15	61.0	64	1	8.88	0.07	960	8210
180	14	62.0	64	1	8.79	0.09	896	9106
196	16	63.0	64	1	8.77	0.06	1024	10130
210	14	64.0	64	1	8.72	0.07	896	11026
222	12	65.0	62	1	8.61	0.10	744	11770
237	15	66.0	62	2	8.63	0.10	930	12700
253	16	67.0	63	1	8.70	0.09	1008	13708
308	68	67.8	60	2	9.22	0.17	4080	17788
Data from letter report for Dynamic Pile Measurements and CAPWAP Analyses from Robert Miner Dynamic Testing, Inc. to ACC West Coast (Hurlen) dated March 6, 2005								

Figure 3.6 below shows the number of hammer blows per foot of drive depth for pile 8. The number of blows per foot was less than that used to drive pile 7 for most of the driven depth. As was the case for pile 8, the number of blows per foot increased very significantly at the end of the drive when the pile achieved its set depth and encountered hard substrate.

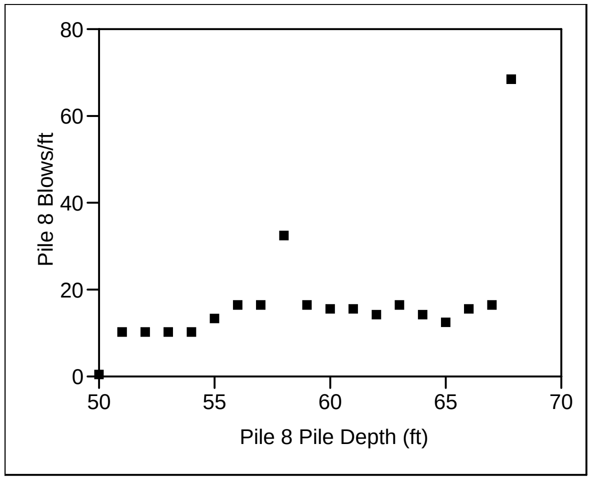

Figure 3.6. The Number of Hammer Blows per foot of Pile Depth for Pile 8

The length of the average hammer stroke per blow over the drive depth for pile 8 is shown in Figure 3.7 below. The hammer used to drive pile 8 was the same as that used for pile 7. Compared to the data for pile 7, the average hammer stroke used to drive pile 8 was initially lower but then increased and remained higher than that used for pile 7 for the last 10 feet of drive depth.

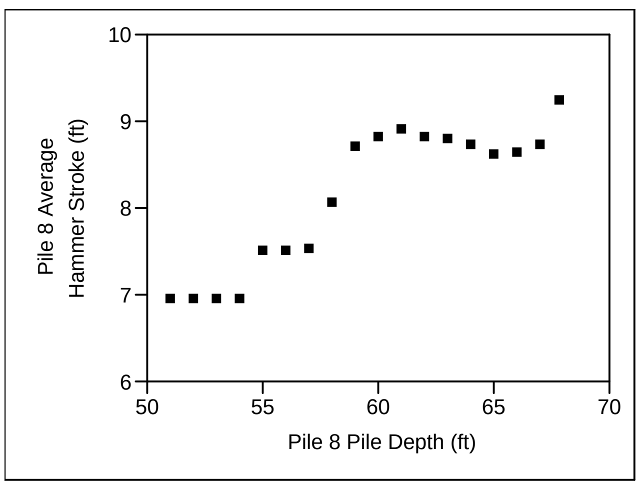

Figure 3.7. The Average Hammer Stroke per Foot of Drive Depth for Pile 8

As was the case for pile 7 data, a line was fit to the average transferred energy and stroke length data for pile 8. The resulting fit is shown in Figure 3.8 and the statistics for the fit are in Table 3.4. The regression accounted for more of the variability (95% compared to 88.6%) in the data for pile 8 than was the case for pile 7. In addition the intercept was lower and the slope higher for pile 8 than pile 7 indicating that the average amount of energy transferred to the pile for each blow was initially lower then moved higher for pile 8 than for pile 7.

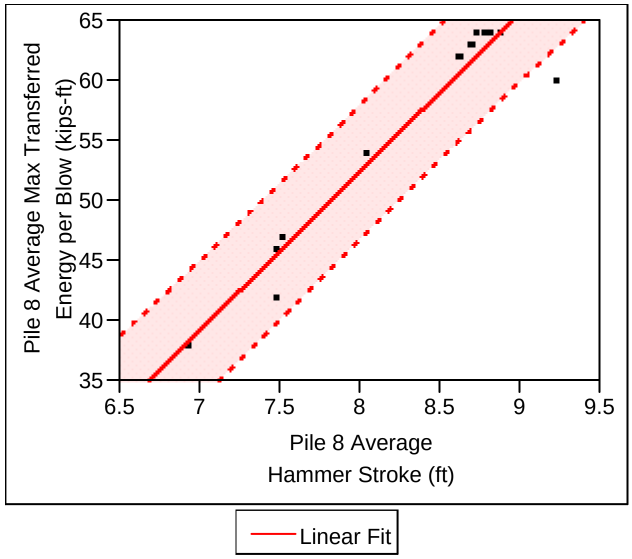

Figure 3.8. Linear Regression of Energy Transfer and Impact Hammer Stroke for Pile 8

Table 3.4. Statistics and Analysis for Regression of Energy Transfer and Impact Hammer Stroke for Pile 8

Linear Fit

Pile 8 Average Max Transferred Energy per Blow (kips-ft) = -53.0433 + 13.185755 Pile 8 Average Hammer Stroke (ft)

Summary of Fit

RSquare	0.950463
RSquare Adj	0.947366
Root Mean Square Error	2.554073
Mean of Response	53.94444
Observations (or Sum Wgts)	18

Lack Of Fit

Source	DF	Sum of Squares	Mean Square	F Ratio
Lack Of Fit	12	96.37260	8.03105	4.0155
Pure Error	4	8.00000	2.00000	Prob > F
Total Error	16	104.37260		0.0953
				Max RSq
				0.9962

Analysis of Variance

Source	DF	Sum of Squares	Mean Square	F Ratio
Model	1	2002.5718	2002.57	306.9881
Error	16	104.3726	6.52	Prob > F
C. Total	17	2106.9444		<.0001

Parameter Estimates

Term	Estimate	Std Error	t Ratio	Prob>|t|
Intercept	-53.0433	6.135835	-8.64	<.0001
Pile 8 Average Hammer Stroke (ft)	13.185755	0.752565	17.52	<.0001

The average maximum transferred energy per blow over the impact hammer drive depth for pile 8 is shown in Figure 3.9. Compared to pile 7, the amount of energy per blow was initially lower but then increased to a level above that measured for pile 7 and remained high through the end of the drive.

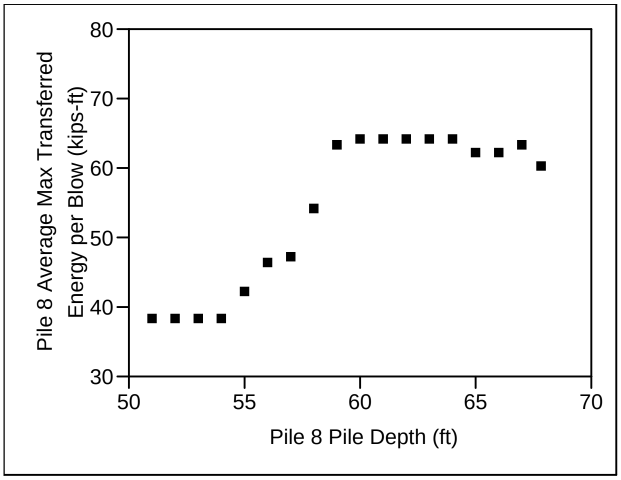

Figure 3.9. The Average Maximum Energy Transferred to the Pile for each Hammer Blow by Pile Depth

The cumulative energy transferred to pile 8 during its drive is shown in Figure 3.10. The cumulative energy transferred to pile 8 was not quite twice that observed for pile 7 even though the drive depth for this pile was 17.8 ft compared to the 6.5 feet for pile 7.

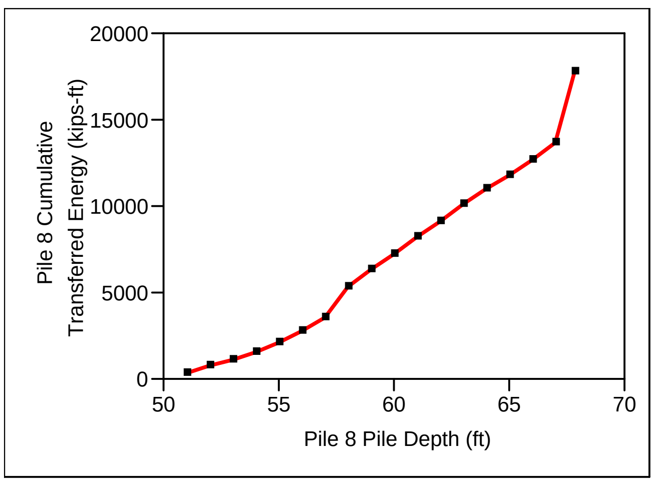

Figure 3.10. Cumulative Energy Transferred to the Pile over the Course of Driving the Pile to its Set Depth

Piles 7 and 8 were identical in construction and were located in close proximity in the bridge seat of the Friday Harbor Ferry Terminal. Both piles were also driven with the same impact hammer. However, the mechanics of driving these two piles was very different. This difference is shown in Figure 3.11. It is clear that the energy per blow was much less for pile 8 initially but increased to a much higher level over the last half of its drive depth. If the wetted length of the two piles was similar and sound production is a function of the energy transferred into a pile, during the driving period it would be reasonable to assume that initially the sound generated would have been higher for pile 7. However, at about half of its drive depth, pile 8 would have produced higher sound levels than those produced by pile 7 at its peak when hammer stroke increased to overcome increased pile drive resistance.

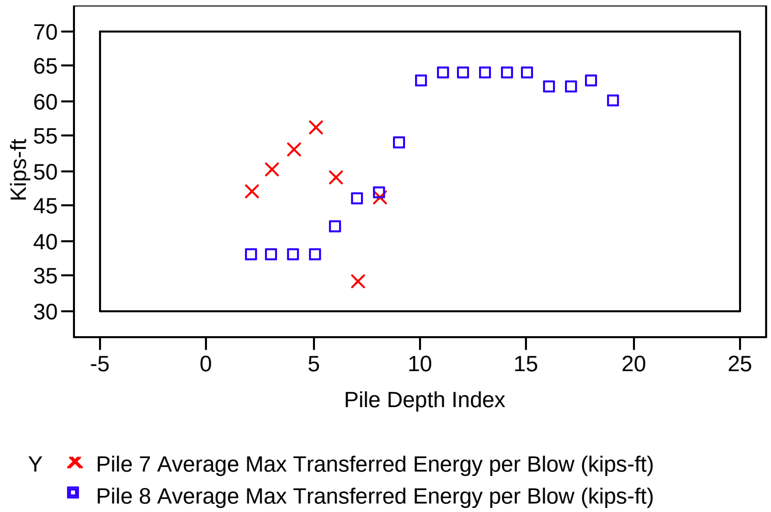

Figure 3.11. The Average Maximum Transferred Energy per Blow for Piles 7 and 8 over their Drive Depths

3.3 Pile 21

Pile 21 was a 30-in. outer-diameter open-end, vertical steel pipe pile with a wall thickness of 1.00 in. Pile 21 is approximately 105 ft long. As with piles 7 and 8, this pile was installed in three phases. In the first phase the pile was placed and driven to a depth of approximately 20 to 30 ft with a vibratory hammer. In the second phase it was driven to its set depth using an impact hammer. After a resting period of a couple of days it was "proofed" to confirm its bearing capacity.

Impact pile driving of pile 21 was conducted using the same model of impact hammer, an ICE 120S open end diesel impact hammer, used to drive piles 7 and 8. The data presented in Table 3.5 below as well as that for pile 16 to be discussed in the next section was abstracted from Miner 2005b. Pile 21 was driven on 3/04/05 at Friday Harbor.

The number of hammer blows per foot of drive depth for pile 21 is shown in Figure 3.12. The number of blows per foot for this pile is similar to that for pile 8 and about half that required for pile 7.

Table 3.5. Dynamic Pile Driving and Related Data for Pile 21

Friday Harbor Tower Base Pile # 21, 30" OD Open End, Vertical Steel Pipe Pile, Wall Thickness 1", Driven 3/04/05								
End Blow #	Blows/ft	Pile Drive Depth in ft	Average Max Transferred Energy per Blow Kips-ft	SD Average Max Transferred Energy per Blow Kips-ft	Average Hammer Stroke in ft	SD Average Hammer Stroke in ft	Transferred Energy per ft of Pile Depth Kips-ft	Cumulative Energy to Drive Pile Kips-ft
1	0	83.0	0	0	0.00	0.00	0	0
18	17	84.0	38	6	7.41	0.71	646	646
28	10	85.0	39	1	7.33	0.10	390	1036
39	11	86.0	39	1	7.28	0.08	429	1465
59	20	87.0	32	14	6.21	2.30	640	2105
68	9	88.0	45	3	7.54	0.19	405	2510
77	9	89.0	42	6	7.42	0.50	378	2888
87	10	90.0	49	9	7.77	0.73	490	3378
102	7	92.0	43	14	7.30	1.14	301	3679
108	6	93.0	48	7	6.55	3.21	288	3967
115	7	94.0	39	9	7.02	0.59	273	4240
125	10	95.0	43	4	6.60	2.33	430	4670
132	7	96.0	51	1	7.88	0.07	357	5027
Data from letter report for Dynamic Pile Measurements and CAPWAP Analyses from Robert Miner Dynamic Testing, Inc. to ACC West Coast (Hurlen) dated March 7, 2005								

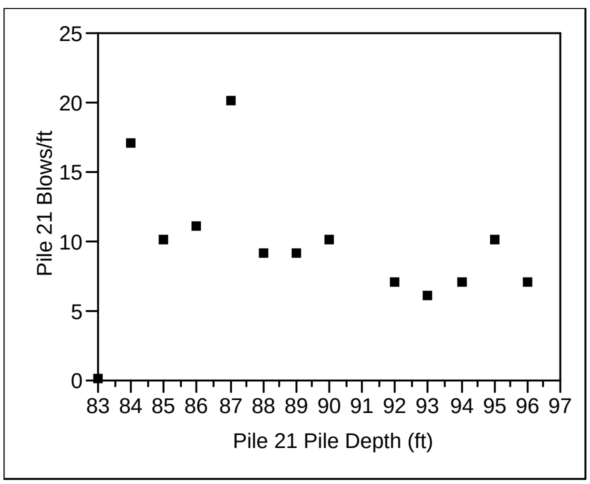

Figure 3.12. The Number of Hammer Blows per Foot of Pile Depth for Pile 21

The average hammer stroke per blow for each foot of drive depth is shown in Figure 3.13 for pile 21. The average hammer stroke length used to drive pile 21 is, in general, slightly less than that used to drive piles 7 and 8 even though 7 and 8 were smaller diameter piles.

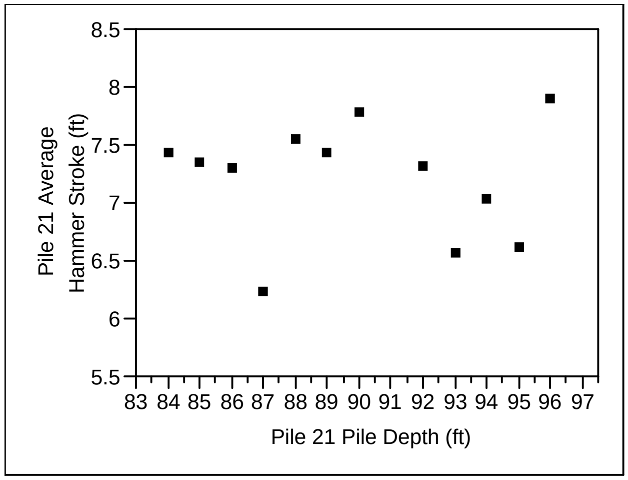

Figure 3.13. The Average Hammer Stroke per Blow for each Foot of Drive Depth for Pile 21

A line was fit to the average maximum transferred energy and average hammer stroke data for pile 21. This line is shown in Figure 3.14 and the statistics describing the fit are shown in Table 3.6. The linear fit only explained about 27% of the variability in the energy and stroke data for this pile. This is in contrast to piles 7 and 8 where a linear fit explained about 88% and 95% respectively of the variability in energy and stroke data. In addition, the intercept and slope for the fit is quite different from that for piles 7 and 8. It is likely the underwater sound that would be produced by this pile would be more variable than that produced by piles 7 and 8. It is also likely that the increased surface area of the 30 in. diameter pile would have increased the energy transferred from the pile into the water. Given the change in diameter alone, not considering wetted length and other variables, an increase in energy of about 25% for 30-in. diameter steel shell piles compared to 24-in. diameter steel shell piles of the same wall thickness would be expected.

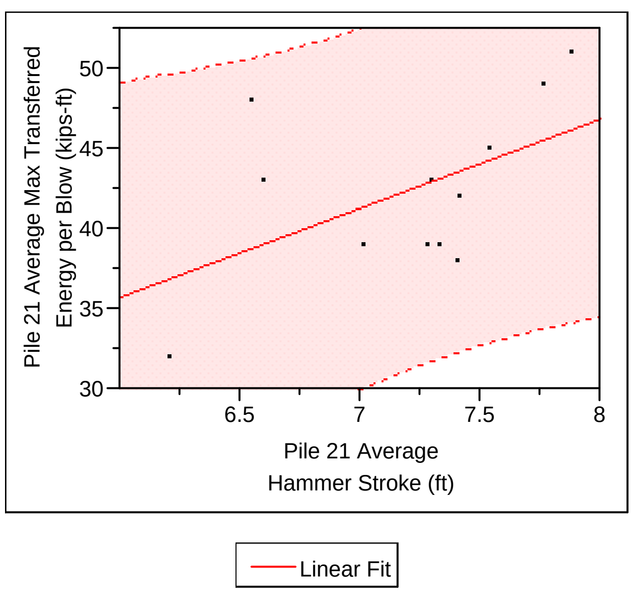

Figure 3.14. Linear Regression of Energy Transfer and Hammer Stroke for Pile 21

Table 3.6. Statistics and Analysis for Regression of Energy Transfer and Impact Hammer Stroke for Pile 21

Linear Fit

Pile 21 Average Max Transferred Energy per Blow (kips-ft) = 2.2564566 + 5.5720371 Pile 21 Average Hammer Stroke (ft)

Summary of Fit

RSquare	0.275046
Rsquare Adj	0.202551
Root Mean Square Error	4.806439
Mean of Response	42.33333
Observations (or Sum Wgts)	12

Analysis of Variance

Source	DF	Sum of Squares	Mean Square	F Ratio
Model	1	87.64814	87.6481	3.7940
Error	10	231.01852	23.1019	Prob > F
C. Total	11	318.66667		0.0800

Parameter Estimates

Term	Estimate	Std Error	t Ratio	Prob>|t|
Intercept	2.2564566	20.62202	0.11	0.9150
Pile 21 Average Hammer Stroke (ft)	5.5720371	2.860659	1.95	0.0800

The average maximum energy transferred to pile 21 per blow by pile depth is shown in Figure 3.15. The variability in energy transfer for this pile from one depth increment to another is higher than either pile 7 or 8. The level of energy transfer is roughly equal to that observed for pile 7 and the first 8 feet of depth for pile 8. It is significantly less than that observed for the last 10 feet of depth for pile 8. It is clear that considerable attention to hammer operation was required by the operator to keep the drive time per foot relatively consistent for this pile.

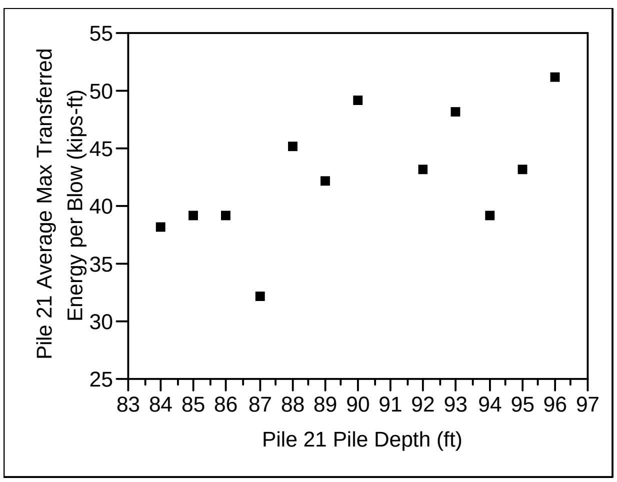

Figure 3.15. The Average Maximum Energy Transferred to the Pile for each Hammer Blow by Pile Depth for Pile 21

Apparently the substrate pile 21 was driven into, plus other factors that contribute to increased drive resistance, varied considerably with depth. The pile driving records indicate the hammer operator had to make frequent changes to hammer operation to achieve a more consistent time to drive the pile a foot over the total distance the pile was driven. The result of this attention to operation is shown in the cumulative energy Figure 3.16. The slope of the cumulative energy line is quite consistent from one depth increment to another, similar to that for piles 7 and 8. The total cumulative energy for pile 21 is considerably less than that for either of the two smaller piles 7 and 8.

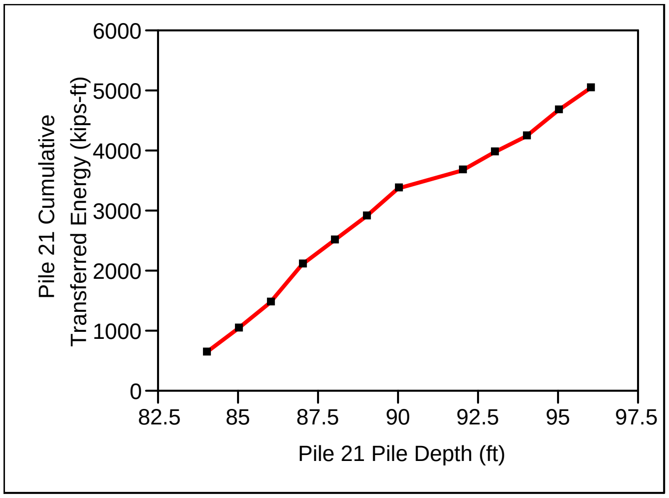

Figure 3.16. Cumulative Energy Transferred to Pile 21over the Course of Driving the Pile to its Set Depth

3.4 Pile 16

Pile 16 was identical to pile 21. Pile 16 was a 30-in. outer-diameter open end, approximately 105 foot long vertical steel pipe pile with a wall thickness of 1.00 in. This pile, as were all other piles discussed in this report, was installed in three phases. In the first phase, the pile was placed and driven to a depth of approximately 20 to 30 ft with a vibratory hammer. In the second phase, it was driven to its set depth using an impact hammer. After a resting period of a couple of days it was “proofed,” to ensure its bearing capacity. The data of importance for our analysis is from the second phase.

Impact pile driving of pile 16 was conducted using the same model of impact hammer, an ICE 120S open-end diesel impact hammer, used to drive piles 7, 8, and 21. The data presented in Table 3.7 below as well as that for pile 16 to be discussed in the next section was abstracted from Miner 2005b. Pile 16 was driven on 3/05/05 at Friday Harbor.

The average hammer stroke over the depth of the pile is shown in Figure 3.17. The hammer stroke for pile 16 was consistently high over the total pile driving period. The only other pile where similar stroke length was used was the last 10 feet of depth for pile 8, a smaller diameter pile.

Table 3.7. Dynamic Pile Driving and Related Data for Pile 16

Friday Harbor Tower Base Pile # 16, 30" OD Open End, Vertical Steel Pipe Pile, Wall Thickness 1", Driven 3/05/05								
End Blow #	Blows/ft	Pile Drive Depth in ft	Average Max Transferred Energy per Blow Kips-ft	SD Average Max Transferred Energy per Blow Kips-ft	Average Hammer Stroke in ft	SD Average Hammer Stroke in ft	Transferred Energy per ft of Pile Depth Kips-ft	Cumulative Energy to Drive Pile Kips-ft
1	0	75.0	0	0	0.00	0.00	0	0
15	14	76.0	38	23	6.95	3.63	532	532
33	18	77.0	55	1	8.98	0.08	990	1522
49	16	78.0	54	1	8.85	0.10	864	2386
64	15	79.0	55	2	8.88	0.12	825	3211
78	14	80.0	54	2	8.86	0.12	756	3967
92	14	81.0	54	1	8.84	0.15	756	4723
107	15	82.0	54	1	8.77	0.10	810	5533
120	13	83.0	52	4	8.57	0.40	676	6209
136	16	84.0	54	1	8.70	0.07	864	7073
148	12	85.0	54	1	8.73	0.06	648	7721
160	12	86.0	64	1	8.72	0.10	768	8489
172	12	87.0	55	1	8.78	0.09	660	9149
184	12	88.0	54	1	8.75	0.09	648	9797
196	12	89.0	54	1	8.74	0.04	648	10445
208	12	90.0	55	1	8.83	0.11	660	11105
219	11	91.0	55	1	8.88	0.07	605	11710
233	14	92.0	54	1	8.84	0.08	756	12466
245	12	93.0	53	3	8.83	0.13	636	13102
Data from letter report for Dynamic Pile Measurements and CAPWAP Analyses from Robert Miner Dynamic Testing, Inc. to ACC West Coast (Hurlen) dated March 7, 2005								

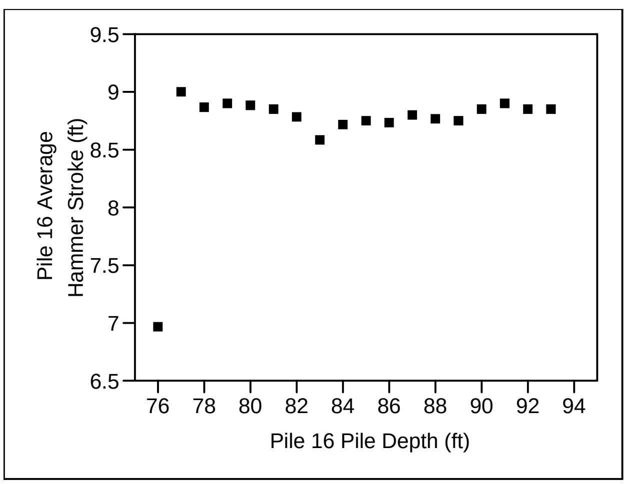

Figure 3.17. The Average Hammer Stroke per Blow for each Foot of Drive Depth for Pile 16

The number of hammer blows per foot of pile depth for pile 16 is shown in Figure 3.18. The number of blows per foot of drive depth for pile 16 was similar to that for the other piles. The only significant departure from blows per foot values in the range of 10 to approximately 20 blows per foot were the final increments in depth for piles 7 and 8.

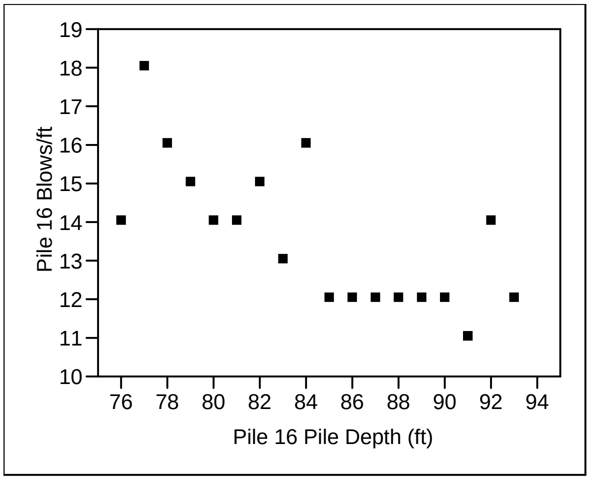

Figure 3.18. The Number of Hammer Blows per Foot of Pile Depth for Pile 16

The average maximum transferred energy per hammer blow for pile 16 is shown in Figure 3.19. As was the case for hammer stroke, the average maximum transferred energy per blow was quite consistent over the total drive. This pattern was different from that observed for the other piles where considerable variation in transferred energy per blow was observed from the beginning to the end of the pile.

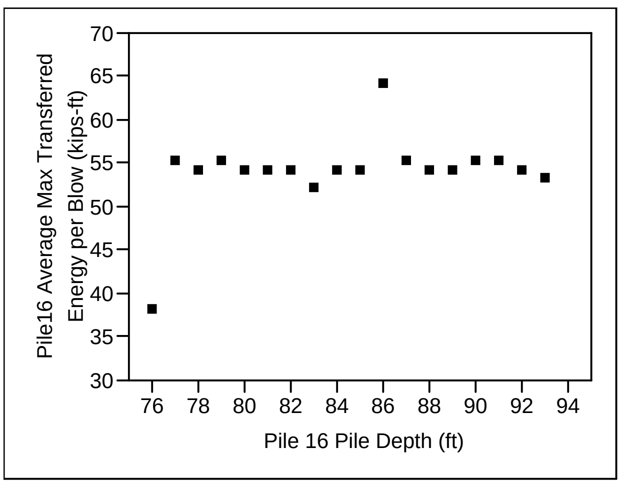

Figure 3.19. The Average Maximum Energy Transferred per Blow for Pile 16

As was done for the other piles, a line was fit to the transferred energy and hammer stroke data. The results of this fit are shown graphically in Figure 3.20 and the statistics describing the fit are given in Table 3.8. The fit explains about 69% of the variation in the energy transfer and stroke data. This is more than was explained by a linear fit to the pile 21 data and less than that explained by linear fits to the data for piles 7 and 8. It is clear that the fit was driven by a single point at a hammer stroke near 7 ft and a cluster near 9 ft.

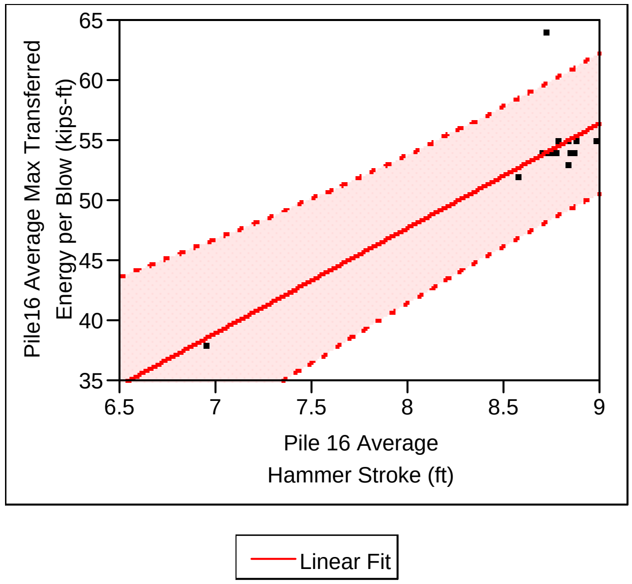

Figure 3.20. Linear Regression of Energy Transfer and Hammer Stroke for Pile 16

Table 3.8. Statistics and Analysis for Regression of Energy Transfer and Impact Hammer Stroke for Pile 16

Linear Fit

Pile16 Average Max Transferred Energy per Blow (kips-ft) = -21.67532 + 8.6783118 Pile 16 Average Hammer Stroke (ft)

Summary of Fit

RSquare	0.69305
RSquare Adj	0.673866
Root Mean Square Error	2.646588
Mean of Response	53.77778
Observations (or Sum Wgts)	18

Lack Of Fit

Source	DF	Sum of Squares	Mean Square	F Ratio
Lack Of Fit	13	110.07082	8.46699	12.7005
Pure Error	3	2.00000	0.66667	Prob > F
Total Error	16	112.07082		0.0296
				Max RSq
				0.9945

Analysis of Variance

Source	DF	Sum of Squares	Mean Square	F Ratio
Model	1	253.04029	253.040	36.1258
Error	16	112.07082	7.004	Prob > F
C. Total	17	365.11111		<.0001

Parameter Estimates

Term	Estimate	Std Error	t Ratio	Prob>|t|
Intercept	-21.67532	12.5691	-1.72	0.1039
Pile 16 Average Hammer Stroke (ft)	8.6783118	1.443865	6.01	<.0001

The cumulative energy over the depth of drive of pile 16 is shown in Figure 3.21. The increment in transferred energy per foot of depth is quite uniform over the drive, which is similar to that observed for piles 7, 8, and 21. It appears that for this pile a different drive strategy was implemented by the hammer operator. For the previous piles, the number of blows per foot was held relatively constant and the hammer stroke was modified as necessary to keep drive times per foot of depth more or less uniform. In the case of this pile it appears that the hammer was operated near its stoke maximum and the number of blows was left to vary. Given that the duty cycle of the hammer is probably set for a particular stroke, it is likely that for this pile the time to drive the pile a foot varied more than for previous piles. Regardless the incremental energy per foot of drive depth was consistent over the drive.

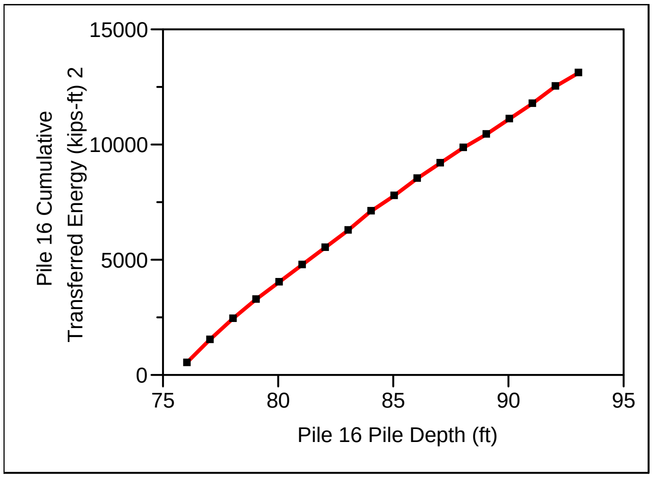

Figure 3.21. Cumulative Energy Transferred to the Pile over the Course of Driving the Pile to its Set Depth

3.5 All Piles Combined

Driving piles economically while protecting the integrity of the pile and obtaining the necessary bearing strengths is a complicated process. Analysis of this process for piles 7, 8, 21, and 16 has shown that, for these piles at least, with limited exception, the blows required per foot of drive depth is quite consistent for all piles regardless of their size and drive location and remained within a relatively narrow band between 10 and 25 blows per foot (Figure 3.22). Also very consistent for all piles examined was the transferred energy per foot of drive depth (Figure 3.23)

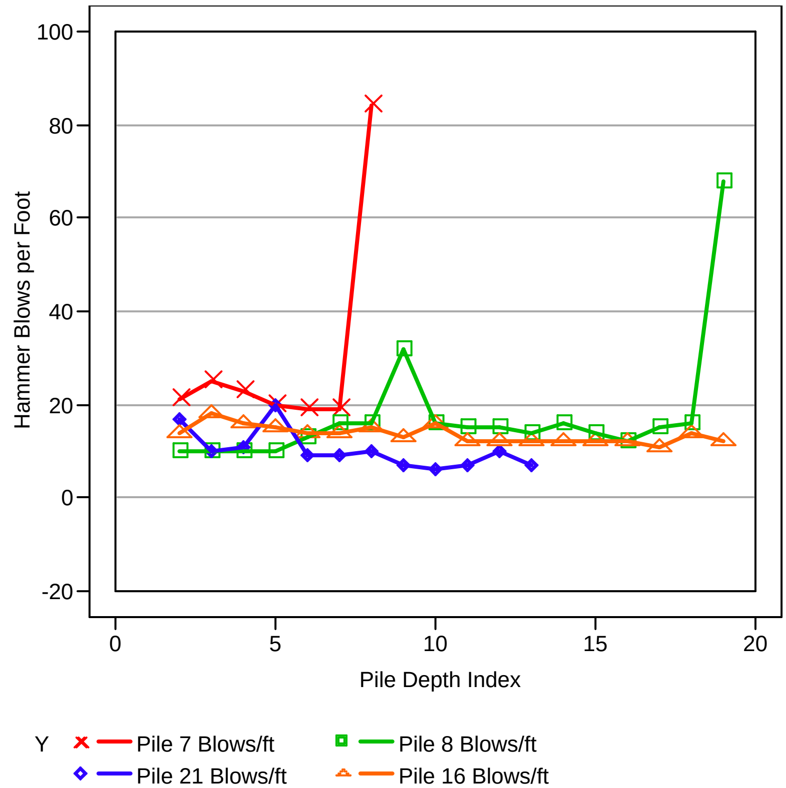

Figure 3.22. The Number of Impact Hammer Blows per Foot of Pile Depth for Piles 7, 8, 21, and 16

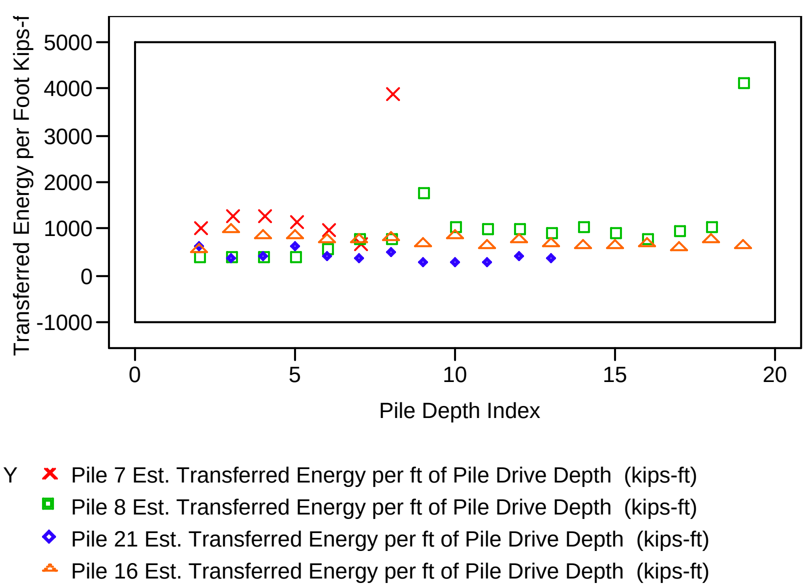

Figure 3.23. The Average Transmitted Energy per Foot of Drive Depth for Piles 7, 8, 21, and 16

The variability between piles in the strategies required to overcome differences in substrate and other conditions affecting driving conditions become apparent when the related measures of average maximum transferred energy per blow and hammer stroke are considered (Figures 3.24 and 3.25). These data show that it is not uncommon for the energy transferred to the pile to double over the driving period as hammer stroke is changed to overcome conditions that are reducing the incremental gain in pile depth with each blow.

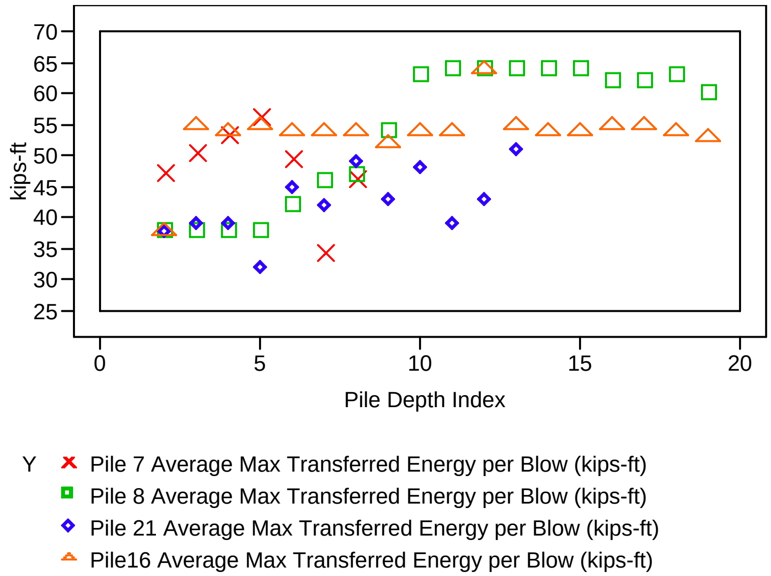

Figure 3.24. The Average Maximum Energy Transferred to Piles 7, 8, 21, and 16 per each Hammer Blow by Pile Depth

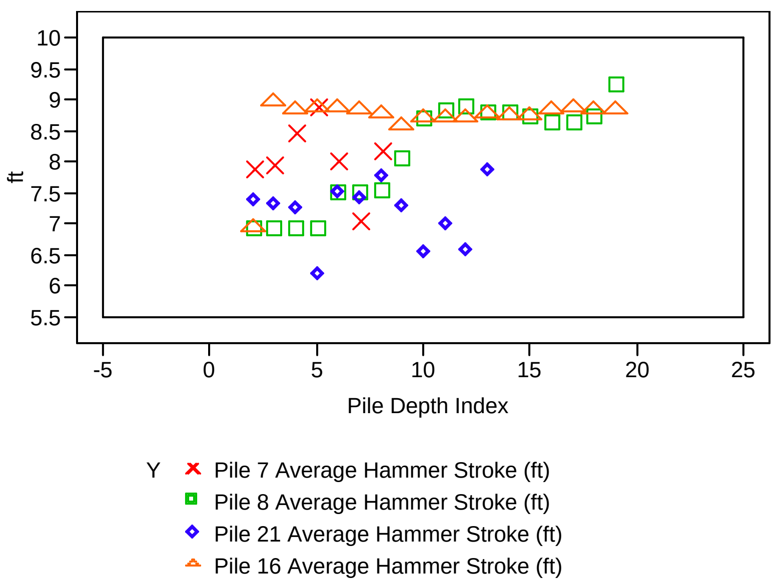

Figure 3.25. The Average Hammer Stroke Length for each Foot of Pile Drive Depth for all Four Piles

The cumulative energy transferred to the pile over the drive period is quite regular for an individual pile. Differences between piles are shown in the slope of the cumulative line which is a measure of the amount of energy required per foot of drive depth (Figure 3.26). The steeper the cumulative energy line the greater the amount of energy required per foot of drive depth. Of the piles considered here, pile 7 required the most energy per foot of pile depth showing a transition to very hard substrate at the end of it drive. Pile 21 required the least energy to drive even though it was a larger pile and was driven to a depth approximately twice that of pile 6 (Table 3.9).

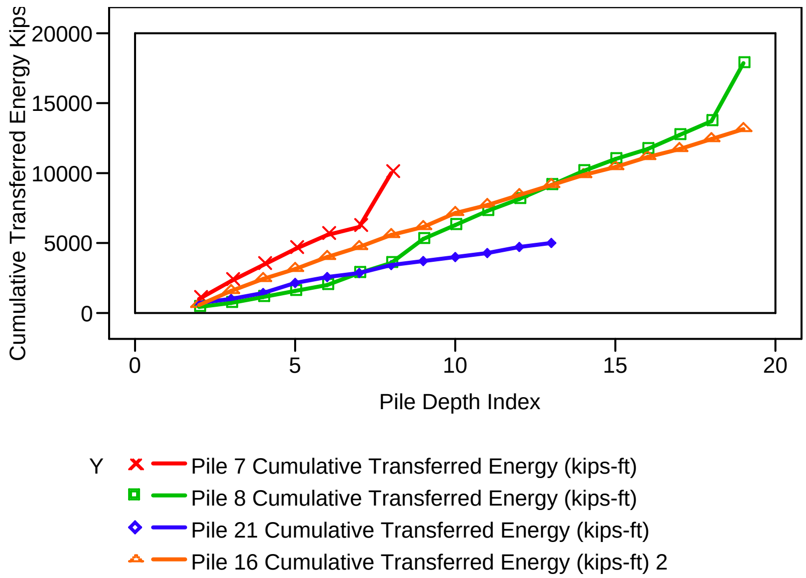

Figure 3.26. Cumulative Energy Transferred to each Pile over the Course of Driving the Pile to its Set Depth

Table 3.9. Depth Driven, Numbers of Blows, and Cumulative Energy Needed to Drive each Pile

Pile Number	Impact Drive Depth (ft)	Number of Blows to Drive Pile	Cumulative Energy to Drive Pile (kips-ft)
7	6.5	170	10,017
8	17.8	308	17,788
21	13.0	132	5,027
16	18.0	245	13,102

It is clear that conditions, i.e., transferred energy per blow, exist during pile driving to account for the large differences in sound production observed over the course of driving a single pile. In Figure 3.27 the lines fit to the data for average maximum energy transferred to the piles and a line fit to manufacturers' hammer energy data for the Model 120S ICE impact hammer are shown (ICE 2007). The hammer energy in kips-ft is shown as a function of hammer stroke by the red line above the cluster of other lines. The cluster of lines below the hammer energy are the regression lines from the line fits to the transferred energy and hammer stroke data acquired during dynamic pile monitoring. This data and the linear fits to the data were discussed previously.

Figure 3.27 shows that considerably more energy is in the hammer blow falling on the pile than is transferred to the pile to increase drive depth. All other factors held constant, it is reasonable to assume that if the drive depth of the pile was static and it was repeatedly struck by the drive hammer using the same stroke every time, the amount of energy radiated into the water as sound would also be relatively constant. Following this logic, it is most likely not so much the characteristics of the substrate the pile is driven through that result in changes in the amount of sound produced. Rather it is the way the driving hammer is operated to overcome the increased (or decreased) resistance to being driven that result in the production of more or less sound.

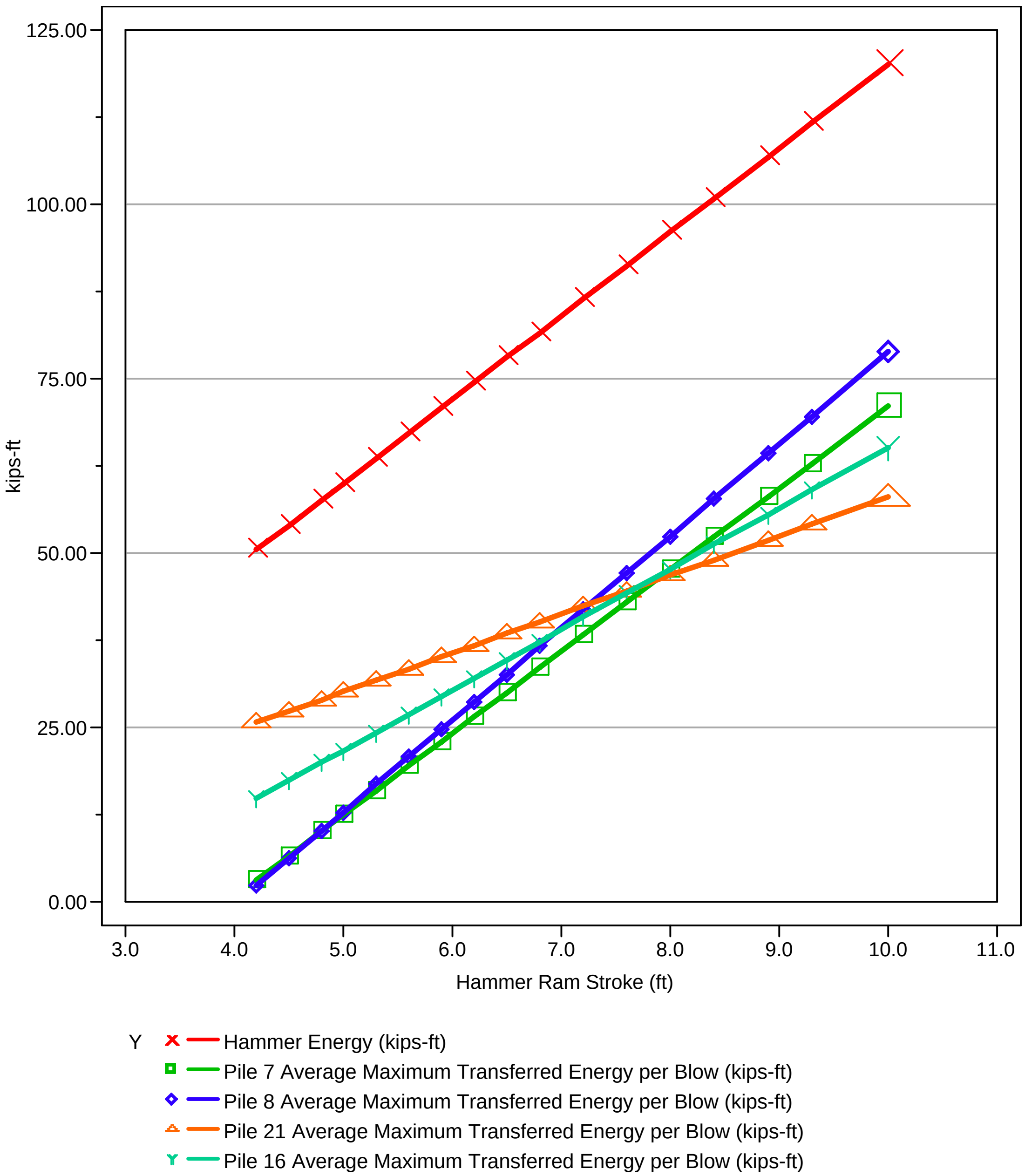

Figure 3.27. Linear Regression of Energy Transfer and Hammer Stroke Length for the Four Pile Drives, Compared to the Manufacturer's Energy Data for the Model 120S ICE Impact Hammer

It is likely that the amount of sound produced per blow is a function of several variables. However it seems likely that a primary determinant will be the amount of energy delivered by the hammer to the pile, which is a linear function of the hammer stroke. The result being that, in general, a longer hammer stroke will result in a higher sound level, all other factors remaining reasonably similar from blow to blow. This in turn suggests that monitoring of hammer stroke (for a particular hammer and type of pile) may be a satisfactory metric for any further study of relationships between sound production and pile driving activity, thereby avoiding the cost and time required for detailed dynamic pile driving data.

3.6 Findings from Friday Harbor Dynamic Pile Driving Data Review

- With the exception of pile 21, the hammer blows per foot of drive depth was relatively constant through a pile drive while hammer stroke was changed in response to changes in pile drive resistance.

- Hammer stroke and the amount of energy transferred to a pile per blow were linearly related.

- The product of the number of hammer blows and transferred energy per blow (hammer stroke) resulted in uniformity for each pile, in the amount of energy required per foot of drive.

- Variability in the characteristics of impulse sound produced by each blow during pile driving is most likely directly related to changes in hammer operation (primarily stroke) in response to changes in pile drive resistance.

- Differences in the total amount of energy required to drive a pile and the total amount of sound energy produced are most likely directly related to the hammer energy (hammer stroke) required to overcome drive resistance and to maintain a drive schedule measured by the number of blows required to achieve a foot of drive depth.

4.0 Pile Driving Impulsive Sound

Observations of impulsive sound generated by pile driving have shown that the level and other characteristics of sound produced can be quite variable during driving of a pile. While there are numerous factors that could contribute to this variability, there is consensus that the characteristics of the pile and the substrate it is driven into are major factors. Based on our analysis in Section 3, we hypothesize that it is hammer operation in response to drive resistance and the mandate to maintain drive schedules that is a primary determinant in impulsive sound variability during a pile drive. We propose that, for a class of pile and potentially hammer type, it may be the operation of the hammer in response to changes in substrate rather than the substrate itself that accounts for changes in the amount and characteristics of sound produced.

In this section we will examine in detail the variability in the amount and characteristics of sound produced by impact pile driving. In Section 5 we will compare the observed variability in sound production with the variability observed in the mechanics of pile driving, particularly the variability in hammer stroke. To perform this comparison, we assume that the pile driving mechanics and implications for sound production identified during analysis of dynamic pile driving information for four piles at Friday Harbor have features that can be extended to the pile driving of any steel shell pile by a diesel hammer. We also assume that the observations of impulsive sound to be examined in this section have features that can be generalized to the production of sound during impact hammer driving of the broader population of intermediate-diameter steel-shell piles.

The impulsive sound signals selected for analysis were acquired during construction work at the Hood Canal Bridge in 2004. This project, the methods for sound signal acquisition, and the initial analysis of these data are reported in Carlson et al. 2005. Table 4.1 provides a summary of the date the piles were driven and other information.

4.1 Results

4.1.1 Wetted Pile Length

Wetted pile length has been suggested as a factor in the characteristics and amount of sound produced by pile driving.

Figure 4.1 shows the distribution of wetted length of piles by pile drive method and bubble curtain factors. There are no strong trends in wetted pile length with drive method and other factors for the Hood Canal data set.

Figures 4.2 and 4.3 and Tables 4.2 and 4.3 show the results of the fit of a line to the mean maximum absolute pressures, mean energy index, and wetted pile lengths for the piles in the Hood Canal data set. The results are clear. There is no relationship between the peak pressures or mean energies observed in the impulsive sound observed for these piles and the wetted length of the piles, whether driven as batter or plumb piles.

The reason for the lack of relationship between wetted depth and impulsive sound metrics is probably the result of how sound is generated by the pile. When the pile is struck, a small segment of the pile is deformed and presses on the surrounding water generating a sound pulse. This deformation propagates up and down the pile until its energy is dissipated. Therefore, only a small circumferential element of the pile generates sound at an instant – not the whole pile (in general – there is most likely some exception to this generality). The result is that, given similar piles and similar impact force, the sound generated at any instant is largely independent of the wetted length of the pile. However, following this argument, the amount of sound and impulsive sound characteristics would be a function of the circumference of a pile and characteristics of its construction that would affect how much it deformed when struck. Larger diameter steel shell piles, given the same impact energy, would generate impulsive sound with higher peak pressures and would contain more energy.

Table 4.1. List of Piles Driven during Construction at the Hood Canal Bridge in 2004 for which Impulsive Sound Monitoring Data Were Available for Re-Analysis

Date	Pile Number	Pile Type	Water Depth (ft)	Bubble Curtain
Sept. 2, 2004	52N	Plumb	40	Type II Conf.
Sept. 2, 2004	50N	Plumb	40	None
Sept. 3, 2004	121N	Plumb	42	Type II Conf.
Sept. 3, 2004	118N	Plumb	39	Type II Conf.
Sept. 3, 2004	120N	Plumb	39	None
Oct. 27, 2004	235	Plumb	4.5	Type II Conf.
Oct. 27, 2004	237	Plumb	4	Type II Conf.
Oct. 27, 2004	238	Plumb	7	Type II Conf.
Oct. 27, 2004	240	Plumb	9	None
Oct. 27, 2004	172	Plumb	20	Type II Conf.
Oct. 28, 2004	171	Plumb	18	Type II Conf.
Oct. 28, 2004	167	Batter	7	Type I Unconf.
Nov. 10, 2004	255	Plumb	33	Type II Conf.
Nov. 10, 2004	252	Plumb	31	Type II Conf.
Nov. 10, 2004	249	Plumb	32	Type II Conf.
Nov. 10, 2004	177	Batter	37	Type I Unconf.
Nov. 10, 2004	174	Batter	29	Type I Unconf.
Nov. 10, 2004	178	Batter	37	None
Nov. 12, 2004	182	Batter	41	Type I Unconf.
Nov. 12, 2004	181	Batter	33	Type I Unconf.
Nov. 12, 2004	244	Batter	20	None

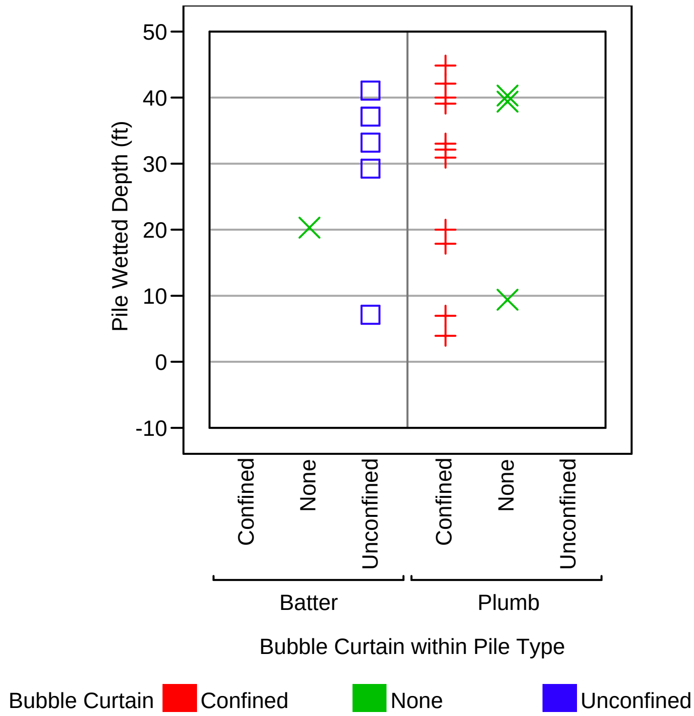

Figure 4.1. Wetted Length (water depth at time of drive) of Monitored Piles by Drive Type (batter or plumb) and Bubble Curtain Type and Presence or Absence

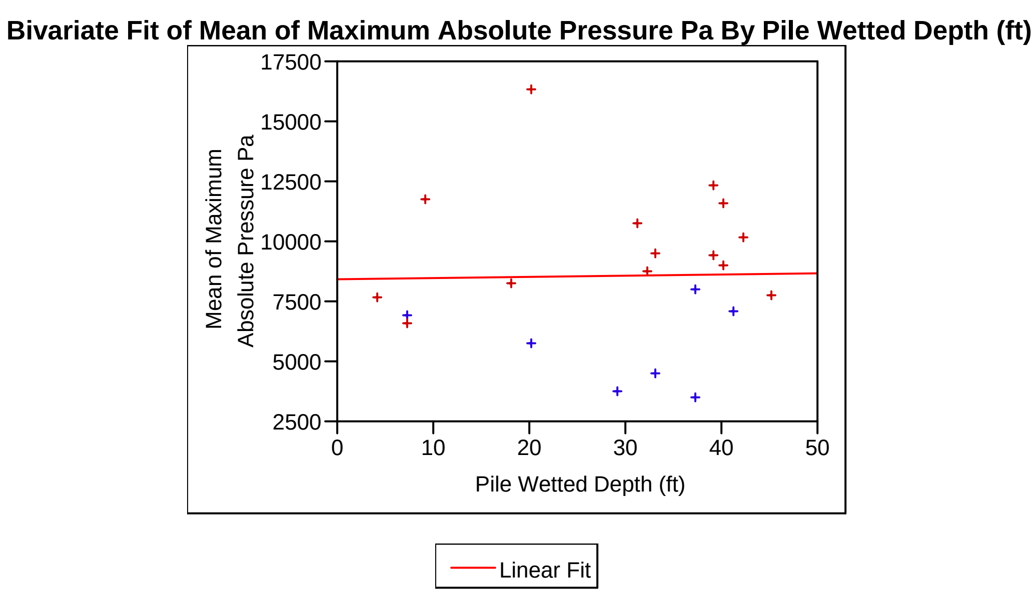

Figure 4.2. Fit of Mean Maximum Absolute Pressure by Pile Wetted Depth. Batter pile data is shown in blue and plumb pile data in red.

Table 4.2. Statistical Summary for Fit of Mean Maximum Absolute Pressure by Pile Wetted Depth

Linear Fit

Mean of Maximum Absolute Pressure Pa = 8401.3522 + 4.9222865 Pile Wetted Depth (ft)

Summary of Fit

RSquare	0.00045
RSquare Adj	-0.05216
Root Mean Square Error	3130.162
Mean of Response	8542.692
Observations (or Sum Wgts)	21

Analysis of Variance

Source	DF	Sum of Squares	Mean Square	F Ratio
Model	1	83790	83790	0.0086
Error	19	186160316	9797911	Prob > F
C. Total	20	186244107		0.9273

Parameter Estimates

Term	Estimate	Std Error	t Ratio	Prob>|t|
Intercept	8401.3522	1674.08	5.02	<.0001
Pile Wetted Depth (ft)	4.9222865	53.22753	0.09	0.9273

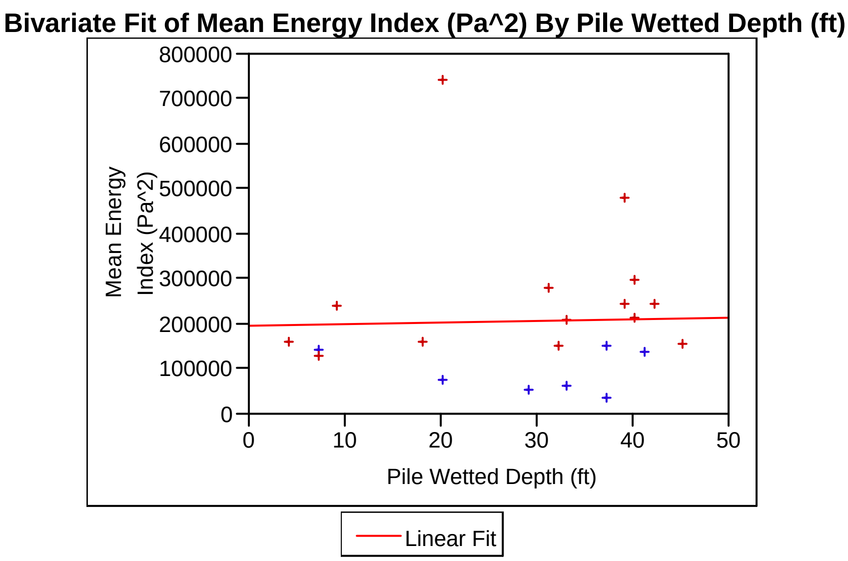

Figure 4.3. Fit of Mean Energy Index by Pile Wetted Depth. Batter pile data is shown in blue and plumb pile data in red.

Table 4.3. Statistical Summary for Fit of Mean Energy Index by Pile Wetted Depth

Linear Fit

Mean Energy Index (Pa^2) = 197547.86 + 359.63478 Pile Wetted Depth (ft)

Summary of Fit

RSquare	0.000901
RSquare Adj	-0.05168
Root Mean Square Error	161583.7
Mean of Response	207874.5
Observations (or Sum Wgts)	21

Analysis of Variance

Source	DF	Sum of Squares	Mean Square	F Ratio
Model	1	447284893	447284893	0.0171
Error	19	4.9608e+11	2.611e+10	Prob > F
C. Total	20	4.9652e+11		0.8972

Parameter Estimates

Term	Estimate	Std Error	t Ratio	Prob>|t|
Intercept	197547.86	86418.55	2.29	0.0339
Pile Wetted Depth (ft)	359.63478	2747.685	0.13	0.8972

4.1.2 Impulsive Sound Characteristics and Relationships between Metrics

Figure 4.4 shows the maximum positive, maximum negative, and maximum absolute pressures observed in each impulse acquired during underwater sound monitoring for all of the piles listed in Table 4.1. All of the observed maximum pressures are bounded at about ±20,000 Pa (~206 dB//μPa). In the majority of cases, it appears that the observed maximum negative pressure was the maximum absolute pressure observed during the impulses. The prevalence of the maximum pressure in an impulsive sound being a negative-going overpressure is the first of a series of differences that will be noted for the Hood Canal data set between sound generated by pile driving and that generated by explosives.

Two related sound impulse metrics are commonly used to describe features of impulse sound believed to present risk of injury to fish. These are sound exposure level, SEL, and sound pressure level, SPL. Both of these metrics are dimensionless units expressed in decibels. They are defined in Carlson et al. 2005 and elsewhere. SPL is the log transformed ratio of the absolute peak pressure of an impulse in Pa relative to a μPa. SEL is an index of the energy in an impulse calculated as the log transformed ratio of the sum of the pressure squared within 90% of the impulse and a μPa^2. The absolute peak pressure in a sound impulse is thought to present a risk of barotrauma to fish with the risk increasing in an unknown way with increasing absolute maximum over-pressure. The energy in an impulsive sound, which is proportional to the sum of the squared pressure in the impulse, is considered a risk to the hearing organs of fish.

Figure 4.5 below shows the results of a linear fit of SPL to SEL for all of the impulsive sound measurements with impulse duration ≤ 0.1 sec made during the Hood Canal construction in 2004. The statistics for the fit are given in Table 4.4. The fit explains about 85% of the variability in the SEL and SPL data. The fit shows that the 95% confidence limits for a predicted value of SPL given SEL would be about 6 dB. A range of 6 dB in SPL is equivalent to a doubling in pressure.

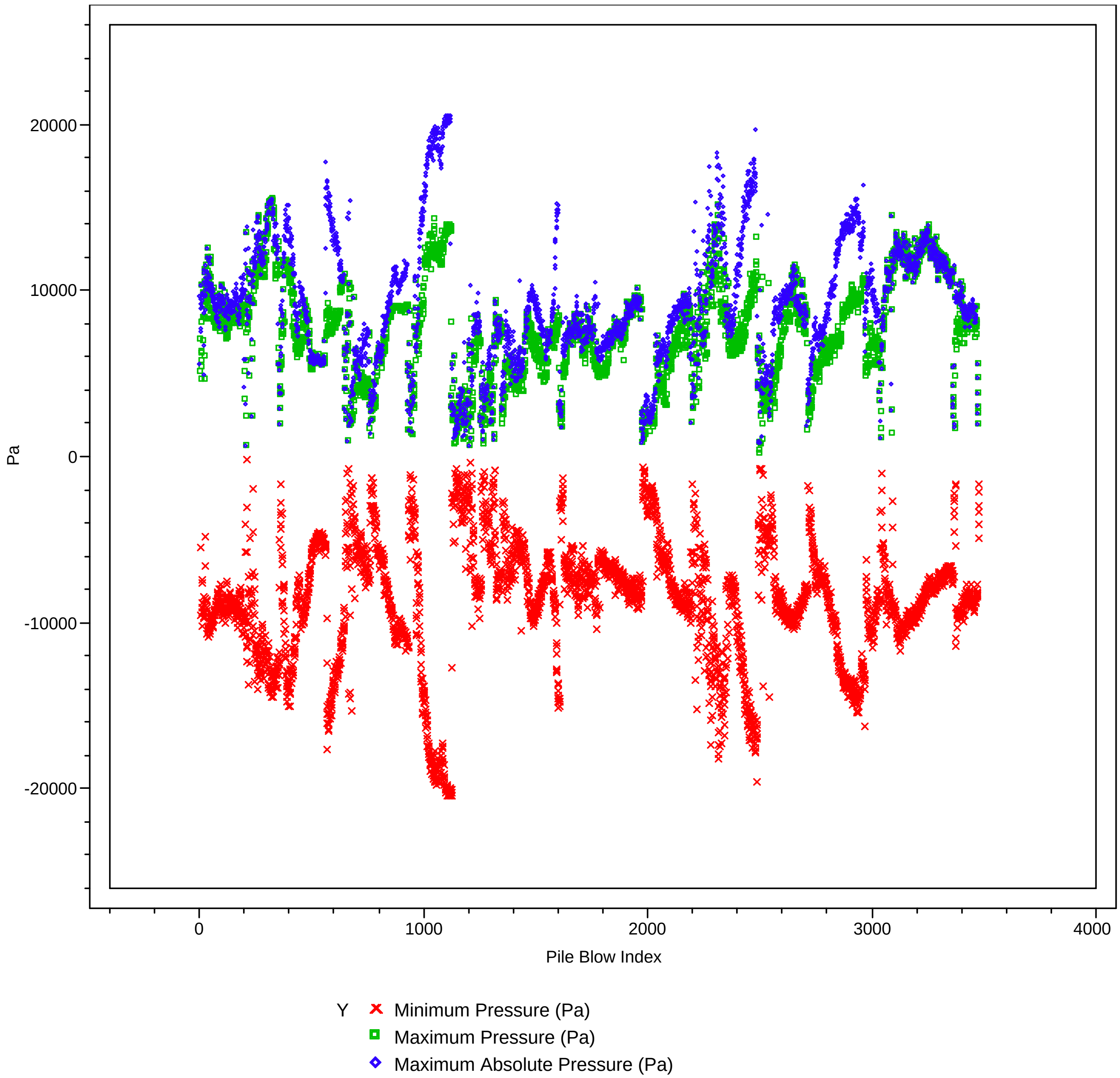

Figure 4.4. The Maximum Positive, Maximum Negative, and Maximum Absolute Sound Pressures Observed for each Impact during Driving of all of the Piles Listed in Table 4.1

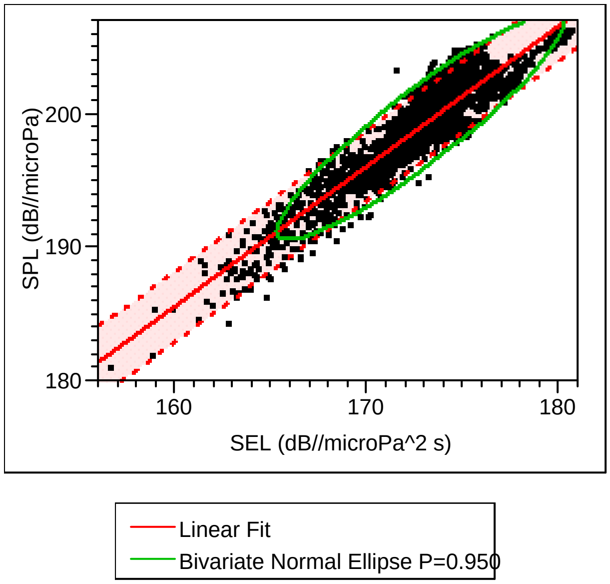

Figure 4.5. Linear Fit of SPL to SEL for all of the Impulsive Sounds Measured at the Hood Canal Project in 2004. The shaded area is the bound for the 95% confidence interval for estimates of specific SPL values given SEL.

Table 4.4. Statistical Summary for the Linear Fit of SPL to SEL

Linear Fit

SPL (dB//microPa) = 18.020879 + 1.0477982 SEL (dB//microPa^2 s)

Summary of Fit

RSquare	0.849472
RSquare Adj	0.849425
Root Mean Square Error	1.344508
Mean of Response	199.0553
Observations (or Sum Wgts)	3218

Analysis of Variance

Source	DF	Sum of Squares	Mean Square	F Ratio
Model	1	32807.679	32807.7	18148.84
Error	3216	5813.568	1.8	Prob > F
C. Total	3217	38621.247		0.0000

Parameter Estimates

Term	Estimate	Std Error	t Ratio	Prob>|t|
Intercept	18.020879	1.344015	13.41	<.0001
SEL (dB//microPa^2 s)	1.0477982	0.007778	134.72	0.0000

Correlation

Variable	Mean	Std Dev	Correlation	Signif. Prob	Number
SEL (dB//microPa^2 s)	172.776	3.047787	0.921668	0.0000	3218
SPL (dB//microPa)	199.0553	3.464875			

While SEL and SPL are 1 to 1 transformations of primary pressure data, their use can result in misunderstanding and misinterpretation of primary pressure data. The confidence limits on the regression in Figure 4.5 are a good example. Here the confidence limits are presented as a relatively narrow band around a highly significant fit to data. However, these limits, which extend over a doubling of peak pressure, are quite wide in terms of potential biological significance. For example, a doubling (or halving) in pressure would correspond to the volume of a fish's swim bladder being reduced by half or doubling in size, depending upon other details of the exposure situation. Such changes are potentially damaging to fish health, depending upon their absolute magnitudes relative to the static pressure at the location of the exposed fish.

Figure 4.6, a scatter plot of impulse maximum absolute pressure and the sum of the impulse squared pressure, is the same data as Figure 4.5 except it is not transformed. As you can see, while the data is still highly correlated, the relationship between the variables is no longer linear and the variability in the basic pressure data is clear.

The high correlation (Table 4.5) between peak pressure and energy in impulsive sounds is understandable because the peak pressure and portions of the sound signal immediately preceding and following the peak have pressure in proportion to the peak pressure.

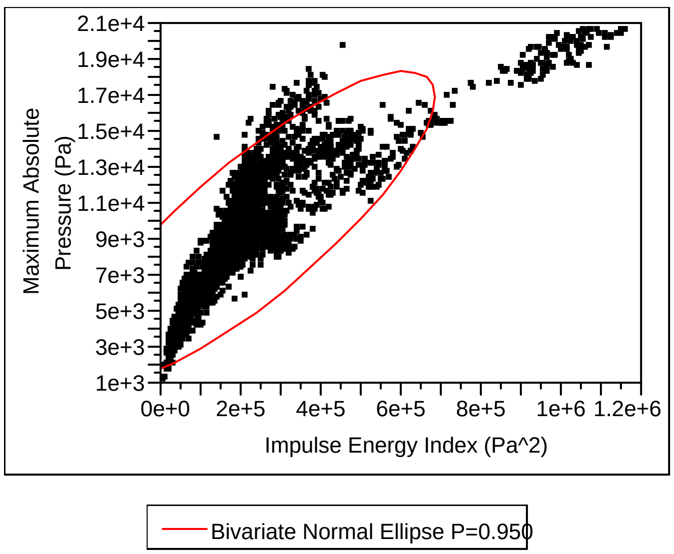

Figure 4.6. Bivariate Plot of Hood Canal Bridge Construction Absolute Maximum Pressure and Sum of Pressure Squared for all Sound Impulses with Duration ≤ 0.1 sec

Table 4.5. Correlation Statistics for Hood Canal Bridge Construction Absolute Maximum Pressure and Sum of Pressure Squared for all Sound Impulses with Duration ≤ 0.1 sec

Correlation

Variable	Mean	Std Dev	Correlation	Signif. Prob	Number
Impulse Energy Index (Pa^2)	238547	182587.3	0.837982	0.0000	3218
Maximum Absolute Pressure (Pa)	9646.118	3536.008			

Figures 4.7 and 4.8 show the probability distribution for SEL and the untransformed primary sum of squared pressure data for the Hood Canal Bridge construction sound impulse data for all monitored piles. While the untransformed data is skewed toward lower values, the transformed data is more normally distributed. This effect is also apparent in Figures 4.9 and 4.10, which show the cumulative frequency distributions for the two data sets.

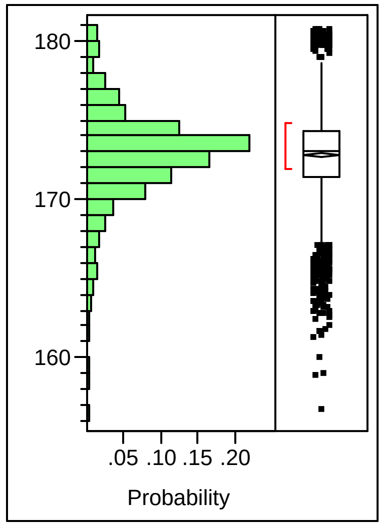

Figure 4.7. Distribution of SEL in dB//microPa²-s for all Hood Canal Bridge Construction Sound Impulse Observations with Duration less than 0.1 sec

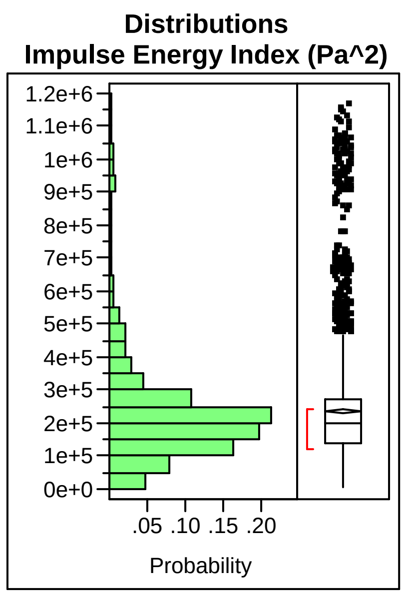

Figure 4.8. Distribution of the Sum of Pressure Squared in Pa² for all Hood Canal Bridge Construction Sound Impulse Observations with Duration less than 0.1 sec

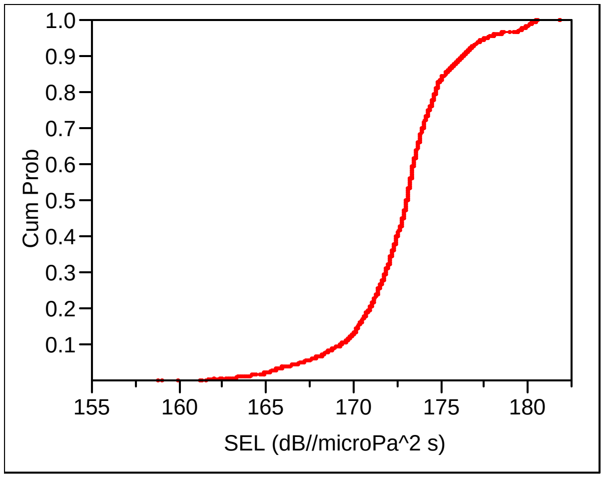

Figure 4.9. Cumulative Distribution of SEL for all Hood Canal Bridge Construction Sound Impulse Observations with Duration less than 0.1 sec

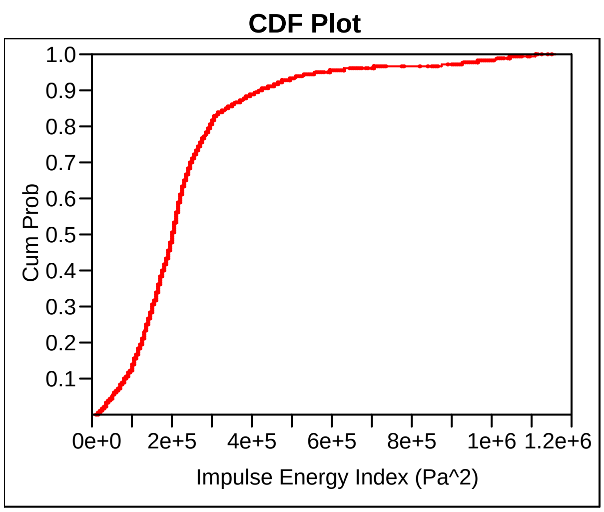

Figure 4.10. Cumulative Frequency Distribution of the Sum of Pressure Squared in Pa² for all Hood Canal Bridge Construction Sound Impulse Observations with Duration less than 0.1 sec

Tables 4.6 and 4.7 give the statistical moments for the two pressure data sets. The coefficients of variation for the transformed and untransformed data are 1.76% and 76.54% respectively.

The peak overpressure is one of the most important metrics for characterization of impulsive sound and has direct implications for the potential of the sound to injure fish. Descriptive information about log-transformed absolute peak pressure for each impulse observed during the Hood Canal Bridge construction is shown in the probability distribution of Figure 4.11, the statistical moments in Table 4.8, and the cumulative frequency distribution in Figure 4.12. The absolute peak data corresponding to the transformed data is shown in Figure 4.13, Table 4.9, and Figure 4.14 respectively. The coefficients of variation for the transformed and original data sets are 1.74% and 36.65% respectively.

Table 4.6. Statistical Moments for SEL in dB//microPa²-s for all Hood Canal Bridge Construction Sound Impulse Observations with Duration less than 0.1 sec

Moments	
Mean	172.77602
Std Dev	3.0477867
Std Err Mean	0.0537269
upper 95% Mean	172.88137
lower 95% Mean	172.67068
N	3218

Table 4.7. Statistical Moments for the Sum of Pressure Squared in Pa² for all Hood Canal Bridge Construction Sound Impulse Observations with Duration less than 0.1 sec

Moments	
Mean	238546.99
Std Dev	182587.26
Std Err Mean	3218.6774
upper 95% Mean	244857.85
lower 95% Mean	232236.12
N	3218

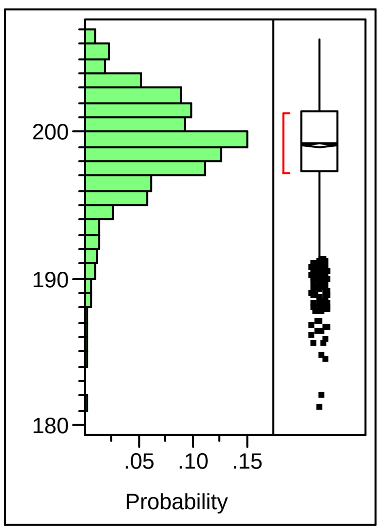

Figure 4.11. Distribution of SPL, the Log Transformed Absolute Peak Pressures, for all Hood Canal Bridge Construction Sound Impulse Observations with Duration less than 0.1 sec

Table 4.8. Statistical Moments for the SPL for all Hood Canal Bridge Construction Sound Impulse Observations with Duration less than 0.1 sec

Moments	
Mean	199.05529
Std Dev	3.4648754
Std Err Mean	0.0610794
upper 95% Mean	199.17505
lower 95% Mean	198.93553
N	3218

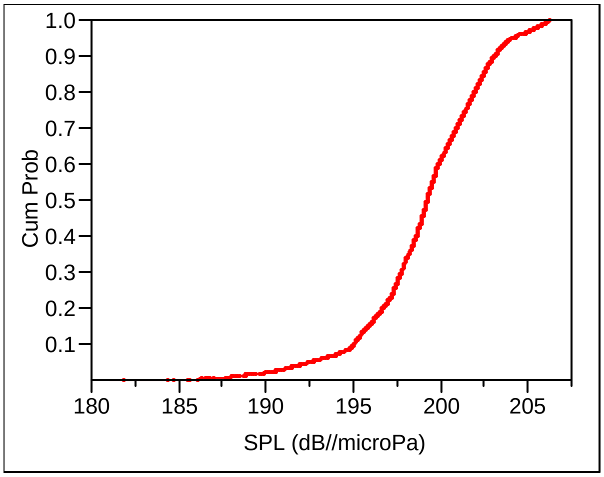

Figure 4.12. Cumulative Frequency Distribution of SPL for all Hood Canal Bridge Construction Sound Impulse Observations with Duration less than 0.1 sec

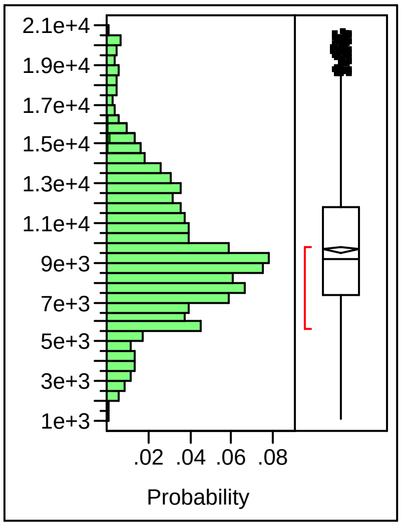

Figure 4.13. Distribution of Absolute Peak Pressure in Pa for all Hood Canal Bridge Construction Sound Impulse Observations with Duration less than 0.1 sec

Table 4.9. Statistical Moments for Absolute Peak Pressure in Pa for all Hood Canal Bridge Construction Sound Impulse Observations with Duration Less than 0.1 sec

Moments	
Mean	9646.1185
Std Dev	3536.0079
Std Err Mean	62.333312
upper 95% Mean	9768.3355
lower 95% Mean	9523.9015
N	3218

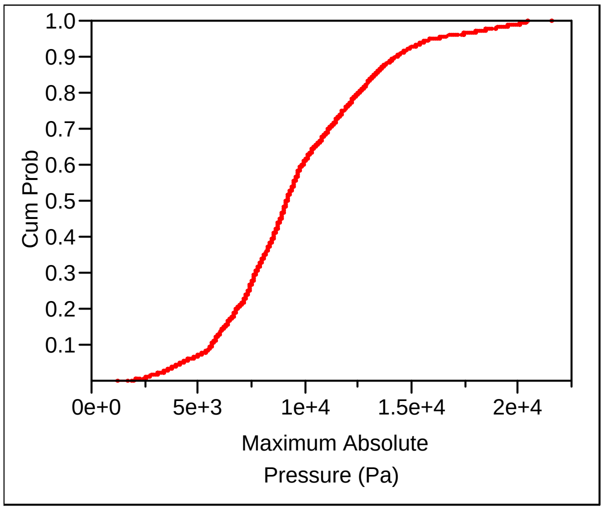

Figure 4.14. Cumulative Frequency Distribution of Absolute Peak Pressure in Pa for all Hood Canal Bridge Construction Sound Impulse Observations with Duration less than 0.1 sec

Assessment of the risk of injury that a sound impulse poses to a fish also considers the rise time, the time from the beginning of the impulse to the highest absolute pressure in the impulse. Unlike sound impulses generated by underwater explosions, the overpressure with the highest amplitude for a pile driving impact can be a negative pressure relative to the static pressure at the measurement depth. In the case of the Hood Canal Bridge construction impulsive sound data set, it was more likely that the peak overpressure would have been negative. In addition, again unlike sound impulses generated by explosions, the absolute peak pressure generated by pile driving may be one or more cycles into the impulse. This feature of pile driving impulsive sound can result in significant differences in rise times between impulses otherwise of equal duration and with equal peak pressure magnitude. There is evidence from experiments done with explosives that longer rise times, given equivalent peak pressures, pose less of a risk of injury to fish.

Figure 4.15 shows the fit of a line to impulse rise and impulse duration data for the Hood Canal Construction impulsive sound data set. It is clear from the plot in this figure as well as the statistical summary in Table 4.10 that very little of the variability in these data are explained by this linear fit. The data do show a tendency for the range of rise times to be fairly consistent to an impulse duration as long as 0.04 sec. Some significantly longer rise times are seen for impulse duration longer than 0.04 sec. Inspection of the waveforms for this data shows that the peak pressure can occur well within the impulse preceded by other pressure cycles with peak pressures that may only be slightly less in magnitude. Insufficient information is available at this time to direct the use of this data to factor barotrauma risk assessments that currently use peak pressure magnitude alone.

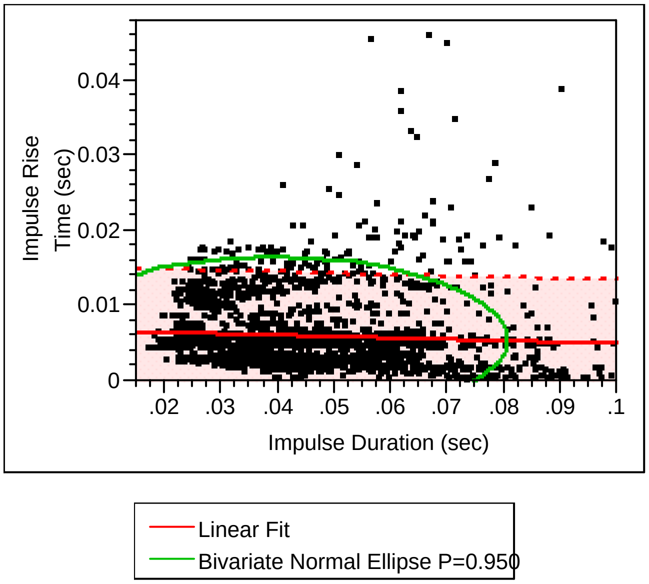

Figure 4.15. Linear Regression of Impulse Rise Time in sec on Impulse Duration in sec for all Impulsive Sounds Observed during the Hood Canal Bridge Construction

Table 4.10. Statistical Summary of Linear Regression of Impulse Rise Time in sec and Impulse Duration in sec for all Impulsive Sounds Observed during the Hood Canal Bridge Construction

Linear Fit

Impulse Rise Time (sec) = 0.0070103 - 0.0190474 Impulse Duration (sec)

Summary of Fit

RSquare	0.00502
RSquare Adj	0.004711
Root Mean Square Error	0.004257
Mean of Response	0.006214
Observations (or Sum Wgts)	3218

Analysis of Variance

Source	DF	Sum of Squares	Mean Square	F Ratio
Model	1	0.00029404	0.000294	16.2255
Error	3216	0.05827979	0.000018	Prob > F
C. Total	3217	0.05857382		<.0001

Parameter Estimates

Term	Estimate	Std Error	t Ratio	Prob>|t|
Intercept	0.0070103	0.000212	33.14	<.0001
Impulse Duration (sec)	-0.019047	0.004729	-4.03	<.0001

Correlation

Variable	Mean	Std Dev	Correlation	Signif. Prob	Number
Impulse Duration (sec)	0.041827	0.015872	-0.07085	<.0001	3218
Impulse Rise Time (sec)	0.006214	0.004267			

The probability distributions, statistical moments, and cumulative frequency distributions for the impulse duration and rise time for the Hood Canal Bridge construction data set are shown in Figures 4.16 and 4.17, Tables 4.11 and 4.12, and Figures 4.18 and 4.19 respectively.

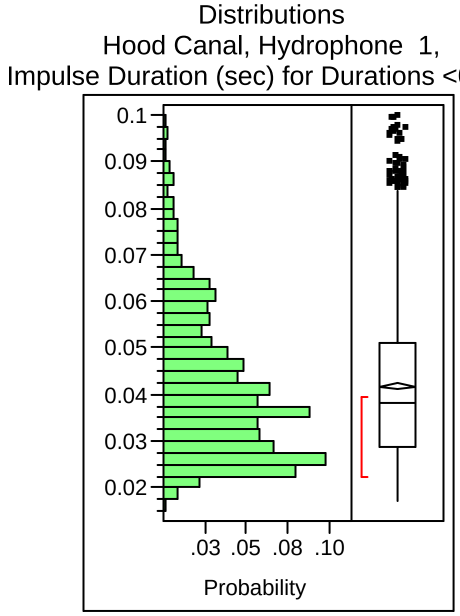

Figure 4.16. Probability Distribution of Impulse Duration for all of the Sound Impulses Observed during the Hood Canal Bridge Construction Project

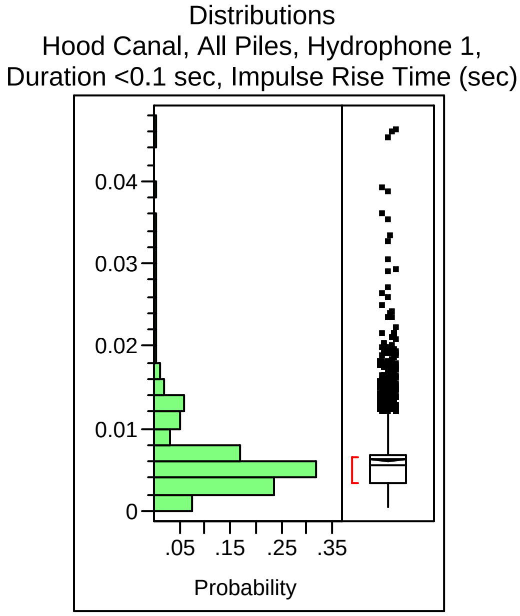

Figure 4.17. Probability Distribution of Impulse Rise Time for all of the Sound Impulses Observed during the Hood Canal Bridge Construction Project

Table 4.11. Statistical Moments for the Impulse Durations Observed during the Hood Canal Bridge Construction Project

Moments	
Mean	0.0418268
Std Dev	0.0158722
Std Err Mean	0.0002798
upper 95% Mean	0.0423754
lower 95% Mean	0.0412782
N	3218

Table 4.12. Statistical Moments for the Impulse Rise Times Observed during the Hood Canal Bridge Construction Project

Moments	
Mean	0.0062136
Std Dev	0.004267
Std Err Mean	7.522e-5
upper 95% Mean	0.0063611
lower 95% Mean	0.0060661
N	3218

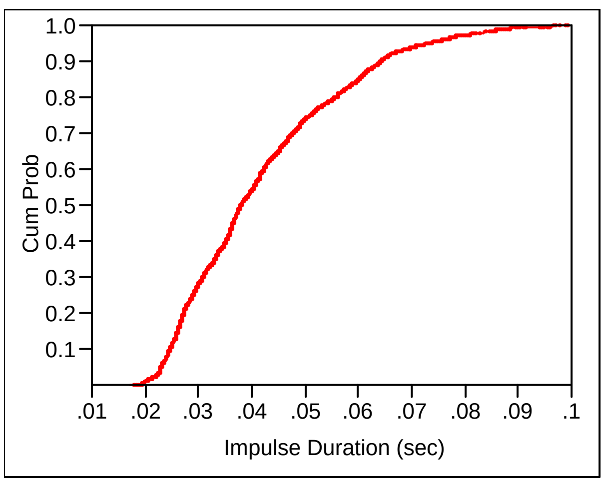

Figure 4.18. Cumulative Frequency Distribution for the Impulse Durations Observed during the Hood Canal Bridge Construction Project

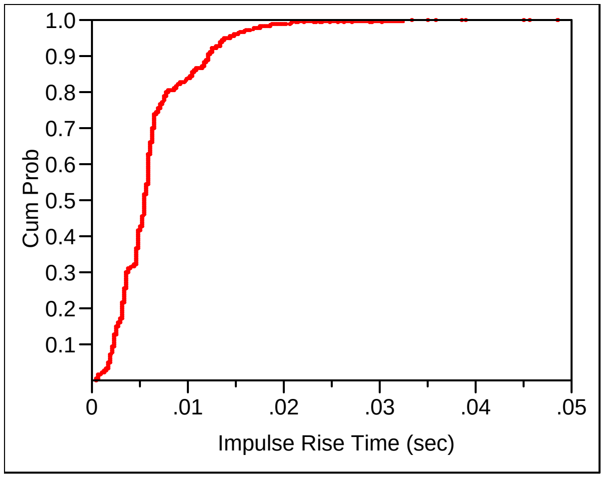

Figure 4.19. Cumulative Frequency Distribution for the Impulse Rise Times Observed during the Hood Canal Bridge Construction Project

4.1.3 Relationships between Pile Drive Method, Bubble Curtain Treatment, and Impulsive Sound Metrics and Variability

Both batter and plumb piles were driven at Hood Canal. In addition to the difference in drive method between these piles, they also differed in construction. Batter piles were steel shell piles 16" in diameter with a wall thickness of 0.5". Plumb piles were 24" in diameter with a wall thickness of 0.5". While not obvious in the summary statistics shown in Section 4.1.2, batter and plumb piles differed in the characteristics of sound they produced, although as shown in Section 4.1.1, the difference in wetted length was not a prominent factor in these differences.

In this section we will examine observed differences in impulsive sound generated by batter and plumb piles. We will focus on mean values of primary impulsive sound descriptive metrics and also on the variability in the data. In Section 3 we examined dynamic pile driving metrics for steel shell piles driven at Friday Harbor. We identified, presented, and discussed primary pile driving metrics obtained from dynamic pile driving data, and the variability in these metrics. In this section we will do the same for impulsive sound metrics obtained for steel shell piles at Hood Canal. In Section 5 we will compare these measures of variability to assess the likely contribution to variability in impulse sound by variability in the energy delivered to a pile by each impact hammer blow.

Figures 4.20 and 4.21 show the mean of maximum absolute peak pressures observed during the driving of Hood Canal piles and their associated standard deviations. These mean and standard deviation values are shown factored by pile drive method (batter or plumb) and bubble curtain treatment (confined, unconfined, or absent). The means show a trend of higher magnitude for plumb versus batter piles and, for plumb piles, higher magnitudes for piles driven without a bubble curtain. These trends, while somewhat less evident, are also shown in the standard deviation values.

An important question to ask is whether the differences in magnitude of sound generated are because of the pile drive method, the difference in the size of the piles, or other factors.

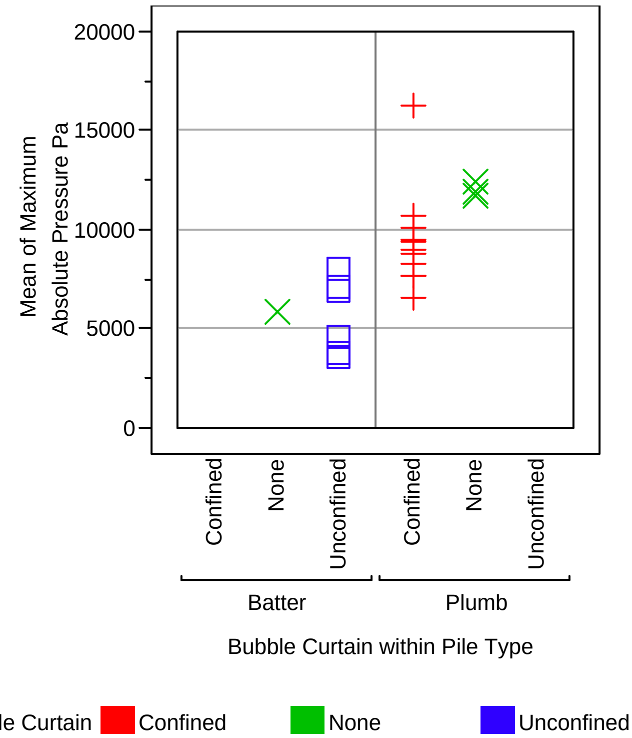

Figure 4.20. Mean Maximum Absolute Pressure for Monitored Piles by Drive Type and Bubble Curtain Type and Presence or Absence

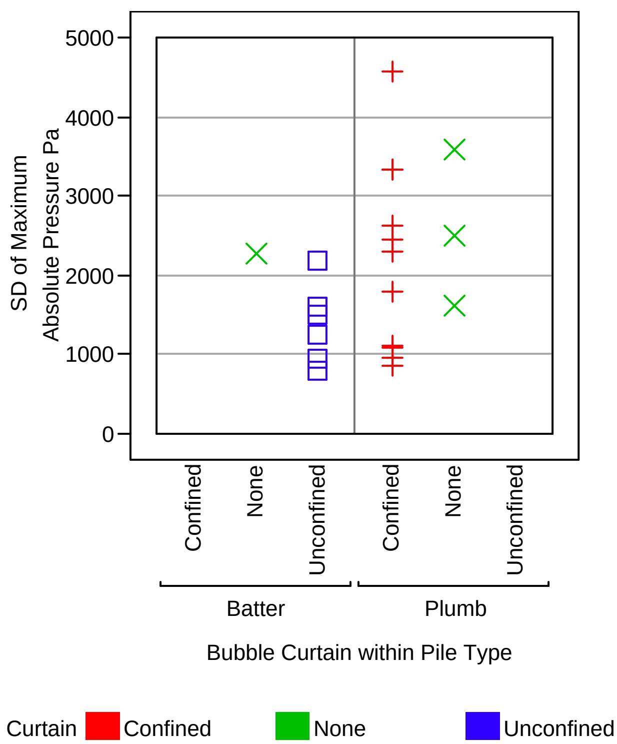

Figure 4.21. Standard Deviation of the Maximum Absolute Pressure for Monitored Piles by Drive Type and Bubble Curtain Type and Presence or Absence

The relationship between the means and standard deviations for the maximum absolute pressures generated for plumb and batter piles driven at Hood Canal was further considered. Figure 4.22 shows the results of a line fit between the means of maximum absolute pressures and associated standard deviations for Hood Canal piles. The data for batter piles is shown in blue and that for plumb piles is in green. The statistical summary for the fit is in Table 4.13. This analysis shows that the means and standard deviations for the summary peak pressure metrics for sound generated by driving batter and plumb piles at Hood Canal are positively correlated. This finding is very important because it means that the ratio of the standard deviation and the mean can be used to compare the variability between data that differs by driving method and pile diameter with that of other pile driving metrics presented in Section 3 for dynamic pile driving data.

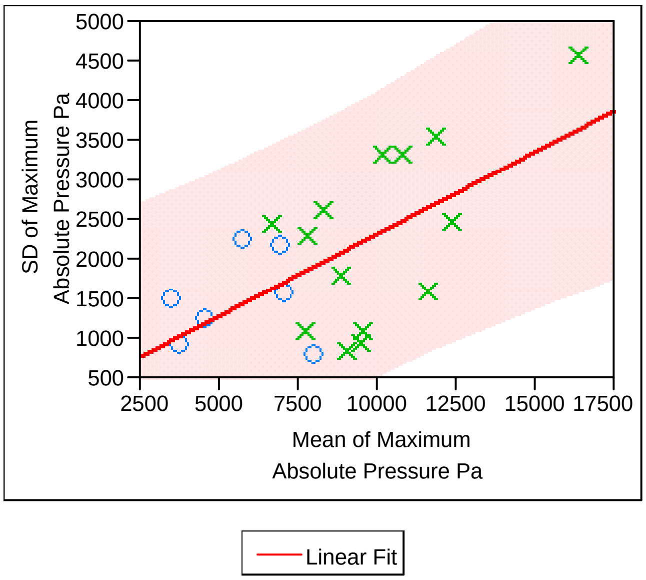

Figure 4.22. Linear Fit of Standard Deviations of Maximum Absolute Pressures to the Means of the Maximum Absolute Pressures for Impulsive Sound Observations made during Hood Canal Bridge Construction

The means and standard deviations of sound energy index for impulsive sound generated by driving piles at Hood Canal are shown in Figures 4.23 and 4.24 respectively. As was the case for maximum pressure, there is a trend in these data that indicate the mean energy in sound impulses was greater for plumb piles than for batter piles. In contrast to observations for mean maximum absolute pressure, the mean energy index for piles driven without a bubble curtain do not show a strong trend of being greater in magnitude than those driven with a bubble curtain. As was the case with the maximum pressure metric, the standard deviation of absolute pressure appears to be correlated with mean absolute pressure.

It is not immediately obvious why the mean energy index of impulsive sound for piles driven without a bubble curtain should be, in general, more or less equal in magnitude to the sound generated by piles driven with a bubble curtain. Possibilities might include factors such as impulse duration elongation caused by reflections between bubbles and the piles by sound before exiting the bubble curtain and propagating away from the pile. If such phenomena were a factor then bubble curtains, while effective at reducing the high frequency content of impulsive sound, would be much less effective at reducing impulsive sound energy.

Table 4.13. Statistics for the Fit of Standard Deviations of Maximum Absolute Pressures to the Means of the Maximum Absolute Pressures for Impulsive Sound Observations made during Hood Canal Bridge Construction

Linear Fit

SD of Maximum Absolute Pressure Pa = 250.45385 + 0.2074841 Mean of Maximum Absolute Pressure Pa

Summary of Fit

RSquare	0.374322
Rsquare Adj	0.341392
Root Mean Square Error	839.8501
Mean of Response	2022.927
Observations (or Sum Wgts)	21

Analysis of Variance

Source	DF	Sum of Squares	Mean Square	F Ratio
Model	1	8017746	8017746	11.3671
Error	19	13401617	705348	Prob > F
C. Total	20	21419363		0.0032

Parameter Estimates

Term	Estimate	Std Error	t Ratio	Prob>|t|
Intercept	250.45385	556.75	0.45	0.6579
Mean of Maximum Absolute Pressure Pa	0.2074841	0.06154	3.37	0.0032

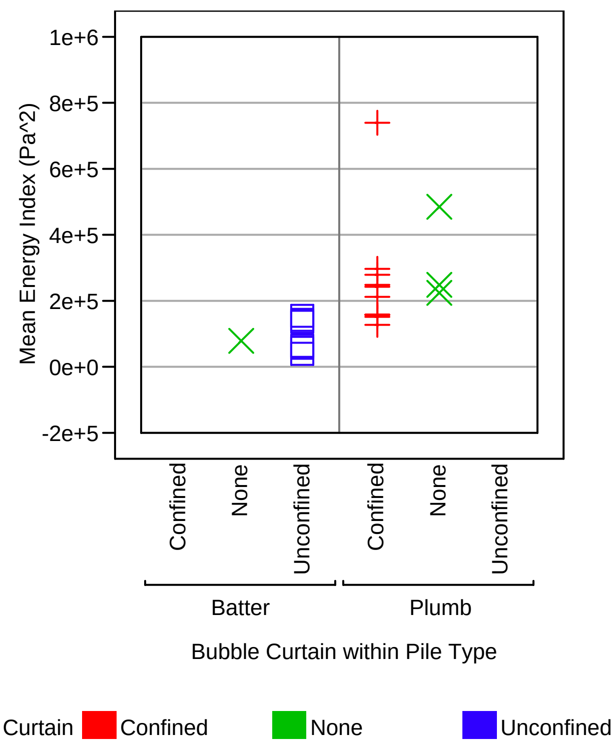

Figure 4.23. Mean Energy Indices for Monitored Piles Driven at Hood Canal by Drive Type and Bubble Curtain Type and Presence or Absence

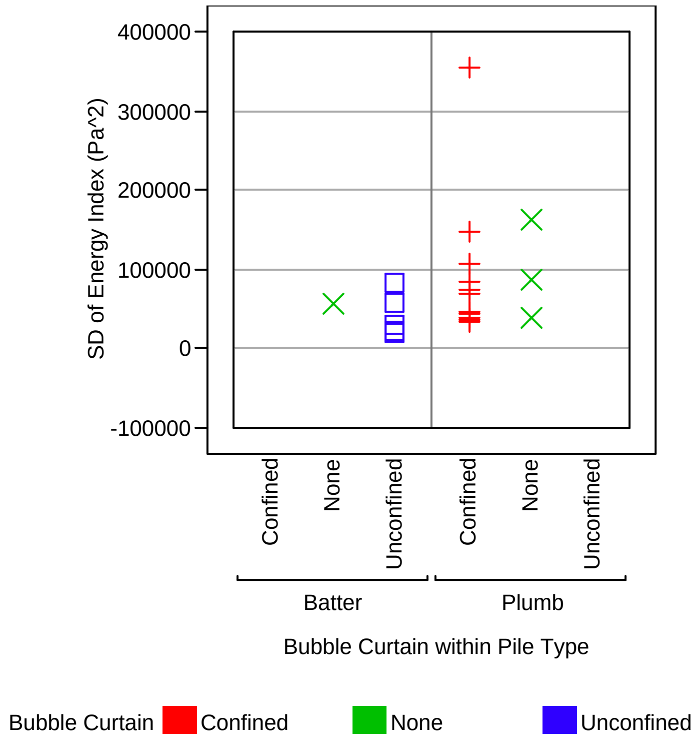

Figure 4.24. Energy Indices Standard Deviations for Monitored Piles Driven at Hood Canal by Drive Type and Bubble Curtain Type and Presence or Absence

Impulse duration has not been identified as an impulsive sound characteristic related to potential injury of fish. However, impulsive sound duration is an important metric helpful in understanding the effects of propagation on the features of sound impulses. Depending upon a number of environmental factors, the characteristics of a sound impulse are continuously modified as it propagates. Important are the loss of energy with distance from the sound source as the sound wave expands and the preferential attenuation of higher frequencies. In shallow water, it is possible for reflections from the bottom and surface to merge with the direct path sound signal and modify its characteristics in other ways. A common observation of modification of sound signals by multipath is elongation.

Figures 4.25 and 4.26 show the sound impulse mean duration and associated standard deviation for Hood Canal piles factored by drive method and bubble curtain treatment. There is an apparent trend for the duration of batter pile impulsive sound to be longer than that for plumb piles. There is no clear trend in impulse mean duration between batter and plumb piles driven without a bubble curtain. As is the case with other impulsive sound metrics, the sample standard deviations appear to be positively correlated with the sample means.

It is not clear why batter-driven piles would have durations that are generally longer than those for plumb-driven piles. It is possible that this results from the attitude of the pile relative to the surface and bottom and resulting reflections that would accentuate multipath effects on signal duration. Less probable are effects resulting from differences in pile diameter.

Also confusing is the trend for several plumb piles driven with a bubble curtain to have mean durations shorter than piles driven without a bubble curtain.

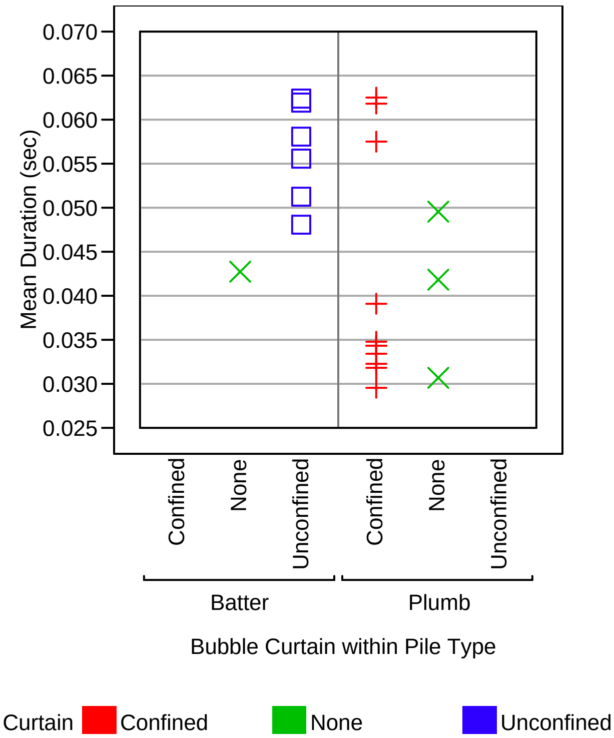

Figure 4.25. Mean Impulse Duration for Monitored Piles Driven at Hood Canal by Drive Type and Bubble Curtain Type and Presence or Absence

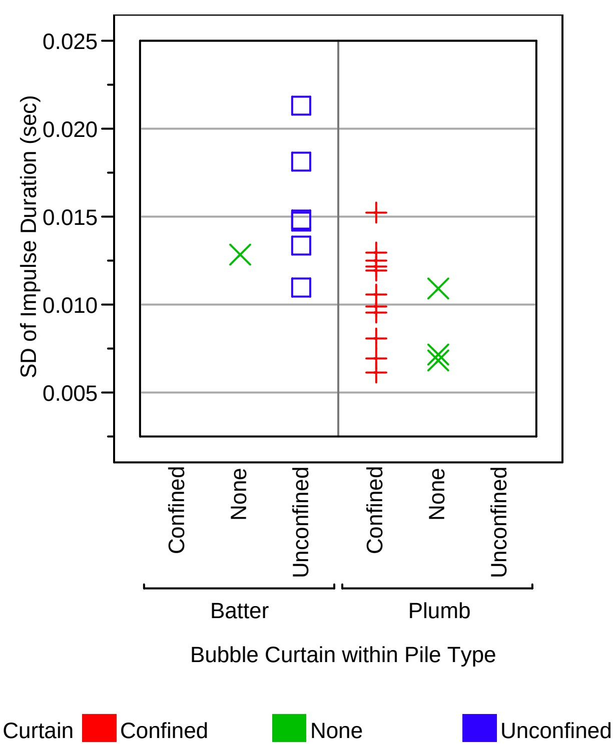

Figure 4.26. Impulse Duration Standard Deviations for Monitored Piles Driven at Hood Canal by Drive Type and Bubble Curtain Type and Presence or Absence

Impulse rise time is considered important for risk of injury to fish by impulsive sound. Faster rise times are thought to present more risk than slower rise time. The means and standard deviations in rise time for Hood Canal piles are shown in Figures 4.27 and 4.28. There is a trend for the rise time of impulsive sound generated by plumb piles driven with a bubble curtain to be shorter than the rise times for impulsive sound generated either by plumb piles driven without a bubble curtain or driven as batter piles. Data presented previously for impulsive sound peak pressure indicated that bubble curtains were effective in reducing peak pressure. It is not clear whether or not impulsive sound rise time is longer for bubble curtain-treated piles than for piles driven without a bubble curtain. There is insufficient data in our data set to answer this question.

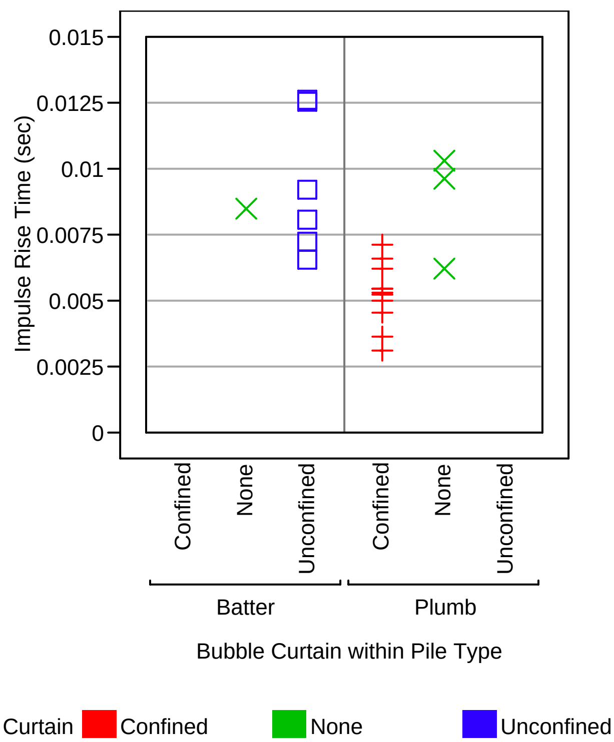

Figure 4.27. Mean Impulse Rise Time for Monitored Piles Driven at Hood Canal by Drive Type and Bubble Curtain Treatment

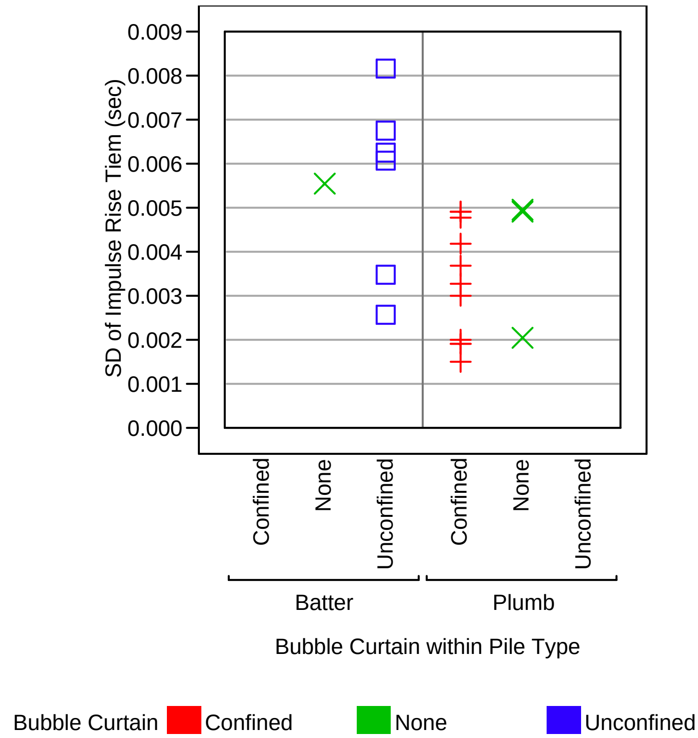

Figure 4.28. Impulse Rise Time Standard Deviations for Monitored Piles Driven at Hood Canal by Drive Type and Bubble Curtain Treatment

4.2 Findings from Hood Canal Impulsive Sound Data Review

- Wetted pile length does not appear to be a factor affecting impulsive sound peak pressure. This is most likely the result of the mechanics of sound production by a pile after it is struck with a hammer.
- The maximum absolute pressure observed for a sound impulse was as likely to result from a negative-going portion of the impulse overpressure as from a positive-going part of the signal.
- Impulse peak pressures were within a band bounded by 20KPa, which is equivalent to SPL values of 206 dB//µPa.
- The means and standard deviations for the samples of impulsive sounds resulting from driving of piles at Hood Canal are positively correlated.
- There is a strong linear relationship between SEL and SPL for the impulsive sounds observed at Hood Canal.
- The log transformation of primary pressure data tends to obscure features of the data, in particular the relationship between peak pressure and energy index and the inherent variability from blow to blow in the peak pressure and energy of generated impulsive sound.

- While still positively correlated, the relationship between maximum absolute pressure and energy index for impulsive sounds is not linear as is the case for the log-transformed versions of these impulsive sound metrics.
- A clear relationship between impulse duration and rise time is not apparent in the Hood Canal data. Impulse duration was considerably more variable than rise time.
- When factored by pile driving method and bubble curtain treatment, the following trends were observed in impulsive sound data:
    - The confined bubble curtains used for plumb piles appear more effective than the unconfined versions used for plumb piles.
    - Plumb pile impulsive sound showed a trend of higher peak pressures than that for batter piles. This may be the consequence of plumb piles being larger in diameter than batter piles; however, other factors may also contribute to the observed differences in peak pressures.
    - The mean energy indices of piles driven with and without bubble curtains appeared similar for both batter and plumb piles.
    - The mean energy indices of plumb piles tended to be higher than those for batter piles.
    - The means and standard deviations for energy indices appeared to be positively correlated.
    - The durations of sound impulses tended to be longer for batter piles than for plumb piles. Bubble curtain treatment did not appear to be a strong factor affecting impulse duration.
    - Impulse duration means and standard deviations appeared to be positively correlated.
    - The rise time of sound impulses tended to be shorter for plumb piles with bubble curtains than for plumb piles without bubble curtains or for batter piles with or without bubble curtains.
    - The means and standard deviations for impulse rise times appear to be positively correlated.

5.0 Comparison of Friday Harbor Dynamic Pile Driving and Hood Canal Impulsive Sound Data

5.1 Comparison of the Diesel Impact Hammers Used at Hood Canal and Friday Harbor

Diesel hammers were used at both Friday Harbor and Hood Canal. The hammer used at Hood Canal was an ICE Model 120S manufactured by International Construction Equipment, Inc. That used at Friday Harbor was an APE Model D46032 manufactured by APE Holland. These hammers are very similar in design and function. The function of the hammers can be evaluated by comparing their rated blows-per-minute, hammer stroke, and energy. Figure 5.1 compares the ram stroke length for the two hammers as a function of operating duty cycle in blows per minute. Figure 5.2 compares their hammer energy as a function of duty cycle. Finally, Figure 5.3 compares their hammer energy as a function of stroke. The data used for this comparison is in Appendix B.

The two hammers are very similar in performance as well as design. The range of hammer stroke used at Friday Harbor is shown in Table 5.1. The overall stroke range was narrow, between 6.2 and 9.2 ft. The performance of the two hammers, while very similar, diverges as hammer stroke increases with the ICE 120S used at Friday Harbor having increasingly larger energy per unit of stroke than the APE D46-32 used at Hood Canal. We assume for purposes of this analysis that these two hammers are functionally equivalent.

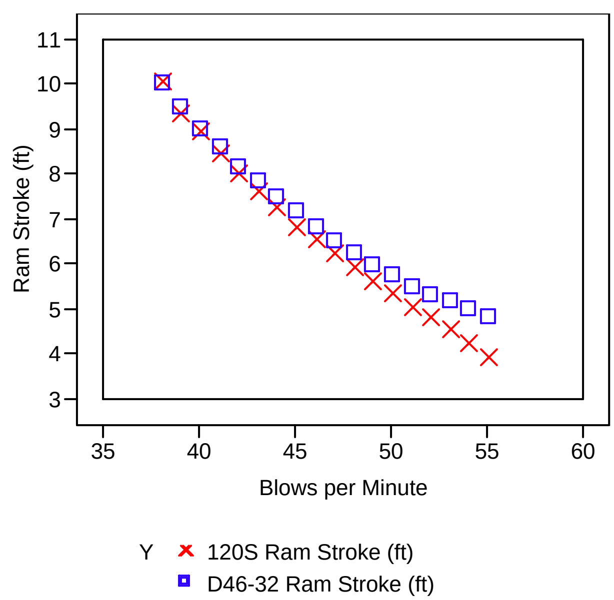

Figure 5.1. Hammer Performance in Terms of Ram Stroke as a Function of Blows per Minute for Diesel Hammers ICE 120S and APE D46-32

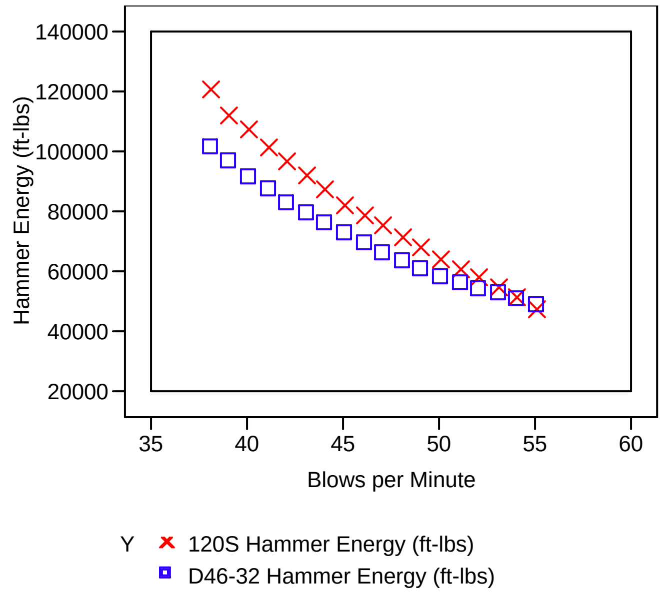

Figure 5.2. Hammer Performance in Terms of Hammer Energy as a Function of Blows per Minute for Diesel Hammers ICE 120S and APE D46-32

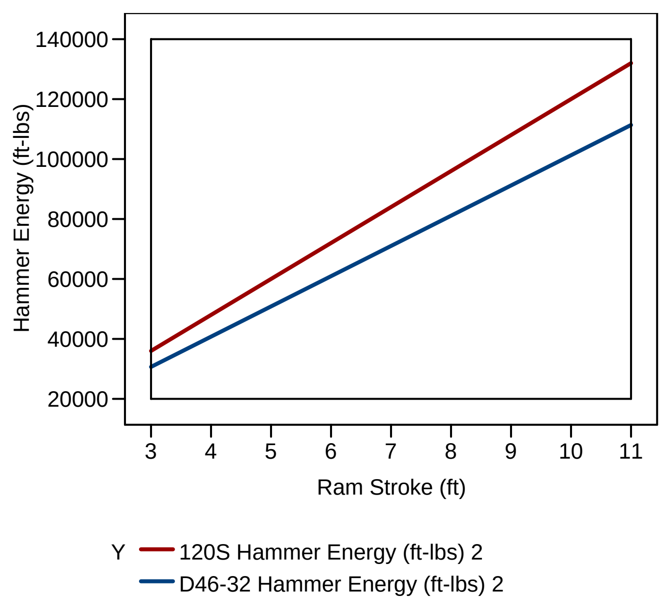

Figure 5.3. Comparison of the Hammer Energy as a Function of Ram Stroke for the ICE 12S Diesel Hammer Used at Hood Canal and the APE D46-32 Used at Friday Harbor

Table 5.1. Minimum and Maximum Hammer Stroke Used at Friday Harbor to Drive Piles 7, 8, 21, and 16 Using an ICE 12S Diesel Impact Hammer

Friday Harbor Dynamic Pile Testing Hammer Stroke for ICE 120S Diesel Impact Hammer by Pile		
	Min	Max
Pile 7 Average Hammer Stroke (ft)	7.02	8.85
Pile 8 Average Hammer Stroke (ft)	6.93	9.22
Pile 21 Average Hammer Stroke (ft)	6.21	7.88
Pile 16 Average Hammer Stroke (ft)	6.95	8.98

5.2 Comparison of Dynamic Pile Driving and Impulsive Sound

In this section we identify measures made during dynamic pile driving that explain some of the variability observed in impulsive underwater sound generated by the pile driving activity. We identified dynamic pile driving and impulsive sound data sets that were available for analysis. These data sets were obtained during WSDOT construction projects using similar hammers and hammer operation methods. The main disadvantage of these data sets is that they were not acquired concurrently.

We addressed the issue of the data sets not being acquired concurrently by carefully examining the data to ensure that the construction materials and methods used for the two projects were not significantly different, and that the resulting data were representative of WSDOT near-shore marine construction projects. In addition, and most important, we identified a statistical measure that permits comparison of the variability in data sets differing in other respects. This measure is ratio of a sample's standard deviation divided by its mean expressed as a percentage. It is called the sample's coefficient of variation (CV).

The Hood Canal Bridge and Friday Harbor dynamic pile driving and impulsive sound data sets were presented and reviewed in the previous section. The Hood Canal impulse sound data, while having the desirable characteristic of no variation in the operation of a bubble curtain during driving of a pile, still differed in that two sizes of steel-shelled pile were used, 16" diameter for batter piles and 24" diameter for plumb piles. There were other differences as well. The design and operation of bubble curtains differed between batter and plumb piles, and some piles were driven without a bubble curtain. There were also differences in the depth of water when the piles were driven. The impulsive sound data set was analyzed to explore the effect of these differences on the principal impulse sound characteristics of absolute pressure, energy index, rise time, and impulse duration.

In the first of the two following sections, we will compare the coefficient of variations for impulsive sound signals with those for hammer stroke and transferred energy to estimate the contribution to impulsive sound variability resulting from hammer operations. In the second section, we will compare cumulative impulsive sound energy and transferred hammer energy data to show another connection between the mechanics of pile driving and resulting impulsive sound.

5.2.1 Comparison of the Coefficient of Variations for Impulse Sound, Impact Hammer Operation, and Hammer Transferred Energy

The coefficients of variation for impulsive sound observed at Hood Canal factored by pile drive method and bubble curtain treatment are shown in Figure 5.4. There are no clear trends in the coefficients by factor, which is expected given the positive correlation between the mean and standard deviation of impulsive sound samples.

The distribution of impulsive sound coefficients of variation are shown in Figure 5.5 and the descriptive statistics for the coefficients are given in Table 5.2. The coefficients for the absolute peak pressures observed for Hood Canal piles have a mean of 24.7 and a standard deviation of 10.2.

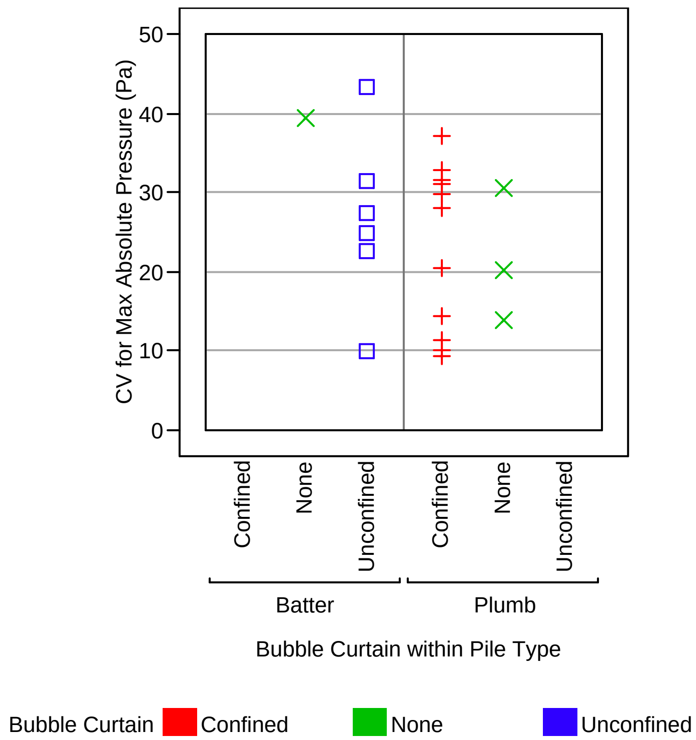

Figure 5.4. Coefficient of Variations for Impulsive Sound Maximum Absolute Pressure Observations Made during Hood Canal Bridge Construction by Pile Installation Method and Bubble Curtain Treatment

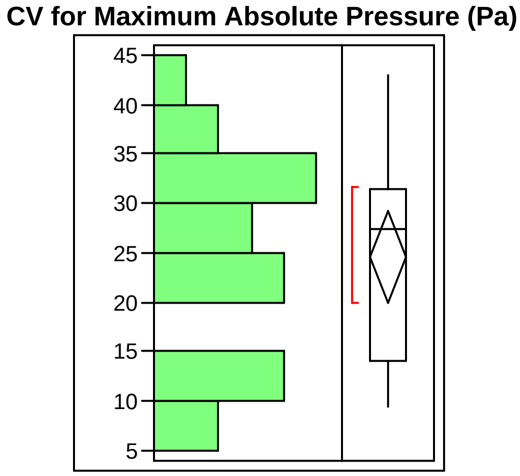

Figure 5.5. Distribution of Coefficients of Variations for Hood Canal Bridge Piles

Table 5.2. Descriptive Statistics for Coefficients of Variations for Hood Canal Bridge Piles

Moments	
Mean	24.676561
Std Dev	10.215631
Std Err Mean	2.2292334
upper 95% Mean	29.32666
lower 95% Mean	20.026461
N	21

The coefficients of variation for hammer stroke and transferred energy obtained from dynamic pile driving measurements are shown in Figure 5.6. The distributions and statistical summaries for these two data sets are given in Figures 5.7 and 5.8, and Tables 5.3 and 5.4. It is clear from Figure 5.14 that the coefficients of variation for energy and stroke are closer for the larger 30” diameter piles 21 and 16 than for the 24” diameter piles. This is most likely the result of the dramatic change in the relationship between hammer stroke and transferred energy for piles 7 and 8 when they approached their set depth (see Figure 3.26). For this reason, the transferred energy coefficient of variations for these piles will be compared with the coefficients of variation for peak pressures observed for impulsive sound at Hood Canal.

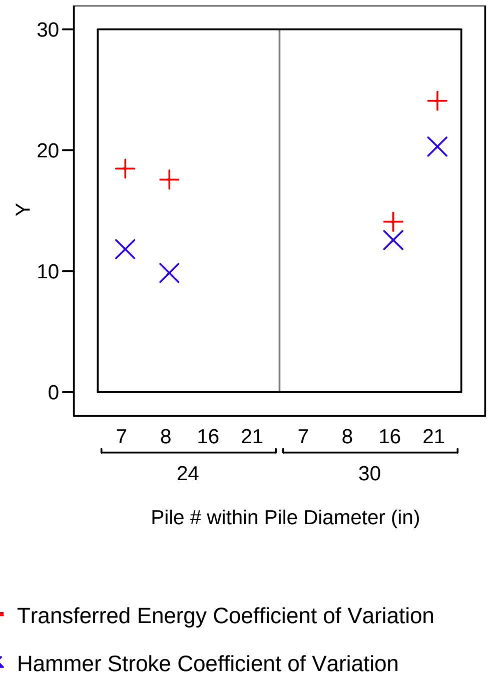

Figure 5.6. Coefficient of Variation of Dynamic Pile Driving Transferred Energy and Hammer Stroke Observations Made during Friday Harbor Ferry Terminal Construction by Pile Diameter

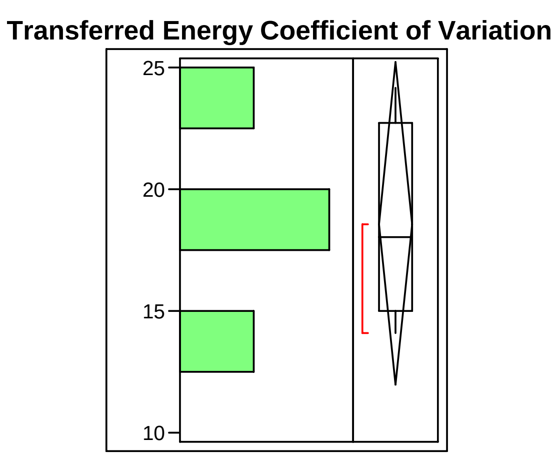

Figure 5.7. Distribution of Coefficients of Variation Transferred Energy Observations Made during Friday Harbor Ferry Terminal Construction

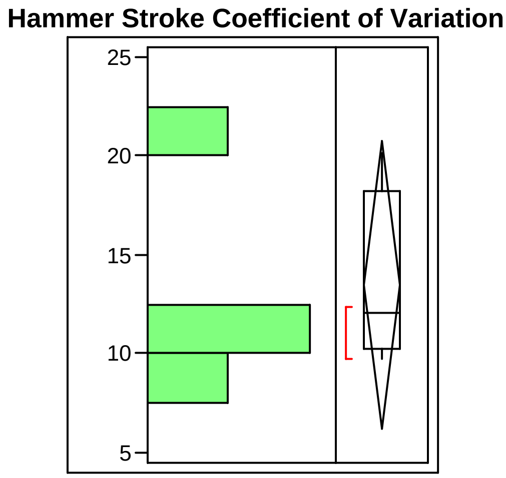

Figure 5.8. Distribution of Coefficients of Variation of Hammer Stroke Observations Made during Friday Harbor Ferry Terminal Construction

Table 5.3. Summary Statistics for Coefficients of Variation of Transferred Energy Observations Made during Friday Harbor Ferry Terminal Construction

Moments	
Mean	18.58648
Std Dev	4.1691643
Std Err Mean	2.0845821
upper 95% Mean	25.220551
lower 95% Mean	11.952409
N	4

Table 5.4. Summary Statistics for Coefficients of Variation of Hammer Stroke Observations Made during Friday Harbor Ferry Terminal Construction

Moments	
Mean	13.487711
Std Dev	4.5903317
Std Err Mean	2.2951658
upper 95% Mean	20.791953
lower 95% Mean	6.1834691
N	4

The means and standard deviations for the coefficients of variation for peak pressures observed for impulsive sound and those observed for transferred energy from dynamic pile driving measurements are given in Table 5.5.

Table 5.5. Comparison of Summary Statistics for Coefficients of Variation of Impulsive Sound Peak Pressure and Dynamic Pile Driving Hammer Stroke Observations Made during Friday Harbor Ferry Terminal and Hood Canal Bridge Construction

Statistic	Summary Statistics for Coefficients of Variation for Samples of Impulsive Sound Peak Pressure Observations	Summary Statistics for Coefficients of Variation for Samples of Transferred Energy from Dynamic Pile Driving Measurements
Mean	24.7	18.6
Standard Deviation	10.2	4.2

The coefficients of variation for impulsive sound peak pressure metrics are similar in magnitude to those observed for energy transfer metrics obtained from dynamic pile driving data. The analysis of dynamic pile driving data discussed in Section 3 showed that maximum transferred energy is linearly related to hammer stroke and thereby to the total energy incident on a pile. It has been assumed for some time that the amount and characteristics of sound generated by a struck pile are related to hammer design and operation. We conclude from our analysis that most of the variability in impulsive sound characteristics, particularly peak pressure, can be explained by variability in hammer operation. We also conclude that variability in hammer operation is in response to changes in resistance to penetration by the pile as a result of change in substrate and other factors. This logic leads to the hypothesis that, for a particular pile, it is not the nature of the substrate that a pile encounters that determines the characteristics of sound produced but the response of the hammer operator to these changes.

5.2.2 Comparison of Sound Energy Produced and Hammer Energy Transferred during Incremental Increases in Pile Drive Depth

Another metric believed to be important for assessing the risk to the health of fish of impulsive sound is sound energy. Two impulsive sound energy statistics are commonly computed. Most frequently what is actually computed is an index of the energy produced because the computed metric is based on pressure measurements alone. The two statistics computed are the energy in each impulsive sound and the sum of the energy in all impulsive sounds generated during driving of a pile. Of course, the total energy in the sound field is not computed, only that observed at a point location in the sound field.

There is an energy metric important for assessment of the efficiency of pile driving operations. This metric is the amount of energy transferred into a pile following impact from a hammer. It is computed from measurements of the acceleration of a pile at impact. These estimates of energy transferred to a pile can be summed for all hammer blows required to drive a pile.

For both energy metrics, the amount of energy produced as sound (as indexed at a monitoring location) and that transferred from an impact hammer during an incremental increase in pile drive depth can be estimated from impulsive sound and transferred energy data.

Figures 5.9 and 5.10 show the cumulative energy index in Pa^2 and SEL for all Hood Canal piles. The effect of the log transformation of primary pressure data is clear when the figures are compared. The cumulative SEL metric is currently receiving attention as a measure of the total energy exposure a fish may experience during driving of a pile.

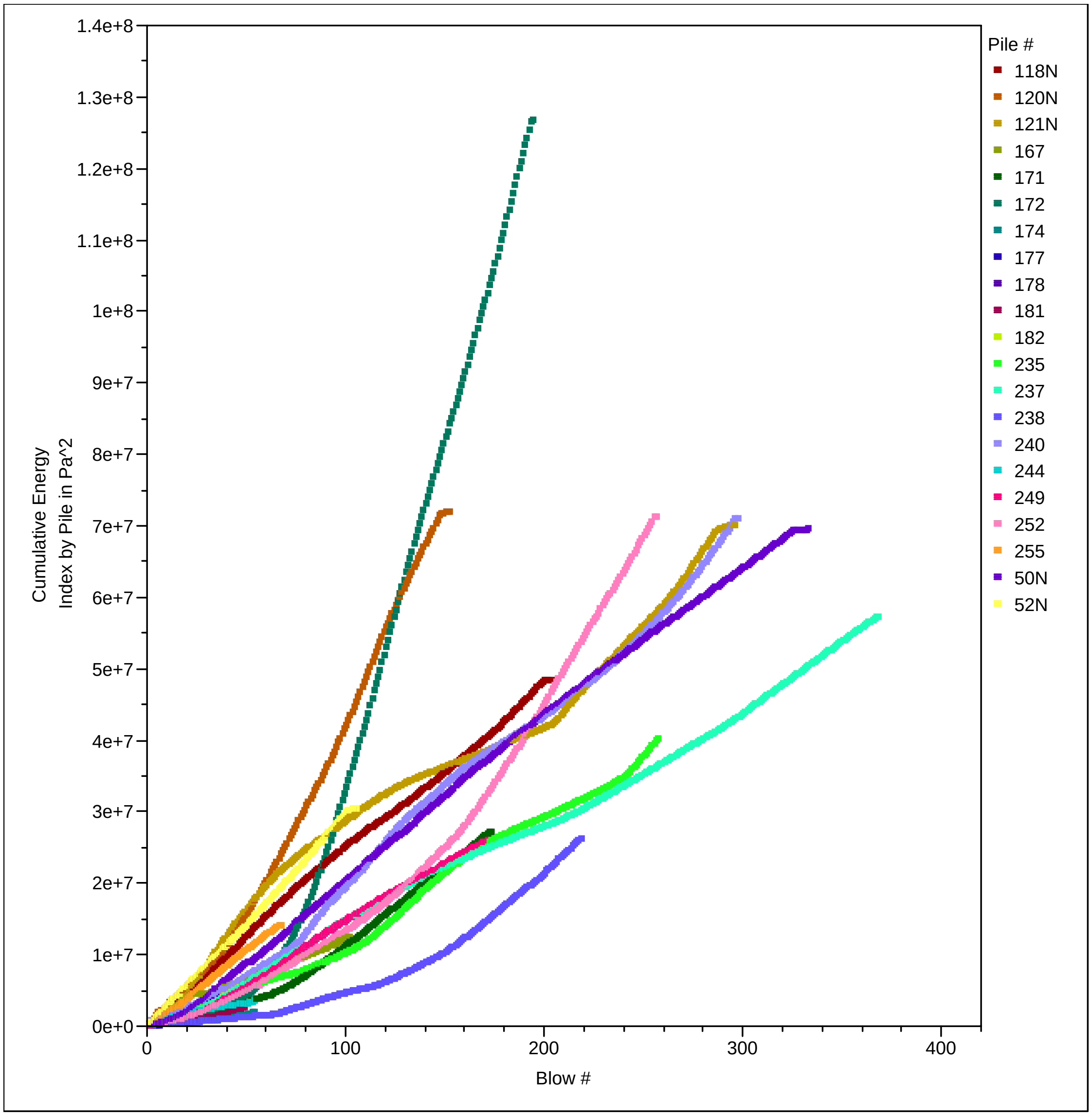

Figure 5.9. Cumulative Energy Index in Pa² for all Hood Canal Piles

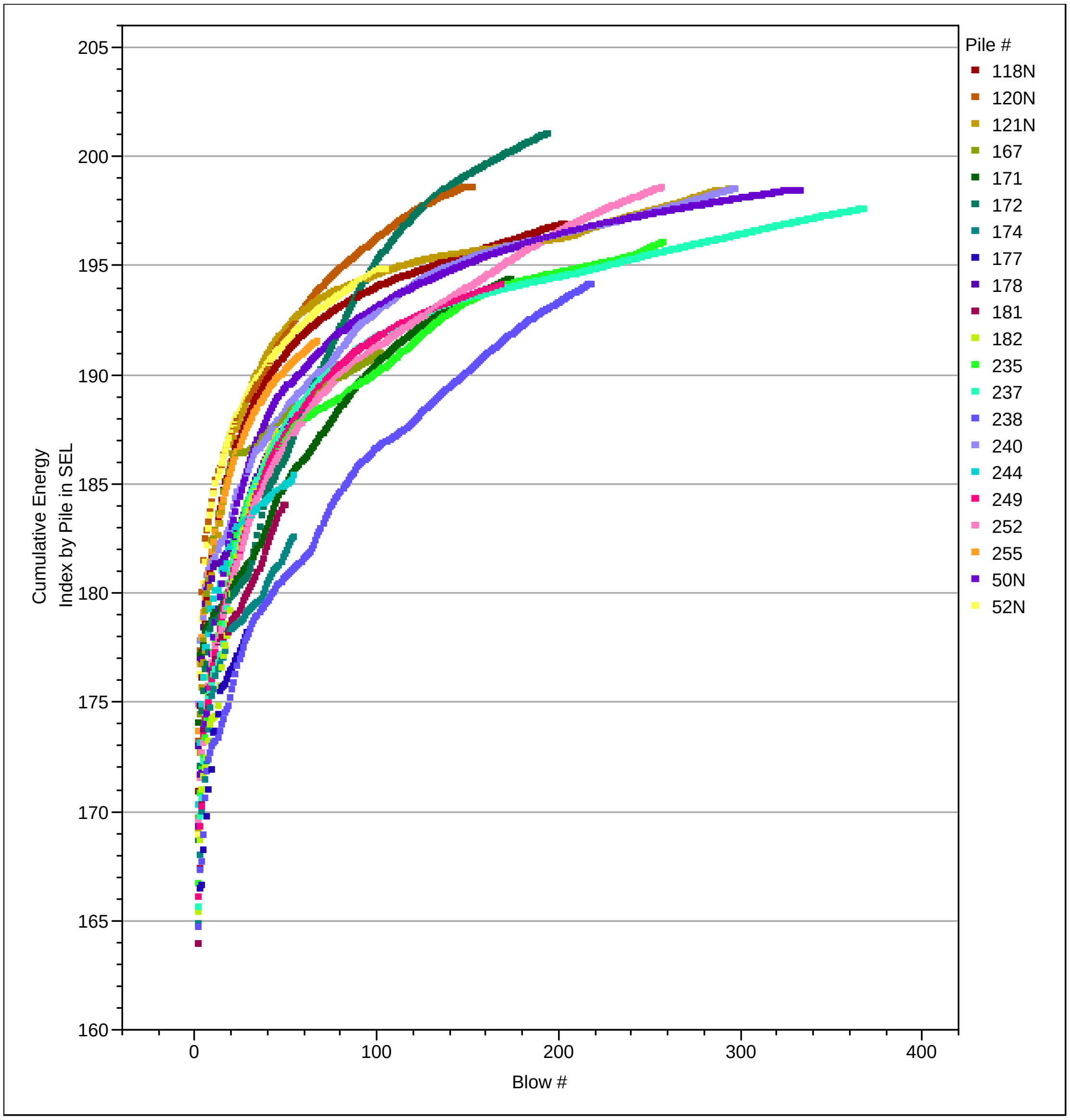

Figure 5.10. Cumulative Energy Index in SEL for all Hood Canal Piles

The cumulative energy data in Pa² for each pile shown in Figure 5.9 were fit with linear models. In most cases, the fit was quite good (see Appendix B). The cumulative transferred energy dynamic pile driving data were also fit to linear models. The last data point for both piles 7 and 8 were excluded from the fit because they were clearly different from the other data points in the cumulative series (Figure 5.11).

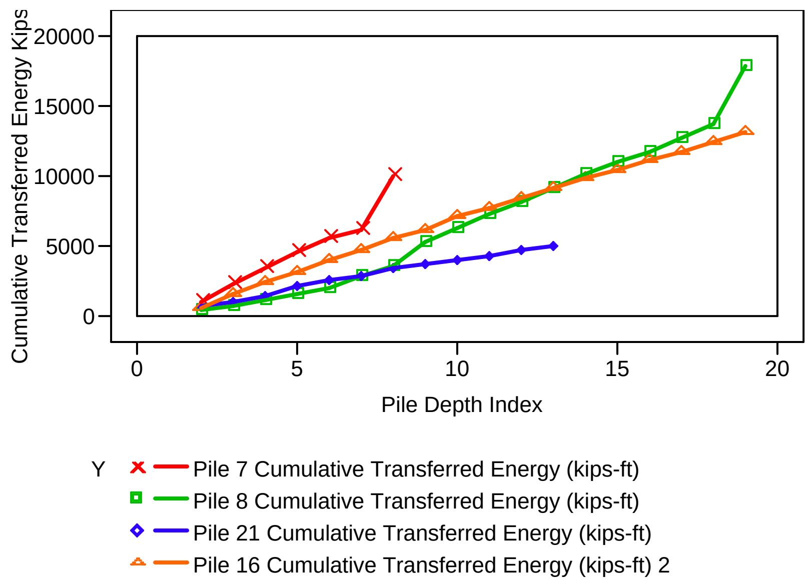

Figure 5.11. Cumulative Energy Transferred to each Pile over the Course of Driving the Pile to its Set Depth

The linear equations resulting from fitting the sound impulse cumulative energy data and the cumulative transferred energy dynamic pile driving data were used to predict the cumulative sound energy for all Hood Canal piles and transferred energy for Friday Harbor piles over a depth index range of 75 to 200. The predicted cumulative data series for each pile was then normalized by dividing the values in each series by the maximum value in the series. The normalization resulted in the line for each pile passing through 1. The results of these data manipulations are shown in Figures 5.12 and 5.13. The legend for these figures is shown as a separate figure, Figure 5.14. Figure 5.13 shows a portion of Figure 5.12 to permit viewing of more detail.

The curves of Figures 5.12 and 5.13 show the normalized incremental sound energy and transferred hammer energy that result from and are required for (respectively) an incremental increase in pile depth. The outcome of the analysis is logical: the steeper the slope, the more energy either created per unit of depth (hammer blow count may be substituted for the depth) or transferred to the pile; the smaller the pile, the less energy that must be transferred to achieve a unit increase in depth and the less sound energy created per incremental increase in depth.

The close agreement in slope between the 24” pile dynamic pile driving data and the 24” plumb pile sound impulse data is particularly interesting. Several of the 24” plumb piles driven at Hood Canal have a sound energy production slope that is quite similar to the transferred energy slope for the 24” plumb piles driven at Friday Harbor.

We conclude from this data that the cumulative sound energy produced during driving of a steel shell pile over the range of 16” to 30” in diameter is a function of the pile diameter and is directly related to the stroke of the hammer used to drive the pile and thereby the energy transferred into the pile.

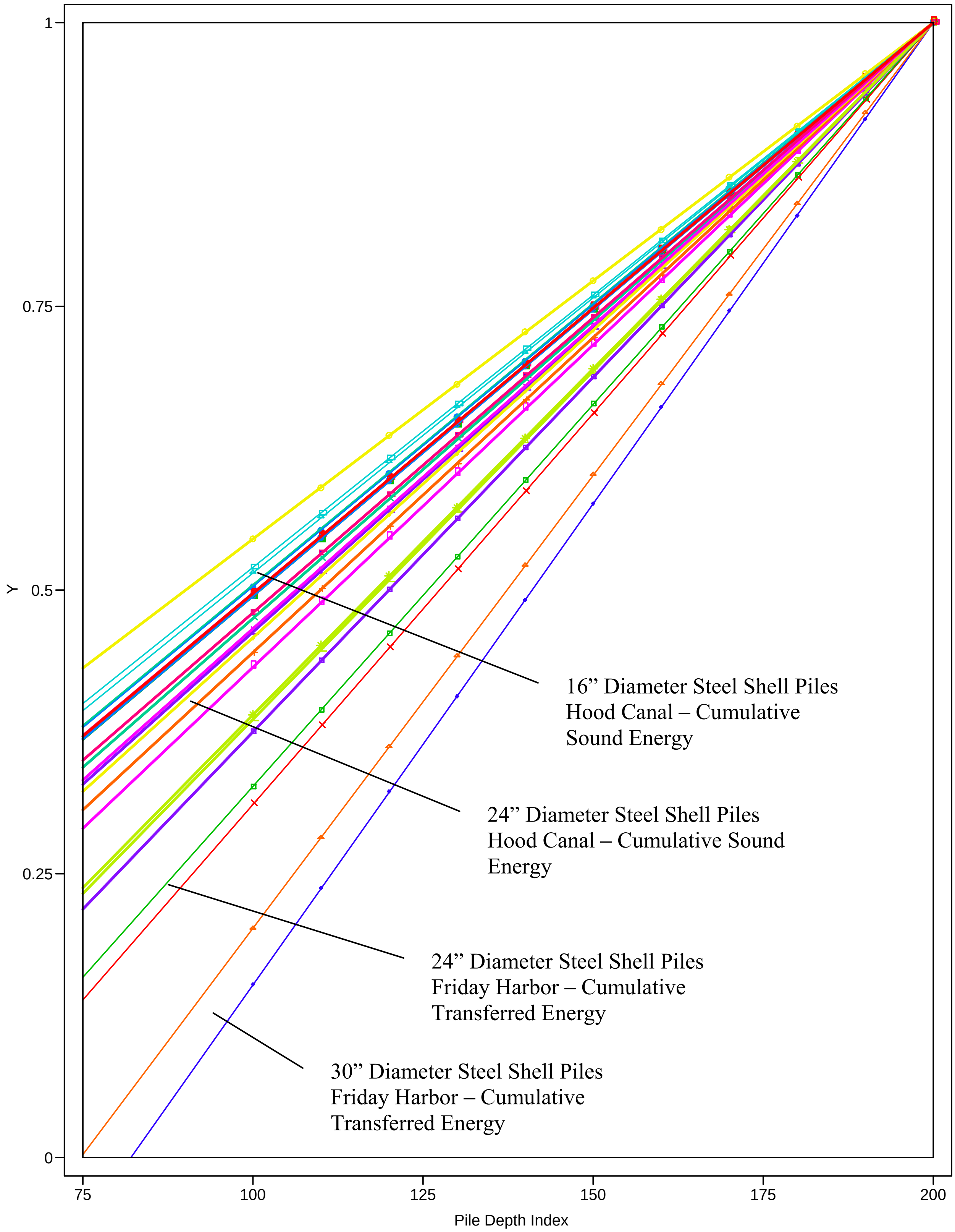

Figure 5.12. Friday Harbor Piles Shown in Dashed Lines – Cumulative Transferred Energy. Hood Canal Plumb Piles Shown in Solid Lines – Cumulative Impulsive Sound Energy. Hood Canal Batter Piles Shown in Dot-Dash Lines – Cumulative Impulsive Sound Energy.

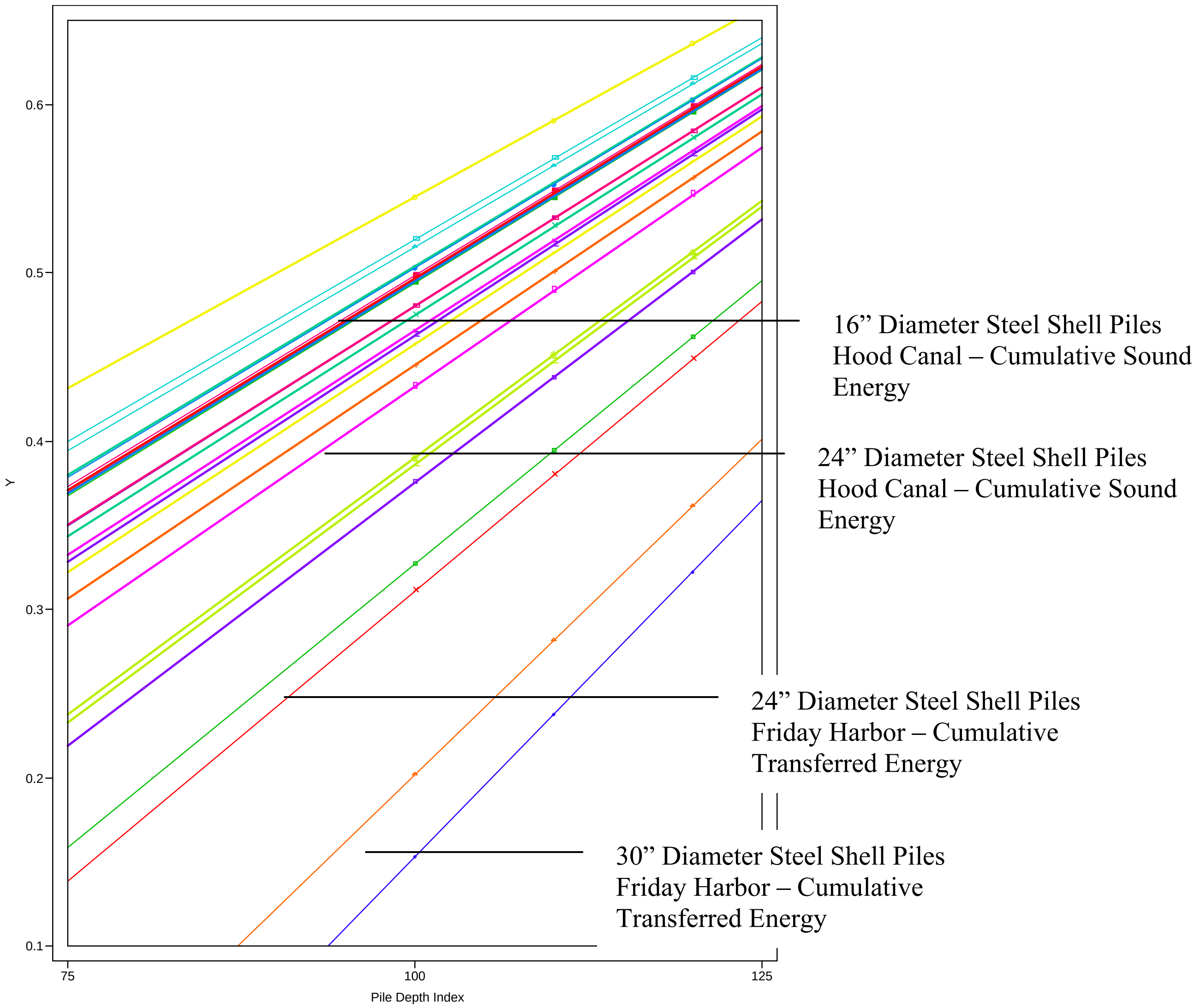

Figure 5.13. Detail of Friday Harbor Piles Shown in Dashed Lines – Cumulative Transferred Energy. Hood Canal Plumb Piles Shown in Solid Lines – Cumulative Impulsive Sound Energy. Hood Canal Batter Piles Shown in Dot-Dash Lines – Cumulative Impulsive Sound Energy.

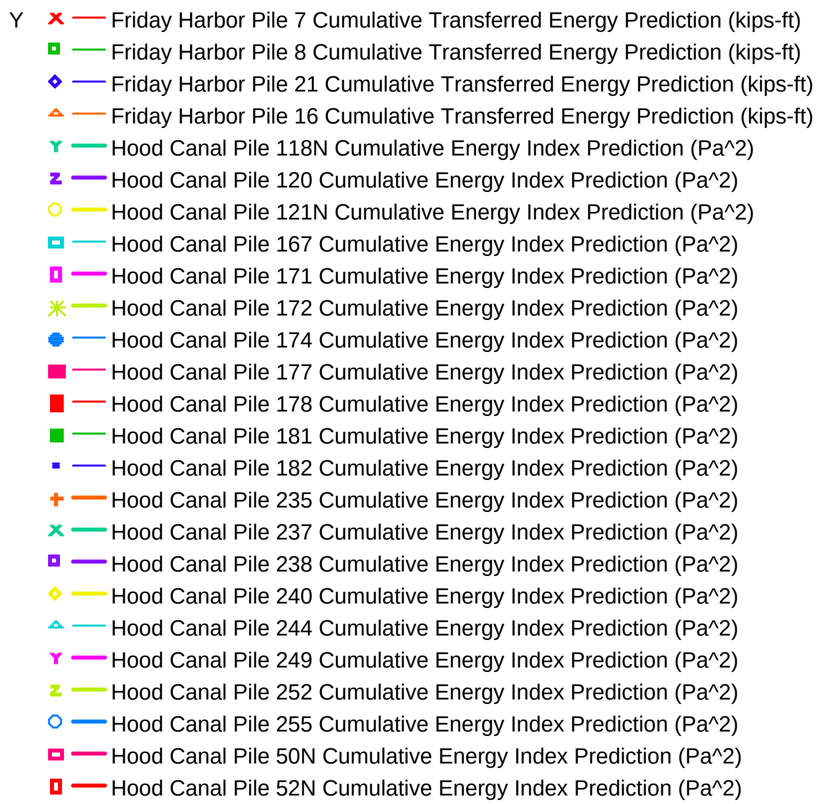

Figure 5.14. Legend for Figures 5.12 and 5.13 – Cumulative Transferred Energy. Hood Canal Plumb Piles Shown in Solid Lines – Cumulative Impulsive Sound Energy. Hood Canal Batter Piles Shown in Dot-Dash Lines – Cumulative Impulsive Sound Energy.

5.3 Findings from Comparison of Friday Harbor Dynamic Pile Driving and Hood Canal Impulsive Sound Data

- The diesel impact hammers used at Friday Harbor and Hood Canal were very similar and were assumed for the purposed of this analysis to be functionally equivalent.
- Comparison of the variability in dynamic pile driving transferred energy and impulsive sound peak pressure data indicated that most of the observed variability in impulsive sound pressure amplitude is proportional to the observed variability in the energy transferred to a pile during driving which is, in turn, directly related to hammer stroke.
- Comparison of the cumulative energy transferred to a pile during driving and the cumulative sound energy produced by a pile during driving indicated that the incremental impulsive sound energy produced during driving of a pile an increment in depth is proportional to the energy that must be transferred to a pile by an impact hammer to achieve an incremental increase in pile depth.

6.0 Conclusions and Recommendations

6.1.1 Conclusions

1. Pile wetted length does not appear to be a factor affecting the absolute peak pressure of impulsive sound generated by driving of 16” and 24” diameter steel shell piles. This finding leads to the conclusion that the mechanics of sound production by struck piles significantly reduces or eliminates wetted length as a factor in sound production as observed at a point in the receiving volume.
2. The variability in impulsive sound absolute peak pressure and related impulsive sound metrics is proportional to the transferred energy and related dynamic pile driving metrics. This finding leads to the conclusion that hammer stroke, not substrate type, is most likely the primary determinant in impulsive sound production.
3. Impulsive sound cumulative energy and the cumulative energy transferred to a pile by an impact hammer appear to be proportional for incremental increases in pile depth. This finding reinforces the conclusion that hammer stroke and resulting transferred energy is the primary determinant in impulsive sound production.
4. It appears that the opportunities for minimization of sound production will become more limited as the diameter of the steel shell pile increases. This follows from the larger increase in transferred energy and, in turn, increased impulsive sound production, for incremental increases in pile depth as pile diameter increases. Strategies that would reduce sound production will necessarily, it seems, also reduce the energy transferred to a pile. Reductions in transferred energy per blow will, according to our analysis, have much less impact on the time required for driving smaller piles than larger piles.

6.1.2 Recommendations

1. Observations of hammer stroke during a pile driving activity combined with manufacturers’ hammer specifications and the characteristics of the pile being driven will probably provide adequate data to more effectively identify causes for observed differences in sound production during pile driving.
2. The use of log transformed pressure data during analysis of impulsive sound produced by pile driving tend to obscure relationships between the mechanics of pile driving, pile characteristics, and impulsive sound production. While useful for many purposes, log transformed data should be avoided for many if not all analyses of the relationships between the mechanics of pile driving and impulsive sound production.
3. Because both sound production and the alternatives for sound reduction appear to decrease as pile diameter increases, sound mitigation alternative development should preferentially focus on piles 30 inches or larger in diameter.

7.0 References

Carlson, T.J, D.L. Woodruff, G.E. Johnson, N.P. Kohn, G.R. Ploskey, M.A. Weiland, J.A. Southard, and S.L. Southard. 2005. *Hydroacoustic Measurements during Pile Driving at the Hood Canal Bridge, September through November 2004.* Report prepared for Washington State Department of Transportation, Olympia, WA.

Laughlin, J. 2005. *Underwater Sound Levels Associated with the Restoration of the Friday Harbor Ferry Terminal.* Washington State Department of Transportation, Seattle, WA.

Miner, R. 2005a. *Dynamic Pile Measurements and CAPWAP Analyses, Piles 7 & 8, Main Slip Bridge Seat Friday Harbor Ferry Terminal.* Letter report prepared for ACC West Coast (Hurlen), Seattle, WA.

Miner, R. 2005b. *Dynamic Pile Measurements and CAPWAP Analyses, Piles 21, 16, & 18, Tower Base Friday Harbor Ferry Terminal.* Letter report prepared for ACC West Coast (Hurlen), Seattle, WA.

Appendix A

Specification Sheets for Hood Canal and Friday Harbor Diesel Impact Hammers

Appendix A

Specification Sheets for Hood Canal and Friday Harbor Diesel Impact Hammers

ICE

Model 120S

Fuel-Injected Diesel Pile Hammers

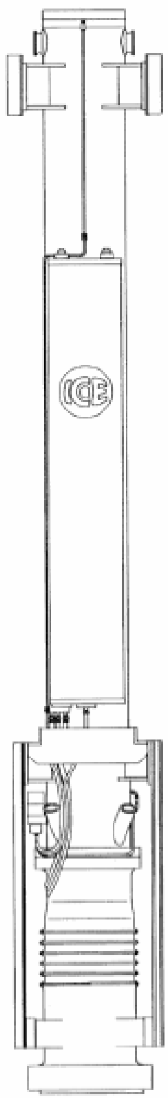

Clean • Efficient • Reliable

Designed and engineered for light-weight driven pile applications.

- High-pressure fuel injection provides easy starts even in extreme weather & soft soil conditions.
- Dual injectors optimize fuel atomization and delivery for clean, efficient operation.
- Remote variable fuel pump.
- Operates on vegetable-based fuel & lubricants without modification, contributing to a clean and toxin-free jobsite.
- Hydraulically-operated remote throttle permits precise control of stroke to match hammer energy to any job or pile condition.
- Upper & lower polymeric ram bearings minimize wear and maximize energy transfer.
- Lower cylinder and other critical components are chemically-treated for superior surface hardness and fatique resistance.
- Ferro-chromium alloy forged ram & anvil exceed strength of cast rams & anvils for durability and long life.
- Weighs less than competitive hammers to move more easily from pile to pile.
- Swinging, fixed and sliding lead set-ups available in 16 and 8 ft. sections.
- Four models of light-to-heavy-duty lead spotters for precise pile positioning.

Working Specifications	
Ram	12,000 lbs (5440 kg)
Maximum energy	149,000 ft-lbs (202 kNm)
Rated continuous energy	120,000 ft-lbs (167.2 kNm)
Minimum energy	48,000 ft-lbs (65.1 kNm)
Speed (blows per minute)	38-55
Weights	
Bare hammer	23,800 lbs (10795 kg)
Typical weight (w/18" concrete cap in 32" leads)	27,400 lbs (12430 kg)
Capacities (adequate for average day of operation)	
Diesel fuel tank	28 gal (105 l)
Lube oil tank	11 gal (40 l)
Dimensions of Hammer	
Width (side to side)	32" (815 mm)
Depth	43" (1095 mm)
Centerline to front	19" (485 mm)
Centerline to rear	24" (610 mm)
Length (hammer only)	19'-10" (6050 mm)
Operating length (top of ram to top of pile)	30'-6" (9300 mm)

INTERNATIONAL CONSTRUCTION EQUIPMENT, INC.

1205-502

Model 120S

Fuel-Injected Diesel Pile Hammers

ICE 120S DIESEL PILE HAMMER BEARING CHART

This chart is based on the Gates formula given below and is provided as a convenience only for those applications where this formula is specified. The Gates formula has been recommended for use by the U.S. DOT Federal Highway Administraion. The formula calculates ultimate pile capacity. The FHWA recommends using a factor of safety of 3.5 with the Gates formula. ICE has no preference for this formula over any other.

Ultimate bearing (tons) = 1/2(1.75*(E)^1/2*log(10N)-100) where E=Hammer energy (ft-lbs) and N=Hammer blows per inch at final penetration.

Blows per Min.	Ram Stroke (feet)	Hammer Energy (ft-lbs)	Pile Set (Blows per inch) 2	3	4	5	6	7	8	9	10	11	12	13	14	15	16	17	18	19	20
38	10.0	"120,000"	344	398	436	466	489	509	527	542	556	569	580	591	601	610	618	626	634	641	647
39	9.3	"111,600"	330	382	418	447	470	489	506	521	535	547	558	568	577	586	594	602	609	616	623
40	8.9	"106,800"	322	372	408	436	458	478	494	509	522	34	545	554	564	572	580	588	595	602	608
41	8.4	"100,800"	311	360	395	422	444	463	479	493	506	517	528	537	546	555	562	570	577	583	589
42	8.0	"96,000"	303	350	384	411	432	450	466	480	492	503	514	523	532	540	548	555	561	568	574
43	7.6	"91,200"	294	340	373	399	420	438	453	466	478	489	499	509	517	525	532	539	546	552	558
44	7.2	"86,400"	285	330	362	387	407	425	439	453	464	475	485	494	502	510	517	524	530	536	542
45	6.8	"81,600"	275	319	350	375	94	411	426	438	450	460	470	478	486	494	501	508	514	520	525
46	6.5	"78,000"	268	311	342	366	386	401	415	428	439	449	458	467	474	482	489	495	501	507	512
47	6.2	"74,400"	261	303	332	355	374	390	404	416	427	437	446	455	462	469	476	482	488	494	499
48	5.9	"70,800"	253	294	323	346	364	380	398	405	416	425	434	442	450	457	463	469	475	481	486
49	5.6	"67,200"	246	285	313	335	53	369	382	393	404	413	422	429	437	444	450	456	462	467	472
50	5.3	"63,600"	237	276	304	325	342	357	370	381	391	400	409	416	424	430	436	442	448	453	458
51	5.0	"60,000"	229	267	293	314	331	346	358	369	379	388	396	403	410	416	422	428	433	438	443
52	4.8	"57,600	223	260	286	307	323	337	350	360	370	379	387	394	401	407	413	418	424	429	433
53	4.5	"54,000	215	250	276	296	312	325	337	347	357	365	373	380	386	392	398	404	409	413	418
54	4.2	"50,400"	206	240	266	284	299	312	324	334	343	351	358	365	372	377	383	388	393	398	402
55	3.9	"46,800"	196	230	253	272	287	299	310	320	329	336	344	350	356	362	367	372	377	381	386

CAUTION: Driving at ten blows per inch is considered practical refusal. Driving in excess of ten blows per inch for more than six inches of driving or driving in excess of 20 blows per inch at all is considered improper use and will void the hammer warranty.

LEADS/SPOTTERS

ICE manufactures leads with 20", 26" 32" and 36" guide rails for all ICE and other pile hammers. Standard components are available in 8' increments for swinging, fixed and sliding lead setups. Two designs are available to provide the most cost-effective configuration for every job. Four models of spotters and three spotter power unit sizes are available.

DRIVE CAPS

ICE offers a drive cap base/insert system for all ICE lead sizes as well as for pipe leads. Drive cap inserts are available for practically any pile type and size. The ICE drive cap system: maintains pile top position under the hammer, protects the hammer from peak stresses,minimizes pile top deformation, and transmits maximum force to pile.

INTERNATIONAL CONSTRUCTION EQUIPMENT, INC.

Corporate offices:
301 Warehouse Drive, Matthews NC 28104
Phones: 704 821-8200, 888 ICEUSA1 (423-8721)
Fax: 704 821-8201
www.iceusa.com e-mail: sales@iceusa.com

APE HOLLAND

APE HOLLAND

MODEL D46-32 DIESEL HAMMER

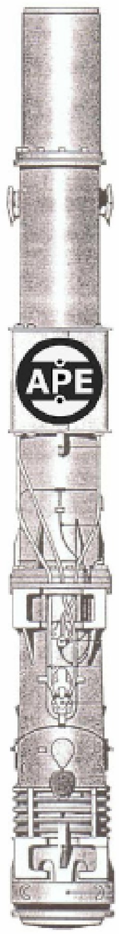

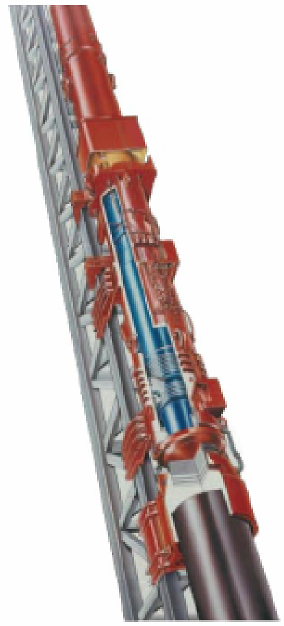

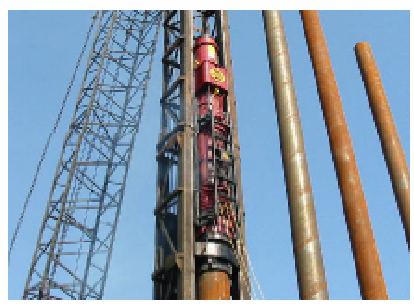

- Fuel injection designed by APE engineers.
- Hardened piston needs no high maintenance wear rings.
- Direct drive available for maximum production on steel piles.
- Fuel pump mounted where heat will not harm it.
- Variable mechanical cam fuel pump – no air pistons or rings.
- Optional hydraulic variable fuel remote control.
- Heavy duty trip system for years of fault free operation.
- Chrome rings for super long life.
- Low maintenance and extremely low parts pricing.
- German design at a reasonable price.

APE HOLLAND

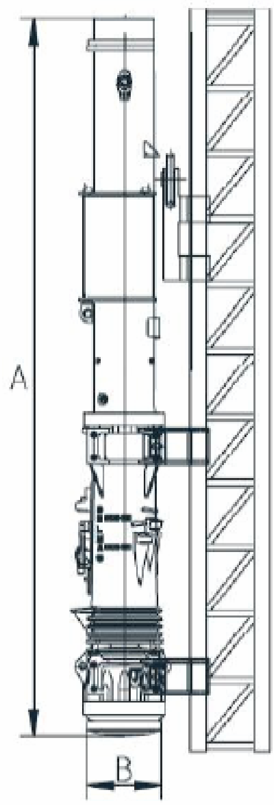

Technical Data		
Impact weight (piston)	kg.	4.600
Energy per blow	kNm	166 - 71
Number of blows	Min^{-1}	35 - 53
Suitable for driving piles. (depending on soil and pile)	kg.	3000 - 16000
Consuption		
Diesel oil	l/h	16
Lubricant	l/h	1,5
Tank capacity		
Diesel oil tank	l	89
Lube tank	l	17
Max. rope diameter for deflector sheave of tripping device.	mm	38
Weight		
Tripping device	kg.	400
Diesel pile hammer	kg.	10.822
Max. inclined pile driving with-out / with extension		1:5 / 1:1
Dimensions		
A. Length of diesel hammer with-out extension	mm.	5.470
B. Outer diameter of impact block	mm.	660
C. Width of diesel hammer	mm.	785
D. Width for connection of guide jaws.	mm.	640
E. Center of hammer to pump guard.	mm.	445
F. Center of hammer to center ofthreads for guide jaw bolts.	mm.	275
G. Depth of diesel hammer	mm.	848
H. Standard distance from center of diesel hammer up to the face of the lead.	mm.	500

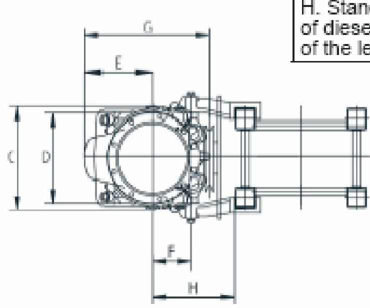

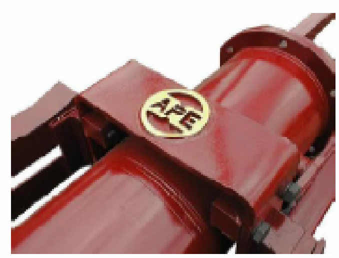

APE Holland BV, P.O. Box 34, 7990 AA Dwingeloo, The Netherlands
Tel.: +31(0) 593 54 08 91, Fax: +31(0) 593 54 27 84, www.apeholland.com, info@apeholland.com

Due to constant improvements we must advise you to call APE Holland for the latest available literature and specifications. 05/06

(800) 248-8498

Diesel Hammer Energy Output and Pile Bearing Chart

APE Model D46-32

The energy output is based on the identical Piston/Travel calculations utilized in the *Pile Driving Analyzer* and the *Saximeter*.

The pile bearing chart is based on the Engineering News formula for pile bearing and is provided for the user's convenience only.

Pile Bearing (tons) = 2E/(S+.1)/2000, where E = Hammer energy (ft-lbs) and S = Pile set (inches per blow)

Ram Weight(lbs): 10,143

APE has no preference for these particular formulas and calculations over any other.

Blows per Minute	Stroke (feet)	Energy (ft-lbs)	Pile Set (Blows per inch) 2	3	4	5	6	7	8	9	10	11	12	13	14	15	16	17	18	19	20
60	4.00	40,572	68	94	116	135	152	167	180	192	203	213	221	229	237	243	250	255	261	266	270
59	4.17	42,296	70	98	121	141	159	174	188	200	211	222	231	239	247	254	260	266	272	277	282
58	4.33	43,919	73	101	125	146	165	181	195	208	220	230	240	248	256	264	270	277	282	288	293
57	4.50	45,644	76	105	130	152	171	188	203	216	228	239	249	258	266	274	281	287	293	299	304
56	4.67	47,368	79	109	135	158	178	195	211	224	237	248	258	268	276	284	291	298	305	310	316
55	4.83	48,991	82	113	140	163	184	202	218	232	245	257	267	277	286	294	301	308	315	321	327
54	5.00	50,715	85	117	145	169	190	209	225	240	254	266	277	287	296	304	312	319	326	332	338
53	5.17	52,439	87	121	150	175	197	216	233	248	262	275	286	296	306	315	323	330	337	344	350
52	5.33	54,062	90	125	154	180	203	223	240	256	270	283	295	306	315	324	333	340	348	354	360
51	5.50	55,787	93	129	159	186	209	230	248	264	279	292	304	315	325	335	343	351	359	365	372
50	5.75	58,322	97	135	167	194	219	240	259	276	292	305	318	330	340	350	359	367	375	382	389
49	6.00	60,858	101	140	174	203	228	251	270	288	304	319	332	344	355	365	375	383	391	399	406
48	6.25	63,394	106	146	181	211	238	261	282	300	317	332	346	358	370	380	390	399	408	415	423
47	6.50	65,930	110	152	188	220	247	271	293	312	330	345	360	373	385	396	406	415	424	432	440
46	6.83	69,277	115	160	198	231	260	285	308	328	346	363	378	392	404	416	426	436	445	454	462
45	7.17	72,725	121	168	208	242	273	299	323	344	364	381	397	411	424	436	448	458	468	476	485
44	7.50	76,073	127	176	217	254	285	313	338	360	380	398	415	430	444	456	468	479	489	498	507
43	7.83	79,420	132	183	227	265	298	327	353	376	397	416	433	449	463	477	489	500	511	520	529
42	8.17	82,868	138	191	237	276	311	341	368	393	414	434	452	468	483	497	510	522	533	543	552
41	8.58	87,027	145	201	249	290	326	358	387	412	435	456	475	492	508	522	536	548	559	570	580
40	9.00	91,287	152	211	261	304	342	376	406	432	456	478	498	516	533	548	562	575	587	598	609
39	9.50	96,359	161	222	275	321	361	397	428	456	482	505	526	545	562	578	593	607	619	631	642
38	10.00	101,430	169	234	290	338	380	418	451	480	507	531	553	573	592	609	624	639	652	665	676
37	10.50	106,502	178	246	304	355	399	439	473	504	533	558	581	602	621	639	655	671	685	698	710
36	11.17	113,297	189	261	324	378	425	467	504	537	566	593	618	640	661	680	697	713	728	742	755

7032 South 196th Street
Kent, WA 98032-2185
Tel: 253/872-0141
Fax:253/872-8710

DIESEL HAMMER BEARING CHAR.XLS D46-32

BLOW ENERGY FOR DRIVING OF BATTER PILES using APE Diesels

Blow energy for the driving of batter piles

The increased friction of the piston and of the impact block causes a decrease in the blow energy when driving batter piles. The wear on the cylinder and guiding components, for example, is also increased. The remaining blow energy can be calculated with the formula shown below:

$$\text{Remaining blow energy (in \% of the max. blow energy)} = \frac{\cos\alpha - 0{,}1\sin\alpha}{\cos\alpha + 0{,}1\sin\alpha} \times 100$$

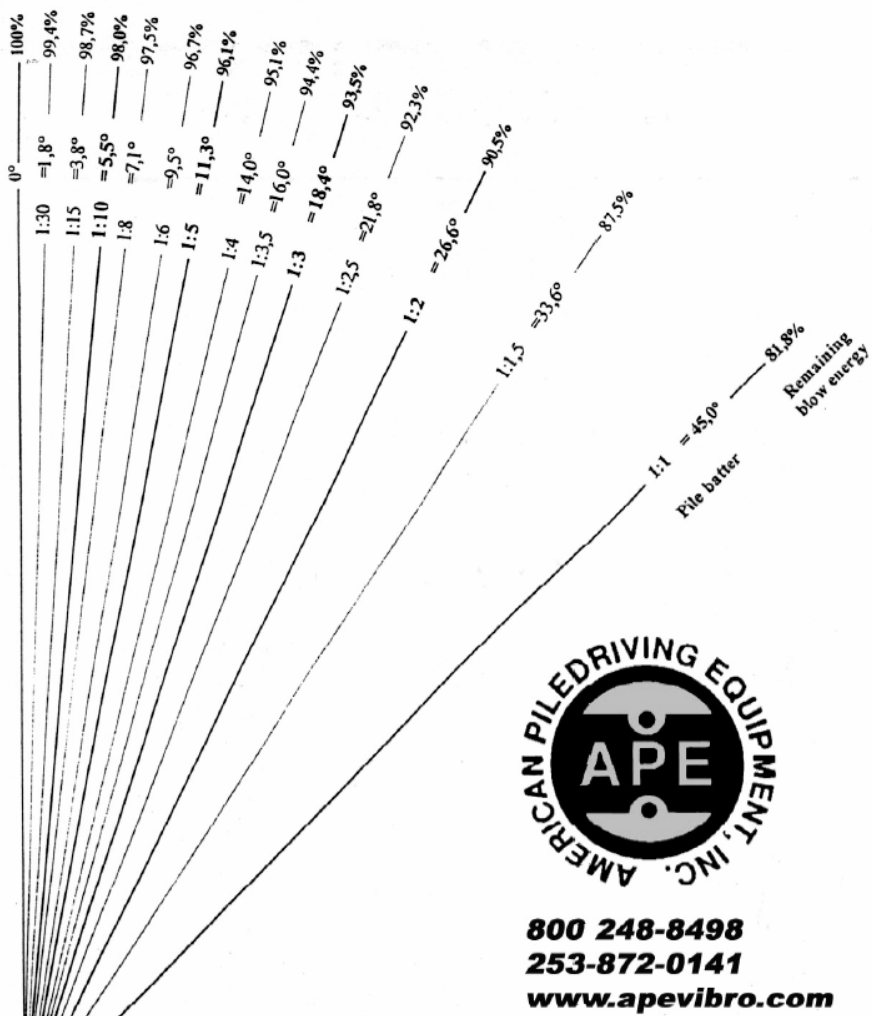

AMERICAN PILEDRIVING EQUIPMENT, INC.

APE

800 248-8498
253-872-0141
www.apevibro.com
www.jandm-usa.com

Appendix B

Data Tables and Plots for Dynamic Pile Driving and Impulsive Sound Data Analyses

Appendix B

Data Tables and Plots for Dynamic Pile Driving and Impulsive Sound Data Analyses

Dynamic Pile Testing - Friday Harbor Ferry Dock			
Source	Mean	Standard Deviation	Coefficient of Variation
Transferred Energy (kips-ft)			
Pile 7	47.84	8.87	18.54%
Pile 8	55.73	9.77	17.53%
Pile 21	40.98	9.90	24.16%
Pile 16	52.99	7.48	14.12%
All Piles	51.01	10.48	20.54%
Hammer Stroke (ft)			
Pile 7	8.04	0.94	11.69%
Pile 8	8.32	0.81	9.74%
Pile 21	7.14	1.44	20.17%
Pile 16	8.66	1.07	12.36%
All Piles	8.16	1.13	13.85%

Impulsive Sound - Hood Canal Bridge - Pile 118N - Plumb Pile - 24" Dia - 0.5" Wall - Steel Shell Pipe - Wetted Depth 39 ft - Type II Confined Bubble Curtain						
Statistic	SPL (dB//microPa)	Maximum Absolute Pressure (Pa)	SEL (dB//microPa^2 s)	Impulse Energy Index (Pa^2)	Impulse Duration (sec)	Impulse Rise Time (sec)
N	197	197	197	197	197	197
Mean	199.4	9428.16	173.8	242635.91	0.062	0.005
Median	199.5	9389.45	173.9	243242.62	0.064	0.005
Std Dev	0.91	955.174	0.86	43425.891	0.012	0.005
CV	0.46	10.13	0.5	17.9	19.29	86.63

Impulsive Sound - Hood Canal Bridge - Pile 120N - Plumb Pile - 24" Dia - 0.5" Wall - Steel Shell Pipe - Wetted Depth 39 ft - No Bubble Curtain						
Statistic	SPL (dB//microPa)	Maximum Absolute Pressure (Pa)	SEL (dB//microPa^2 s)	Impulse Energy Index (Pa^2)	Impulse Duration (sec)	Impulse Rise Time (sec)
N	149	149	149	149	149	149
Mean	201.6	12322.5	176.4	479211.22	0.042	0.01
Median	202	12613.6	177.2	520183.98	0.037	0.01
Std Dev	2.39	2470.48	2.27	159410.26	0.011	0.005
CV	1.18	20.05	1.29	33.27	25.82	47.75

Impulsive Sound - Hood Canal Bridge - Pile 121N - Plumb Pile - 24" Dia - 0.5" Wall - Steel Shell Pipe - Wetted Depth 42 ft - Type II Confined Bubble Curtain						
Statistic	SPL (dB//microPa)	Maximum Absolute Pressure (Pa)	SEL (dB//microPa^2 s)	Impulse Energy Index (Pa^2)	Impulse Duration (sec)	Impulse Rise Time (sec)
N	277	277	277	277	277	277
Mean	199.6	10141.9	173.4	246067.61	0.063	0.004
Median	200	10050.8	174	250504.85	0.061	0.003
Std Dev	3.08	3334.49	2.14	107325.17	0.013	0.004
CV	1.54	32.88	1.23	43.62	20.8	115.3

Impulsive Sound - Hood Canal Bridge - Pile 167 - Batter Pile - 16" Dia - 0.5" Wall - Steel Shell Pipe - Wetted Depth 7 ft - Type II Unconfined Bubble Curtain						
Statistic	SPL (dB//microPa)	Maximum Absolute Pressure (Pa)	SEL (dB//microPa^2 s)	Impulse Energy Index (Pa^2)	Impulse Duration (sec)	Impulse Rise Time (sec)
N	75	75	75	75	75	75
Mean	196.5	6911.18	171	141606.98	0.055	0.007
Median	196.2	6428.91	170.7	118091.95	0.049	0.006
Std Dev	2.19	2167.23	1.87	81619.868	0.021	0.003
CV	1.12	31.36	1.1	57.64	38.3	52.68

Impulsive Sound - Hood Canal Bridge - Pile 171 - Plumb Pile - 24" Dia - 0.5" Wall - Steel Shell Pipe - Wetted Depth 18 ft - Type II Confined Bubble Curtain						
Statistic	SPL (dB//microPa)	Maximum Absolute Pressure (Pa)	SEL (dB//microPa^2 s)	Impulse Energy Index (Pa^2)	Impulse Duration (sec)	Impulse Rise Time (sec)
N	166	166	166	166	166	166
Mean	197.8	8267.88	171.2	159578.94	0.035	0.005
Median	199	8954.05	173	200832.35	0.033	0.006
Std Dev	3.36	2620.25	3.18	73499.356	0.011	0.002
CV	1.7	31.69	1.86	46.06	30.38	41.36

Impulsive Sound - Hood Canal Bridge - Pile 172 - Plumb Pile - 24" Dia - 0.5" Wall - Steel Shell Pipe - Wetted Depth 20 ft - Type II Confined Bubble Curtain						
Statistic	SPL (dB//microPa)	Maximum Absolute Pressure (Pa)	SEL (dB//microPa^2 s)	Impulse Energy Index (Pa^2)	Impulse Duration (sec)	Impulse Rise Time (sec)
N	169	169	169	169	169	169
Mean	203.7	16306.5	177.7	740804.54	0.03	0.007
Median	205.3	18376.8	179.6	920251.6	0.025	0.007
Std Dev	3.39	4570.34	3.63	353351.95	0.012	0.002
CV	1.66	28.03	2.04	47.7	41.2	27.98

Impulsive Sound - Hood Canal Bridge - Pile 174 - Batter Pile - 16" Dia - 0.5" Wall - Steel Shell Pipe - Wetted Depth 29 ft - Type I Unconfined Bubble Curtain						
Statistic	SPL (dB//microPa)	Maximum Absolute Pressure (Pa)	SEL (dB//microPa^2 s)	Impulse Energy Index (Pa^2)	Impulse Duration (sec)	Impulse Rise Time (sec)
N	22	22	22	22	22	22
Mean	191.3	3767.51	166.9	51602.208	0.062	0.009
Median	191.2	3622.09	167.5	56718.763	0.057	0.01
Std Dev	2.02	929.075	1.6	18140.796	0.013	0.007
CV	1.06	24.66	0.96	35.16	21.45	73.5

Impulsive Sound - Hood Canal Bridge - Pile 177 - Batter Pile - 16" Dia - 0.5" Wall - Steel Shell Pipe - Wetted Depth 37 ft - Type I Unconfined Bubble Curtain						
Statistic	SPL (dB//microPa)	Maximum Absolute Pressure (Pa)	SEL (dB//microPa^2 s)	Impulse Energy Index (Pa^2)	Impulse Duration (sec)	Impulse Rise Time (sec)
N	11	11	11	11	11	11
Mean	190.2	3488.83	165.2	37107.278	0.058	0.013
Median	189.9	3116.32	165	31974.853	0.054	0.015
Std Dev	3.28	1502.42	2.1	20229.447	0.015	0.006
CV	1.73	43.06	1.27	54.52	25.35	49.54

Impulsive Sound - Hood Canal Bridge - Pile 178 - Batter Pile - 16" Dia - 0.5" Wall - Steel Shell Pipe - Wetted Depth 37 ft - No Bubble Curtain						
Statistic	SPL (dB//microPa)	Maximum Absolute Pressure (Pa)	SEL (dB//microPa^2 s)	Impulse Energy Index (Pa^2)	Impulse Duration (sec)	Impulse Rise Time (sec)
N	25	25	25	25	25	25
Mean	198	7995.02	171.8	152267.25	0.062	0.012
Median	197.9	7894.78	171.8	151247.9	0.063	0.009
Std Dev	0.82	792.799	0.53	18752.955	0.015	0.008
CV	0.42	9.916	0.31	12.32	23.7	65.07

Impulsive Sound - Hood Canal Bridge - Pile 181 - Batter Pile - 16" Dia - 0.5" Wall - Steel Shell Pipe - Wetted Depth 33 ft - Type I Unconfined Bubble Curtain						
Statistic	SPL (dB//microPa)	Maximum Absolute Pressure (Pa)	SEL (dB//microPa^2 s)	Impulse Energy Index (Pa^2)	Impulse Duration (sec)	Impulse Rise Time (sec)
N	36	36	36	36	36	36
Mean	192.8	4534.2	167.4	62630.361	0.051	0.007
Median	192.6	4269.99	167.6	57219.14	0.05	0.006
Std Dev	2.68	1241.11	2.58	29127.898	0.018	0.006
CV	1.39	27.37	1.54	46.51	35.21	84.35

Impulsive Sound - Hood Canal Bridge - Pile 182 - Batter Pile - 16" Dia - 0.5" Wall - Steel Shell Pipe - Wetted Depth 41 ft - Type I Unconfined Bubble Curtain						
Statistic	SPL (dB//microPa)	Maximum Absolute Pressure (Pa)	SEL (dB//microPa^2 s)	Impulse Energy Index (Pa^2)	Impulse Duration (sec)	Impulse Rise Time (sec)
N	39	39	39	39	39	39
Mean	196.7	7082.21	170.7	136258.05	0.048	0.008
Median	197.5	7489.23	171.9	156395.18	0.044	0.007
Std Dev	2.52	1584.77	2.77	56692.38	0.011	0.003
CV	1.28	22.38	1.63	41.61	22.82	31.6

Impulsive Sound - Hood Canal Bridge - Pile 235 - Plumb Pile - 24" Dia - 0.5" Wall - Steel Shell Pipe - Wetted Depth 4.5 ft - Type II Confined Bubble Curtain						
Statistic	SPL (dB//microPa)	Maximum Absolute Pressure (Pa)	SEL (dB//microPa^2 s)	Impulse Energy Index (Pa^2)	Impulse Duration (sec)	Impulse Rise Time (sec)
N	253	253	253	253	253	253
Mean	197.4	7725.84	171.6	157375.94	0.034	0.005
Median	197.5	7507.3	171.3	134631.81	0.033	0.004
Std Dev	2.5	2295.52	1.88	69332.131	0.008	0.003
CV	1.27	29.71	1.1	44.06	23.64	60.32

Impulsive Sound - Hood Canal Bridge - Pile 237 - Plumb Pile - 24" Dia - 0.5" Wall - Steel Shell Pipe - Wetted Depth 4 ft - Type II Confined Bubble Curtain						
Statistic	SPL (dB//microPa)	Maximum Absolute Pressure (Pa)	SEL (dB//microPa^2 s)	Impulse Energy Index (Pa^2)	Impulse Duration (sec)	Impulse Rise Time (sec)
N	358	358	358	358	358	358
Mean	197.6	7682.82	171.9	158747.38	0.034	0.006
Median	197.6	7585.98	172	159396.72	0.035	0.005
Std Dev	1.41	1101.51	1.19	35498.404	0.007	0.004
CV	0.71	14.34	0.69	22.36	20.14	59.54

Impulsive Sound - Hood Canal Bridge - Pile 238 - Plumb Pile - 24" Dia - 0.5" Wall - Steel Shell Pipe - Wetted Depth 7 ft - Type II Confined Bubble Curtain						
Statistic	SPL (dB//microPa)	Maximum Absolute Pressure (Pa)	SEL (dB//microPa^2 s)	Impulse Energy Index (Pa^2)	Impulse Duration (sec)	Impulse Rise Time (sec)
N	202	202	202	202	202	202
Mean	195.6	6609.47	169.8	127512.49	0.032	0.007
Median	196.9	7015.16	170.1	103063.17	0.024	0.005
Std Dev	4.2	2460.03	3.73	84412.157	0.015	0.005
CV	2.15	37.22	2.2	66.2	47.95	74.39

Impulsive Sound - Hood Canal Bridge - Pile 240 - Plumb Pile - 24" Dia - 0.5" Wall - Steel Shell Pipe - Wetted Depth 9 ft - No Bubble Curtain						
Statistic	SPL (dB//microPa)	Maximum Absolute Pressure (Pa)	SEL (dB//microPa^2 s)	Impulse Energy Index (Pa^2)	Impulse Duration (sec)	Impulse Rise Time (sec)
N	291	291	291	291	291	291
Mean	201	11787.8	173.5	241768.89	0.03	0.01
Median	201.5	11914.4	173.7	232782.8	0.029	0.01
Std Dev	2.98	3560.55	1.85	84140.686	0.007	0.005
CV	1.48	30.21	1.07	34.8	22.1	51.13

Impulsive Sound - Hood Canal Bridge - Pile 244 - Batter Pile - 16" Dia - 0.5" Wall - Steel Shell Pipe - Wetted Depth 20 ft - No Bubble Curtain						
Statistic	SPL (dB//microPa)	Maximum Absolute Pressure (Pa)	SEL (dB//microPa^2 s)	Impulse Energy Index (Pa^2)	Impulse Duration (sec)	Impulse Rise Time (sec)
N	41	41	41	41	41	41
Mean	194.7	5732.19	168	75076.938	0.042	0.008
Median	194.2	5122.08	167.2	51924.115	0.038	0.006
Std Dev	2.48	2242.33	2.44	53353.481	0.013	0.006
CV	1.27	39.12	1.45	71.07	29.84	65.59

Impulsive Sound - Hood Canal Bridge - Pile 249 - Plumb Pile - 24" Dia - 0.5" Wall - Steel Shell Pipe - Wetted Depth 32 ft - Type II Confined Bubble Curtain						
Statistic	SPL (dB//microPa)	Maximum Absolute Pressure (Pa)	SEL (dB//microPa^2 s)	Impulse Energy Index (Pa^2)	Impulse Duration (sec)	Impulse Rise Time (sec)
N	166	166	166	166	166	166
Mean	198.6	8790.33	171.5	151817.18	0.039	0.003
Median	199.3	9193.19	172.1	160743.15	0.037	0.002
Std Dev	2.48	1796.48	2.08	45307.988	0.01	0.003
CV	1.25	20.44	1.21	29.84	24.43	97.15

Impulsive Sound - Hood Canal Bridge - Pile 252 - Plumb Pile - 24" Dia - 0.5" Wall - Steel Shell Pipe - Wetted Depth 31 ft - Type II Confined Bubble Curtain						
Statistic	SPL (dB//microPa)	Maximum Absolute Pressure (Pa)	SEL (dB//microPa^2 s)	Impulse Energy Index (Pa^2)	Impulse Duration (sec)	Impulse Rise Time (sec)
N	252	252	252	252	252	252
Mean	200.1	10724.3	173.7	281529.24	0.033	0.005
Median	201.4	11805.9	174	252079.89	0.028	0.006
Std Dev	3.14	3326.02	2.77	146786.97	0.013	0.002
CV	1.57	31.01	1.59	52.14	37.48	36.5

Impulsive Sound - Hood Canal Bridge - Pile 255 - Plumb Pile - 24" Dia - 0.5" Wall - Steel Shell Pipe - Wetted Depth 33 ft - Type II Confined Bubble Curtain						
Statistic	SPL (dB//microPa)	Maximum Absolute Pressure (Pa)	SEL (dB//microPa^2 s)	Impulse Energy Index (Pa^2)	Impulse Duration (sec)	Impulse Rise Time (sec)
N	67	67	67	67	67	67
Mean	199.5	9501.7	173.2	210636.61	0.032	0.005
Median	199.5	9400.98	173.4	217088.16	0.031	0.005
Std Dev	1.05	1090.72	0.85	34356.748	0.006	0.002
CV	0.53	11.48	0.49	16.31	18.84	30.43

Impulsive Sound - Hood Canal Bridge - Pile 50N - Plumb Pile - 24" Dia - 0.5" Wall - Steel Shell Pipe - Wetted Depth 40 ft - No Bubble Curtain						
Statistic	SPL (dB//microPa)	Maximum Absolute Pressure (Pa)	SEL (dB//microPa^2 s)	Impulse Energy Index (Pa^2)	Impulse Duration (sec)	Impulse Rise Time (sec)
N	321	321	321	321	321	321
Mean	201.1	11578.6	173.2	215156.26	0.049	0.006
Median	201.5	11871.6	173.4	217849.68	0.048	0.006
Std Dev	1.8	1590.01	1.34	36326.012	0.007	0.002
CV	0.89	13.73	0.77	16.88	14.33	32.9

Impulsive Sound - Hood Canal Bridge - Pile 52N - Plumb Pile - 24" Dia - 0.5" Wall - Steel Shell Pipe - Wetted Depth 40 ft - Type II Confined Bubble Curtain						
Statistic	SPL (dB//microPa)	Maximum Absolute Pressure (Pa)	SEL (dB//microPa^ 2 s)	Impulse Energy Index (Pa^2)	Impulse Duration (sec)	Impulse Rise Time (sec)
N	101	101	101	101	101	101
Mean	199.1	9017.49	174.7	295973.64	0.058	0.005
Median	199.1	8978.74	174.7	295762.77	0.056	0.003
Std Dev	0.92	850.155	0.8	37985.521	0.01	0.005
CV	0.46	9.428	0.46	12.83	17.27	92.66

Overlay Plot Pile #=118N, Pile Driving Method=Plumb, Bubble Curtain=Bubble Curtain Present

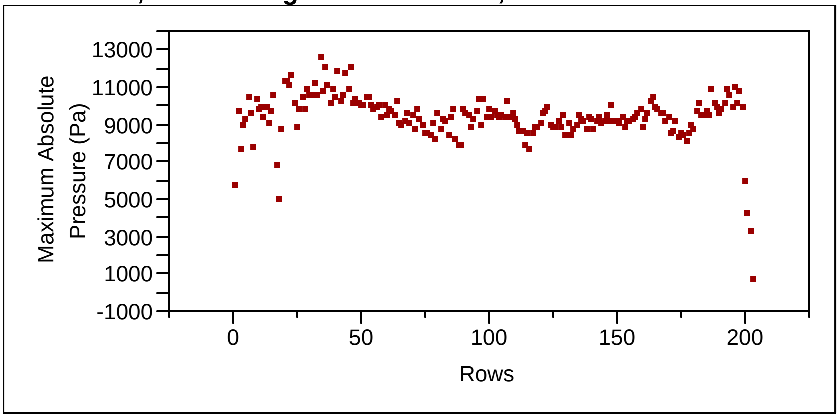

Overlay Plot Pile #=118N, Pile Driving Method=Plumb

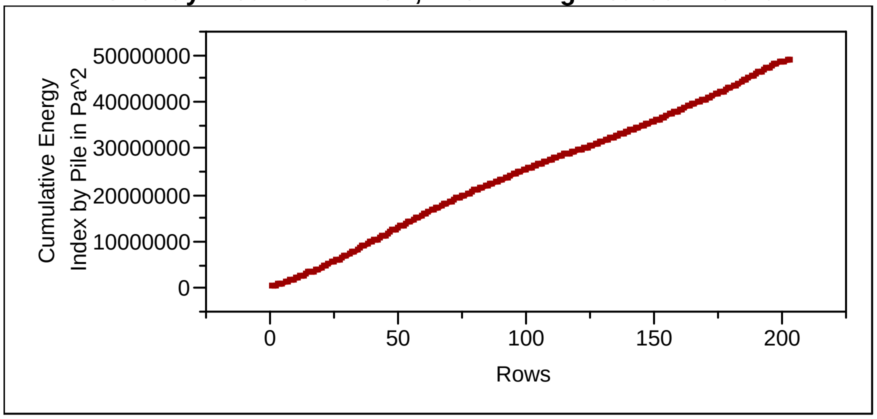

Overlay Plot Pile #=120N, Pile Driving Method=Plumb, Bubble Curtain=No Bubble Curtain

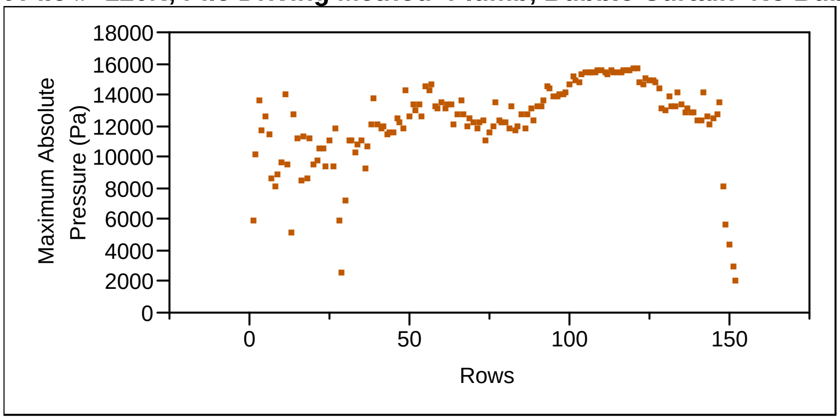

Overlay Plot Pile #=120N, Pile Driving Method=Plumb

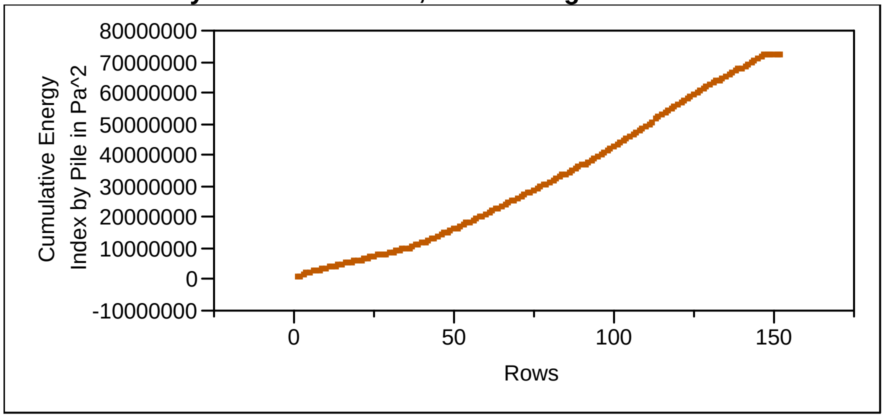

Overlay Plot Pile #=121N, Pile Driving Method=Plumb, Bubble Curtain=Bubble Curtain Present

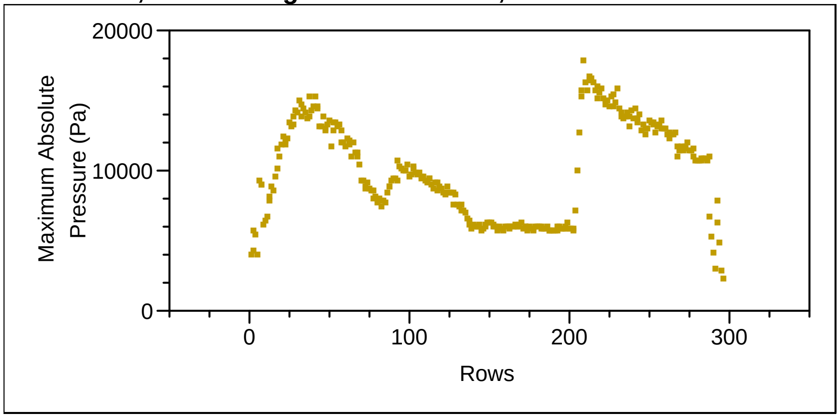

Overlay Plot Pile #=121N, Pile Driving Method=Plumb

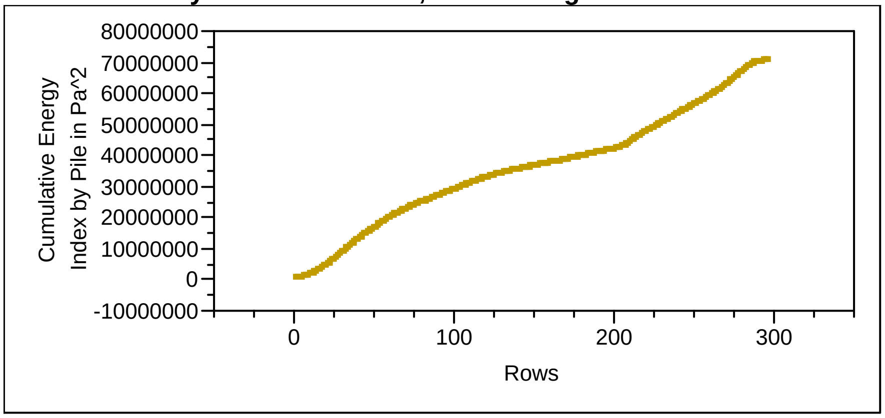

Overlay Plot Pile #=167, Pile Driving Method=Batter, Bubble Curtain=Bubble Curtain Present

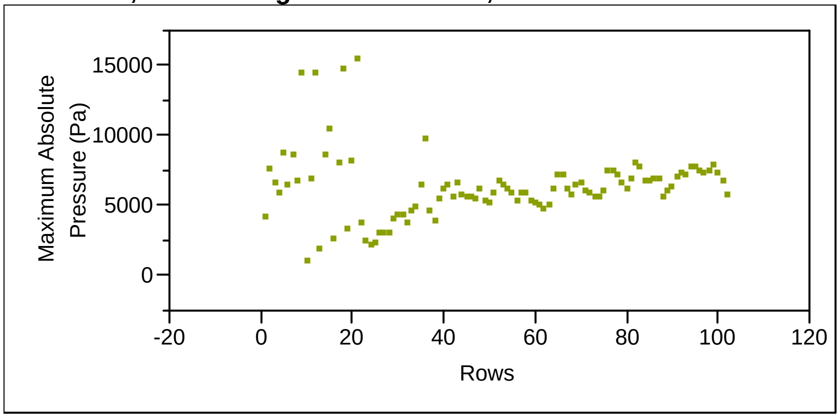

Overlay Plot Pile #=167, Pile Driving Method=Batter

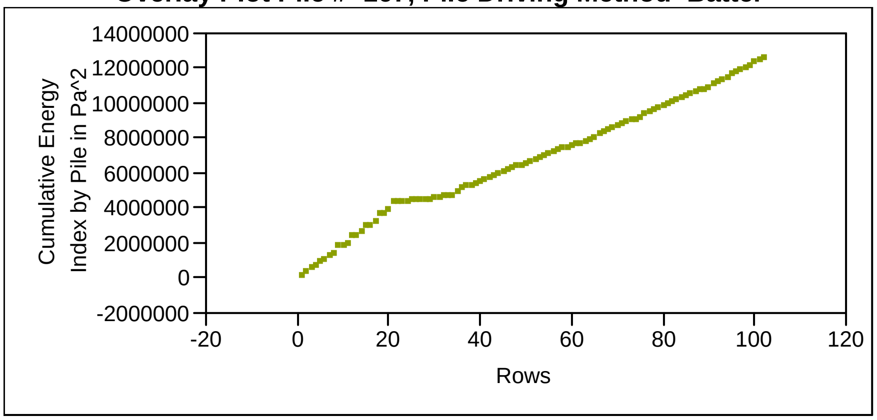

Overlay Plot Pile #=171, Pile Driving Method=Plumb, Bubble Curtain=Bubble Curtain Present

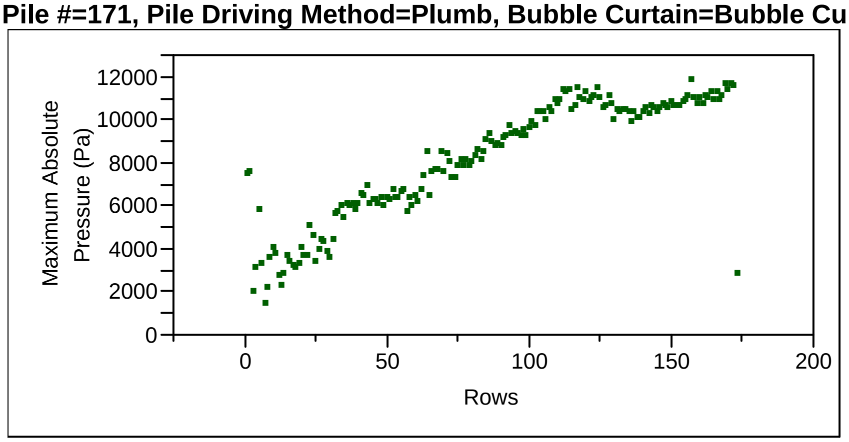

Overlay Plot Pile #=171, Pile Driving Method=Plumb

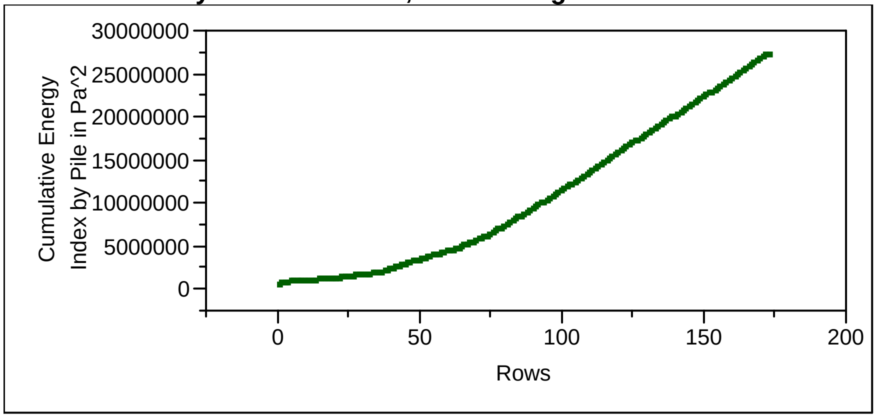

Overlay Plot Pile #=172, Pile Driving Method=Plumb, Bubble Curtain=Bubble Curtain Present

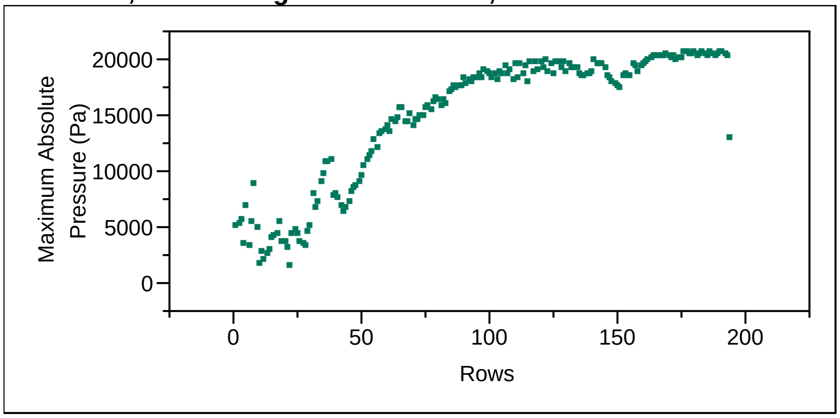

Overlay Plot Pile #=172, Pile Driving Method=Plumb

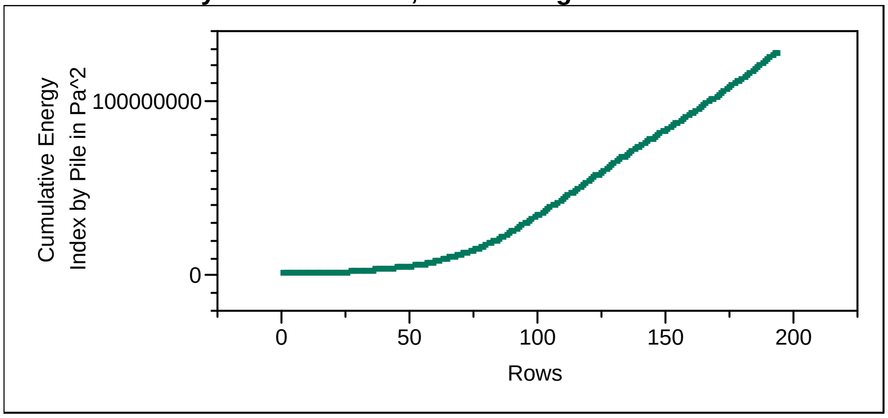

Overlay Plot Pile #=174, Pile Driving Method=Batter, Bubble Curtain=Bubble Curtain Present

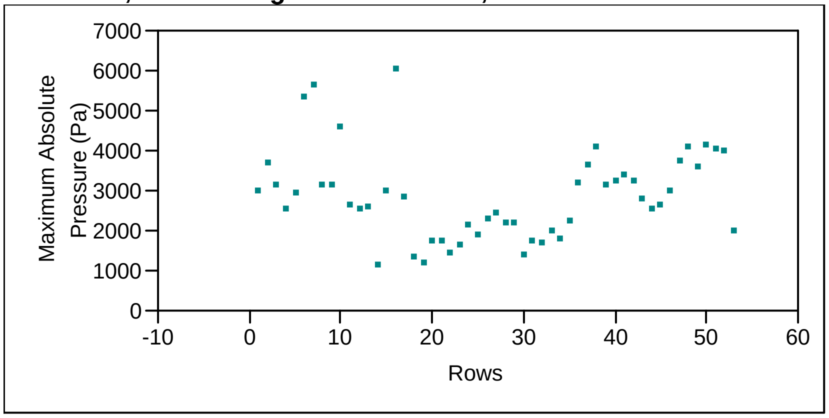

Overlay Plot Pile #=174, Pile Driving Method=Batter

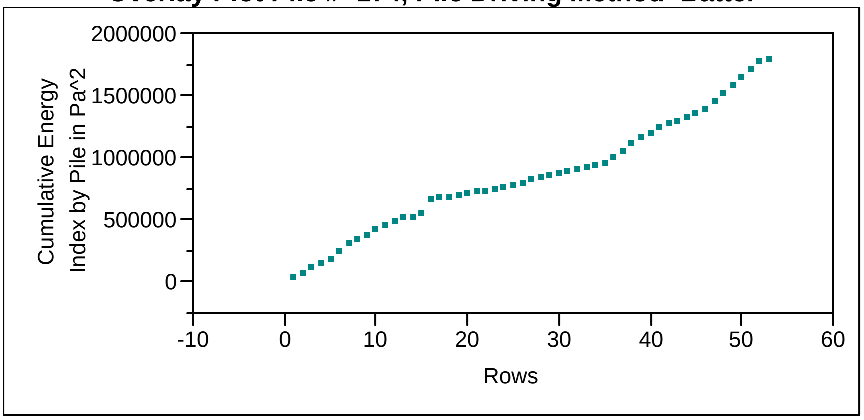

Overlay Plot Pile #=177, Pile Driving Method=Batter, Bubble Curtain=Bubble Curtain Present

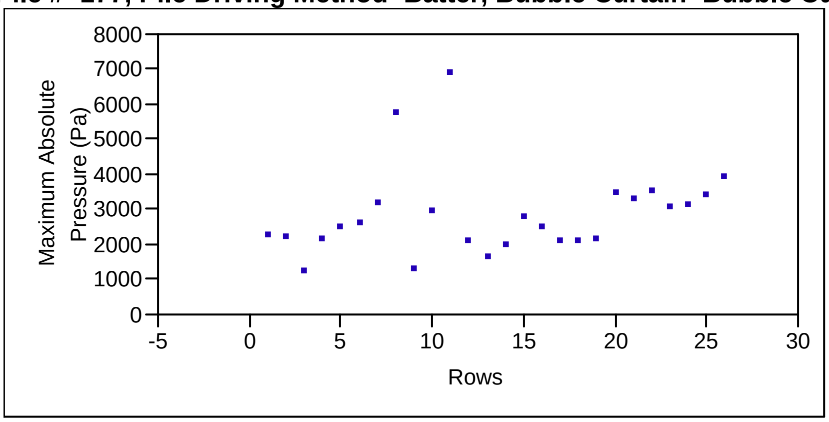

Overlay Plot Pile #=177, Pile Driving Method=Batter

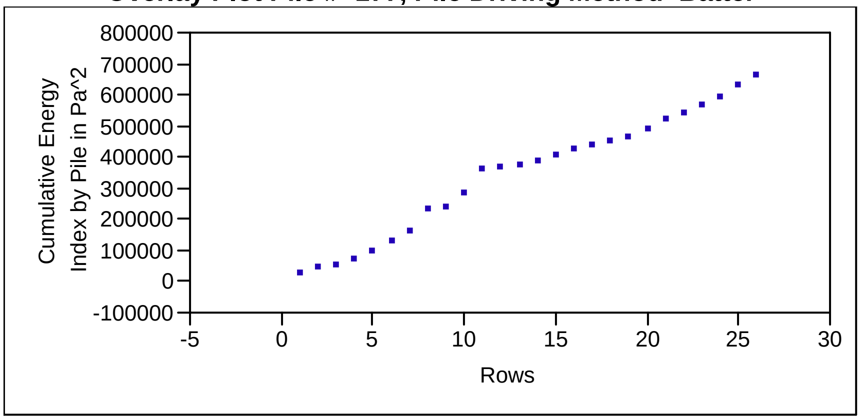

Overlay Plot Pile #=178, Pile Driving Method=Batter, Bubble Curtain=No Bubble Curtain

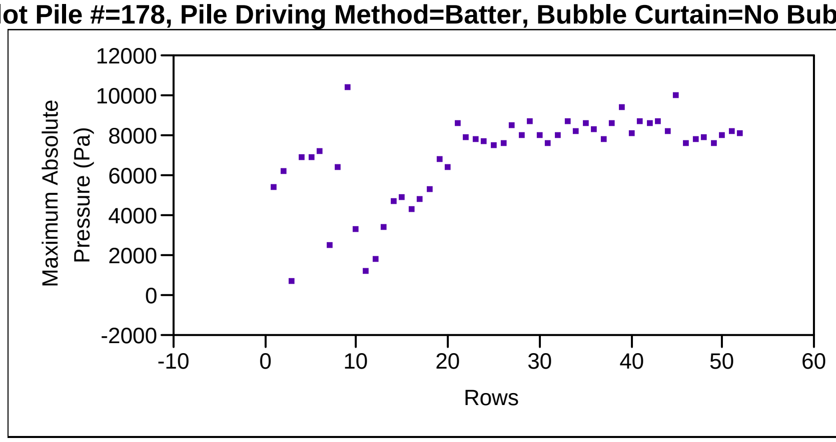

Overlay Plot Pile #=178, Pile Driving Method=Batter

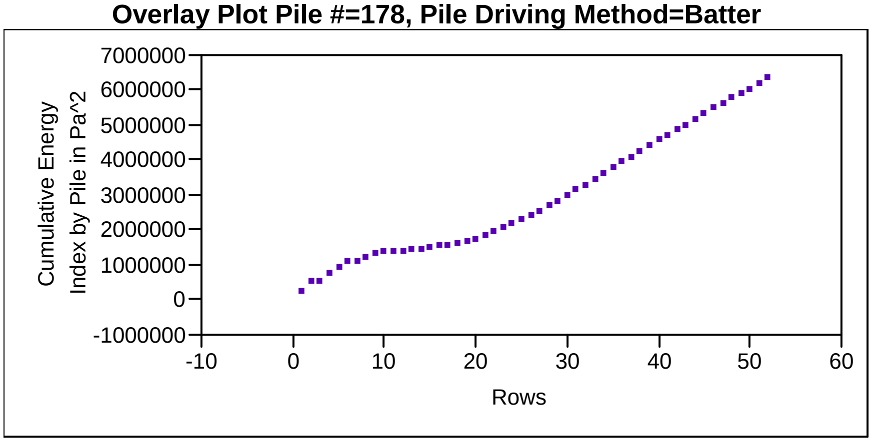

Overlay Plot Pile #=181, Pile Driving Method=Batter, Bubble Curtain=Bubble Curtain Present

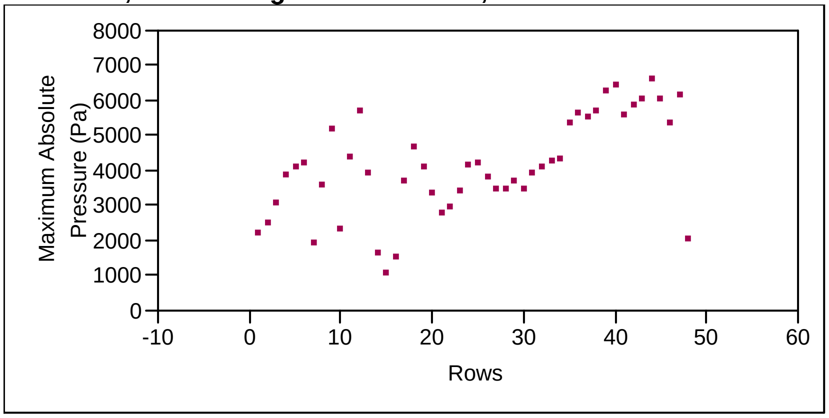

Overlay Plot Pile #=181, Pile Driving Method=Batter

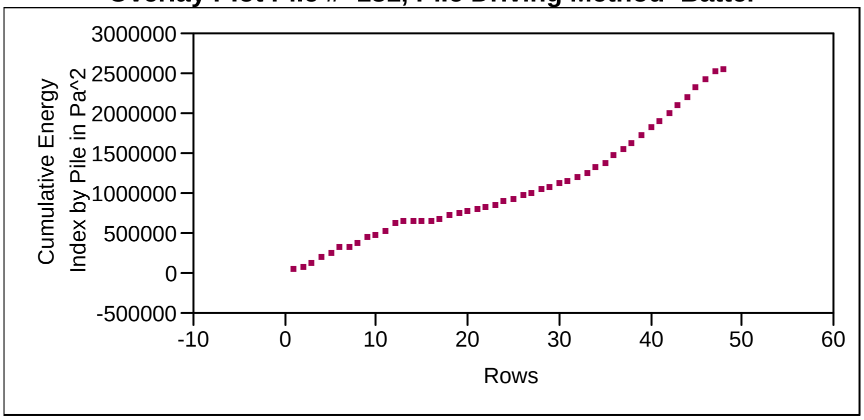

Overlay Plot Pile #=182, Pile Driving Method=Batter, Bubble Curtain=Bubble Curtain Present

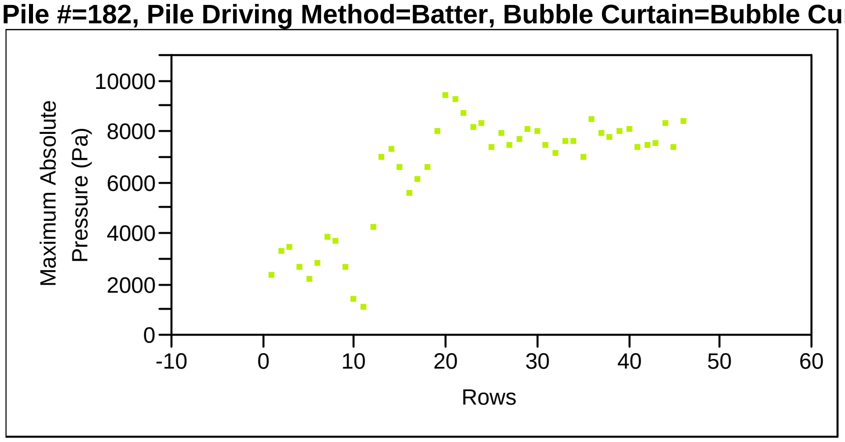

Overlay Plot Pile #=182, Pile Driving Method=Batter

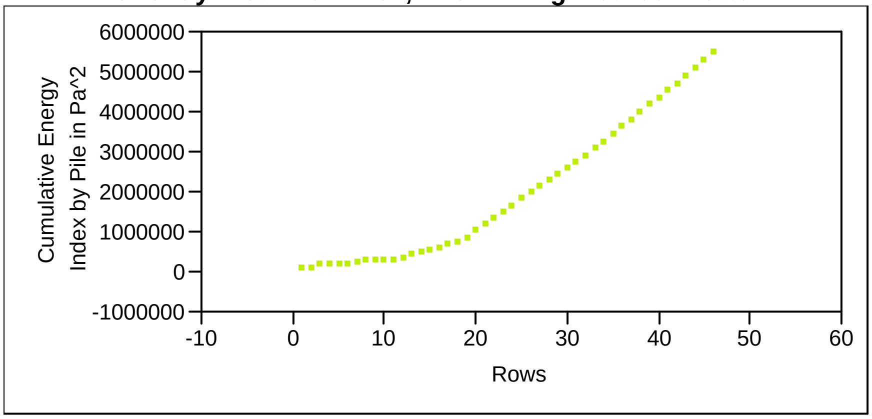

Overlay Plot Pile #=235, Pile Driving Method=Plumb, Bubble Curtain=Bubble Curtain Present

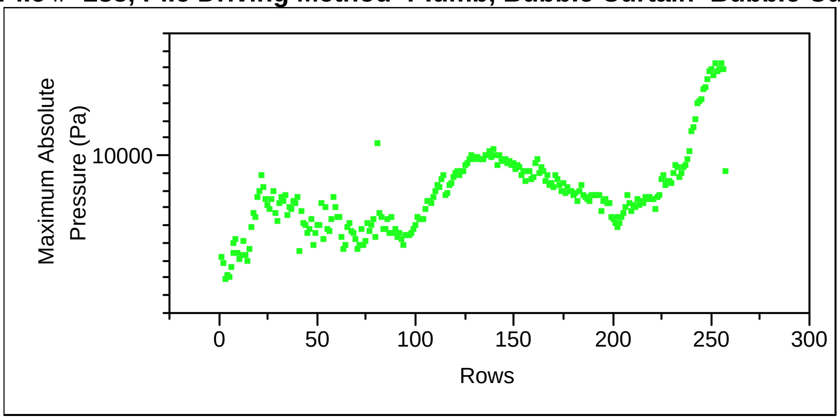

Overlay Plot Pile #=235, Pile Driving Method=Plumb

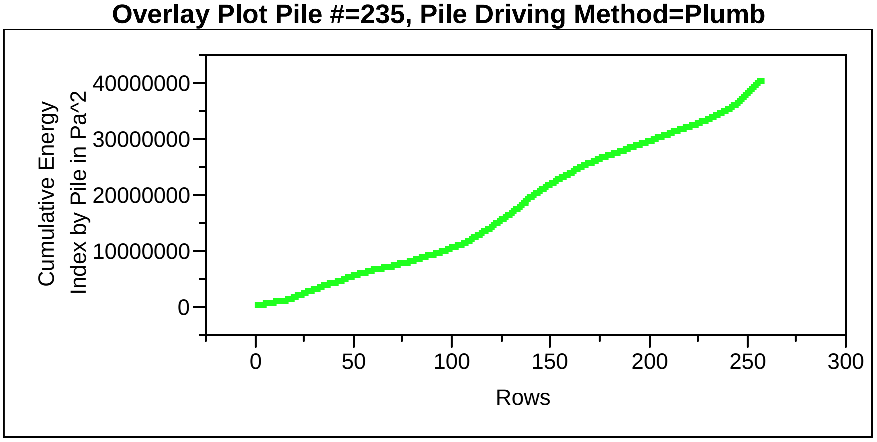

Overlay Plot Pile #=237, Pile Driving Method=Plumb, Bubble Curtain=Bubble Curtain Present

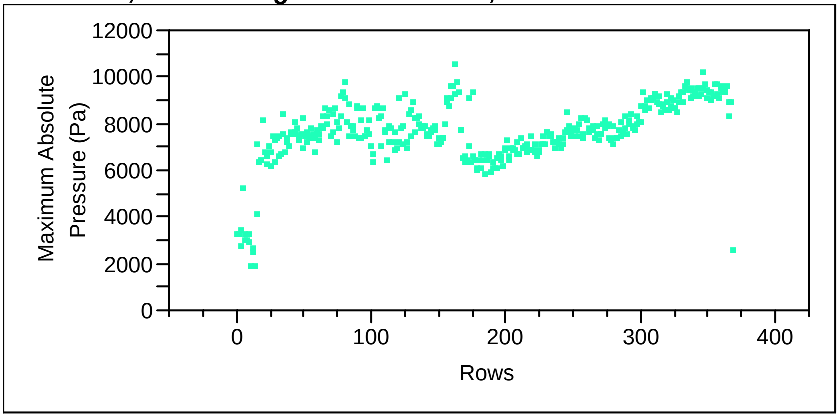

Overlay Plot Pile #=237, Pile Driving Method=Plumb

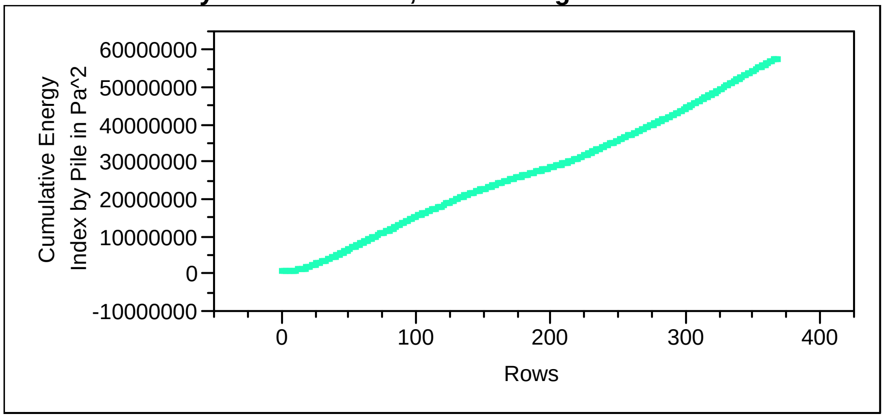

Overlay Plot Pile #=238, Pile Driving Method=Plumb, Bubble Curtain=Bubble Curtain Present

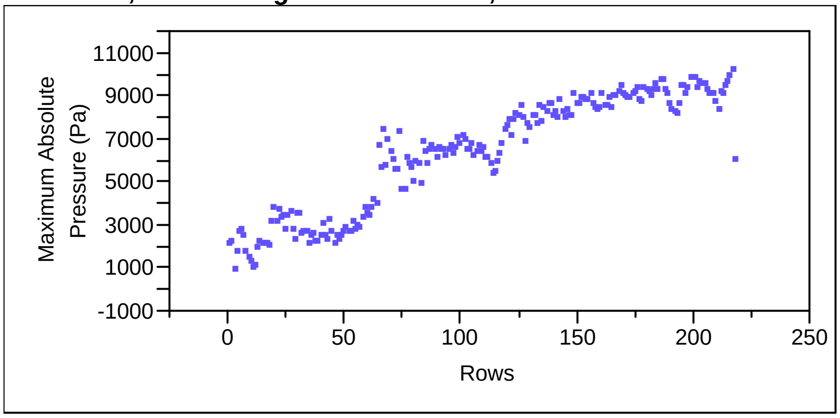

Overlay Plot Pile #=238, Pile Driving Method=Plumb

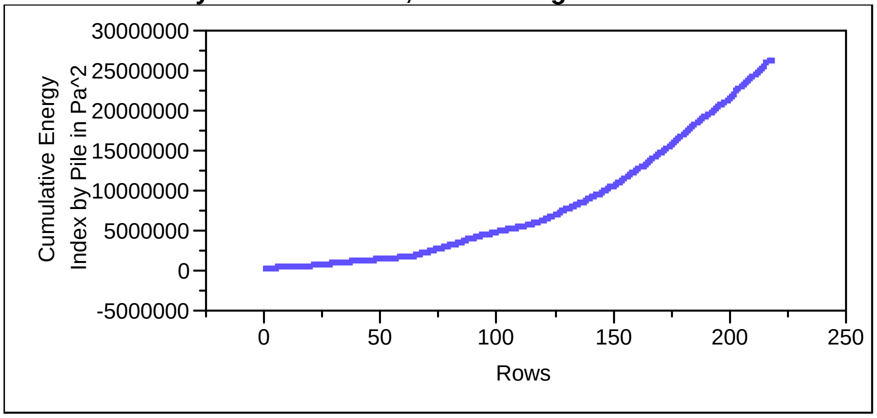

Overlay Plot Pile #=240, Pile Driving Method=Plumb, Bubble Curtain=No Bubble Curtain

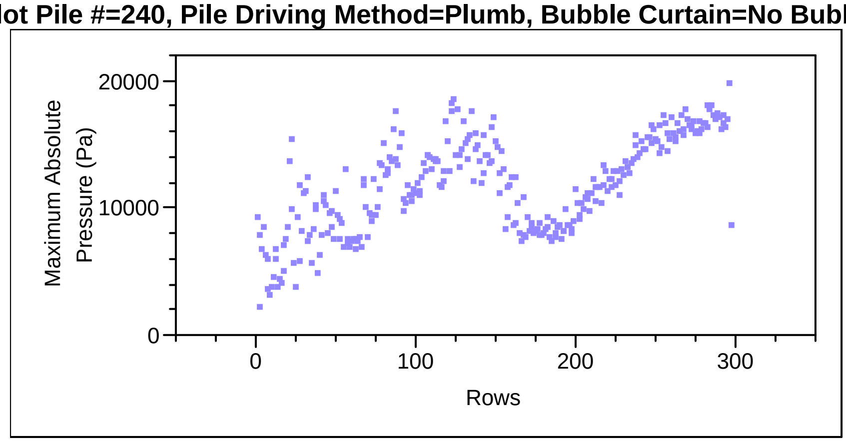

Overlay Plot Pile #=240, Pile Driving Method=Plumb

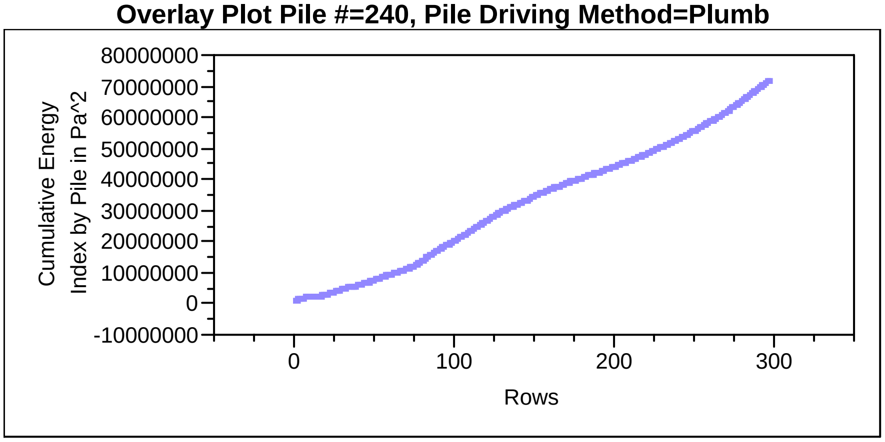

Overlay Plot Pile #=244, Pile Driving Method=Batter, Bubble Curtain=No Bubble Curtain

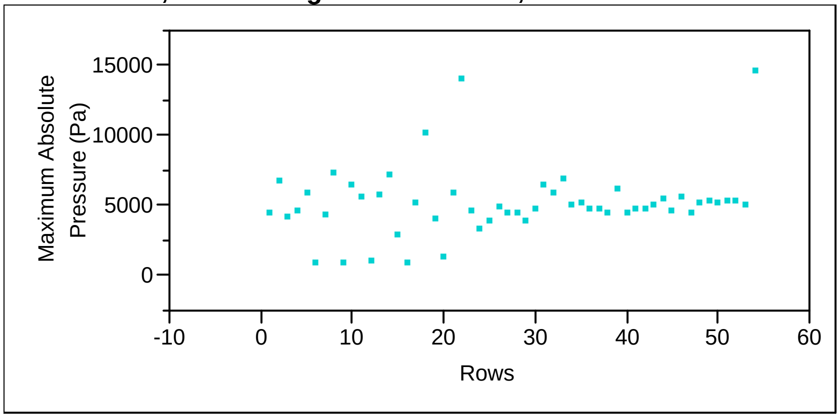

Overlay Plot Pile #=244, Pile Driving Method=Batter

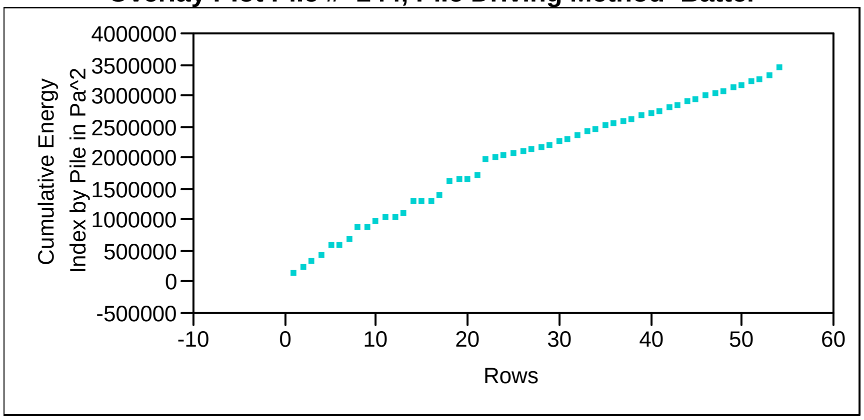

Overlay Plot Pile #=249, Pile Driving Method=Plumb, Bubble Curtain=Bubble Curtain Present

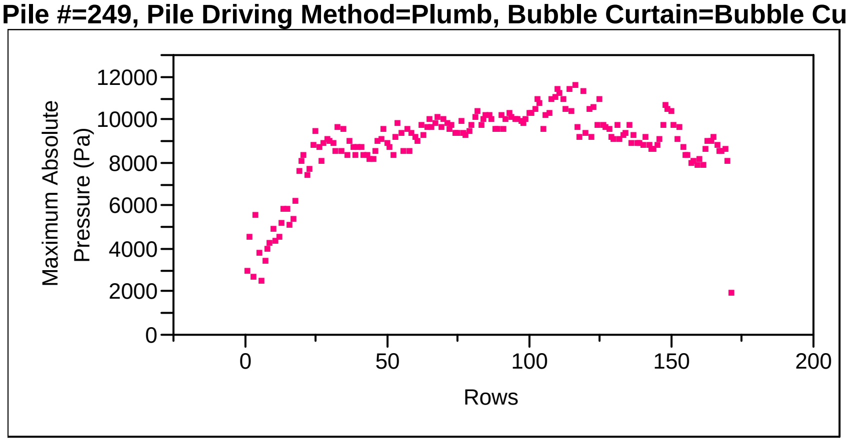

Overlay Plot Pile #=249, Pile Driving Method=Plumb

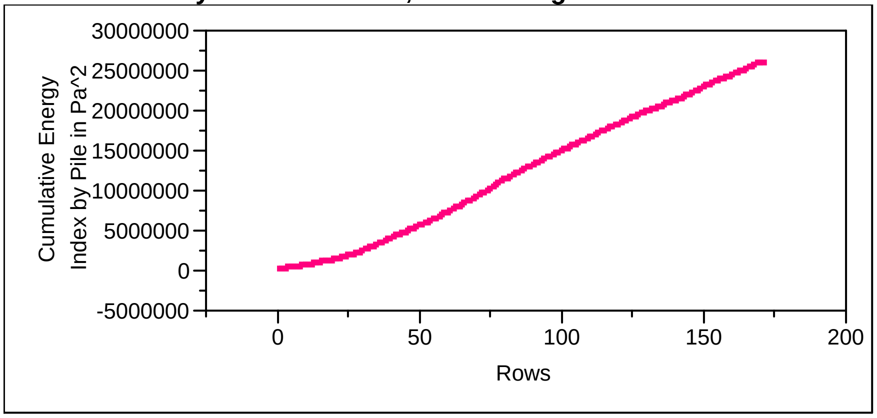

Overlay Plot Pile #=252, Pile Driving Method=Plumb, Bubble Curtain=Bubble Curtain Present

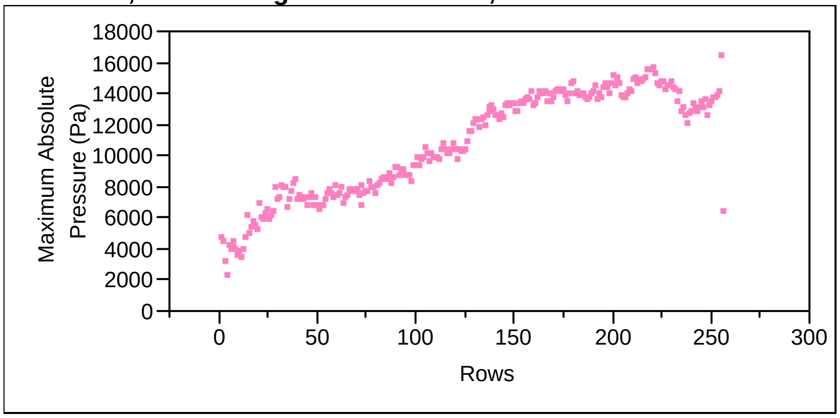

Overlay Plot Pile #=252, Pile Driving Method=Plumb

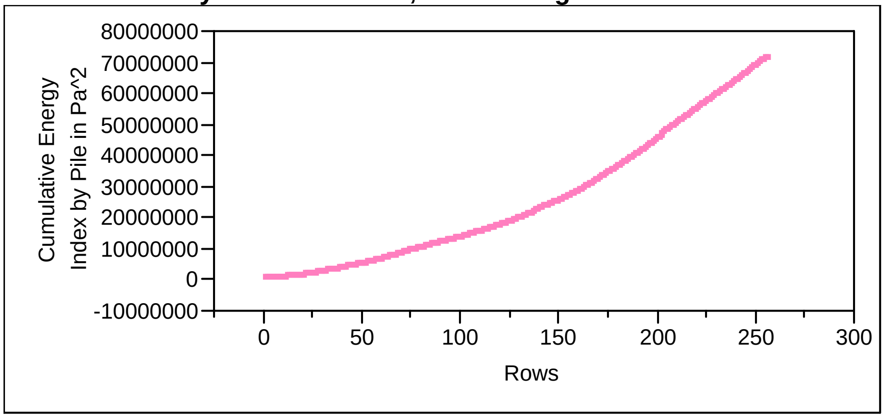

Overlay Plot Pile #=255, Pile Driving Method=Plumb, Bubble Curtain=Bubble Curtain Present

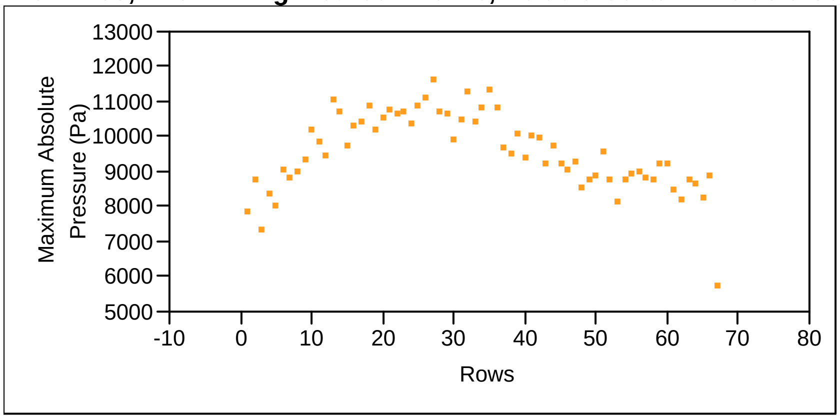

Overlay Plot Pile #=255, Pile Driving Method=Plumb

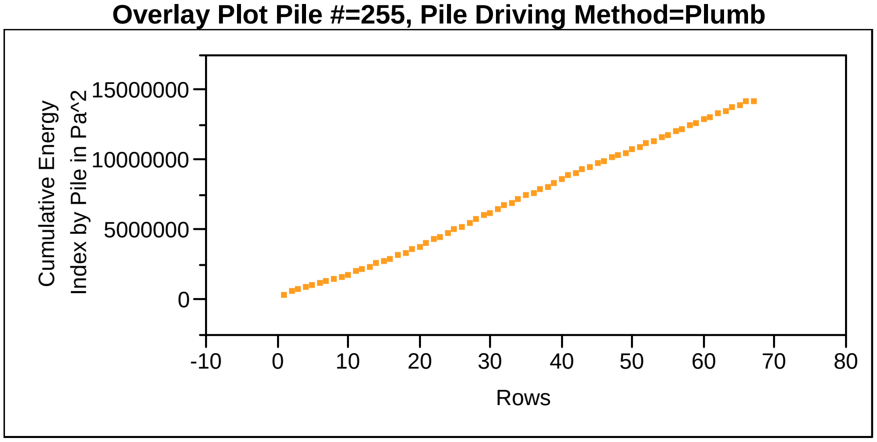

Overlay Plot Pile #=50N, Pile Driving Method=Plumb, Bubble Curtain=No Bubble Curtain

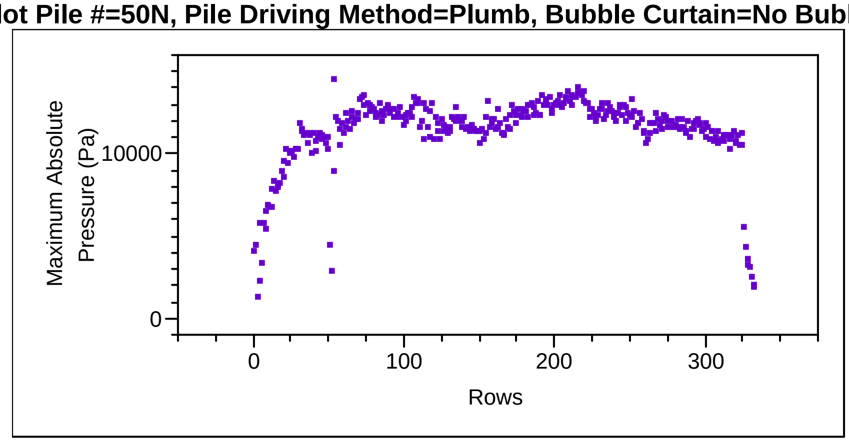

Overlay Plot Pile #=50N, Pile Driving Method=Plumb

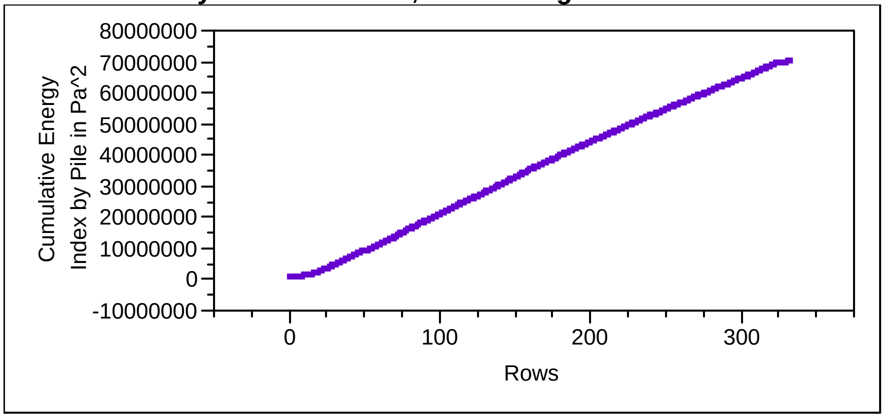

Overlay Plot Pile #=52N, Pile Driving Method=Plumb, Bubble Curtain=Bubble Curtain Present

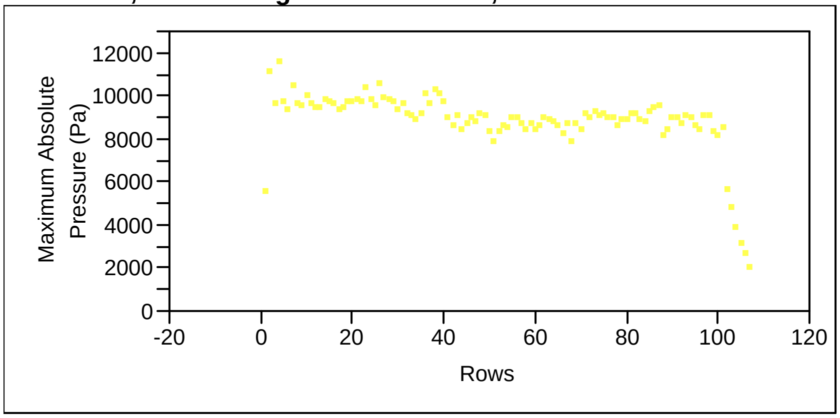

Overlay Plot Pile #=52N, Pile Driving Method=Plumb

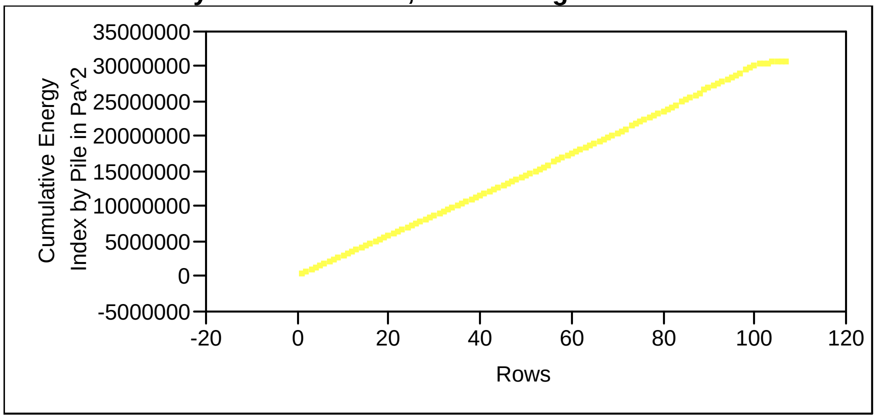

Bivariate Fit of Cumulative Energy Index by Pile in Pa^2 By Blow # Pile #=118N

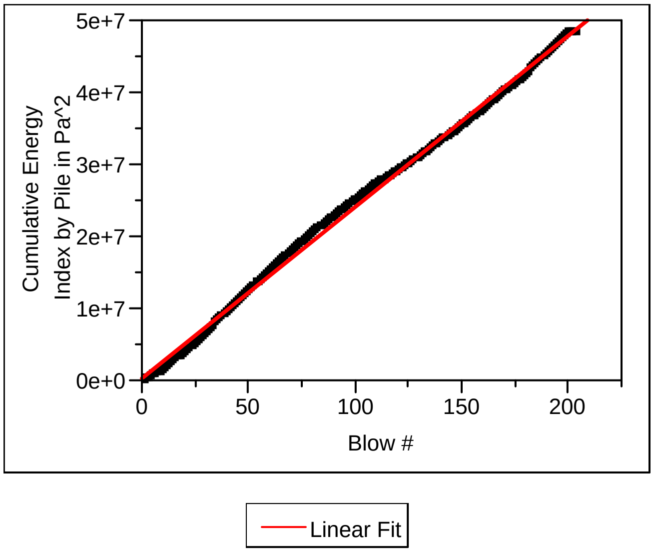

Linear Fit

Cumulative Energy Index by Pile in Pa^2 = 347287.31 + 238024.67 Blow #

Summary of Fit

RSquare	0.997359
RSquare Adj	0.997346
Root Mean Square Error	721329
Mean of Response	24625804
Observations (or Sum Wgts)	203

Analysis of Variance

Source	DF	Sum of Squares	Mean Square	F Ratio
Model	1	3.9495e+16	3.949e+16	75905.55
Error	201	1.0458e+14	5.203e+11	Prob > F
C. Total	202	3.9599e+16		<.0001

Parameter Estimates

Term	Estimate	Std Error	t Ratio	Prob>|t|
Intercept	347287.31	101630	3.42	0.0008
Blow #	238024.67	863.9432	275.51	<.0001

Bivariate Fit of Cumulative Energy Index by Pile in Pa^2 By Blow # Pile #=120N

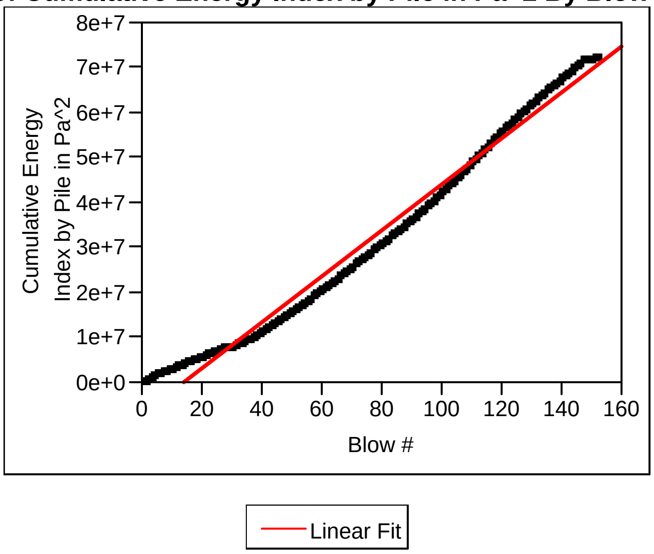

Linear Fit

Cumulative Energy Index by Pile in Pa^2 = -7087255 + 510019.85 Blow #

Summary of Fit

RSquare	0.983382
RSquare Adj	0.983271
Root Mean Square Error	2928475
Mean of Response	31929264
Observations (or Sum Wgts)	152

Analysis of Variance

Source	DF	Sum of Squares	Mean Square	F Ratio
Model	1	7.6121e+16	7.612e+16	8876.093
Error	150	1.2864e+15	8.576e+12	Prob > F
C. Total	151	7.7407e+16		<.0001

Parameter Estimates

Term	Estimate	Std Error	t Ratio	Prob>|t|
Intercept	-7087255	477415.1	-14.85	<.0001
Blow #	510019.85	5413.475	94.21	<.0001

Bivariate Fit of Cumulative Energy Index by Pile in Pa^2 By Blow # Pile #=121N

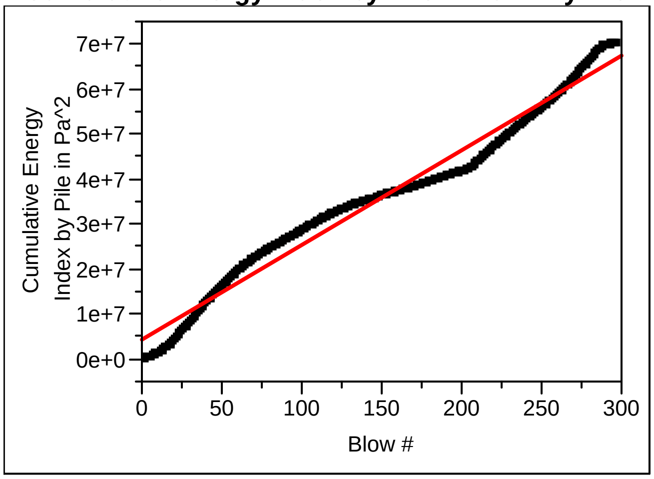

Linear Fit

Cumulative Energy Index by Pile in Pa^2 = 4166782.3 + 210828.6 Blow #

Summary of Fit

RSquare	0.973502
RSquare Adj	0.973412
Root Mean Square Error	2982217
Mean of Response	35474829
Observations (or Sum Wgts)	296

Analysis of Variance

Source	DF	Sum of Squares	Mean Square	F Ratio
Model	1	9.6061e+16	9.606e+16	10801.14
Error	294	2.6147e+15	8.894e+12	Prob > F
C. Total	295	9.8676e+16		<.0001

Parameter Estimates

Term	Estimate	Std Error	t Ratio	Prob>|t|
Intercept	4166782.3	347555.9	11.99	<.0001
Blow #	210828.6	2028.592	103.93	<.0001

Bivariate Fit of Cumulative Energy Index by Pile in Pa^2 By Blow # Pile #=167

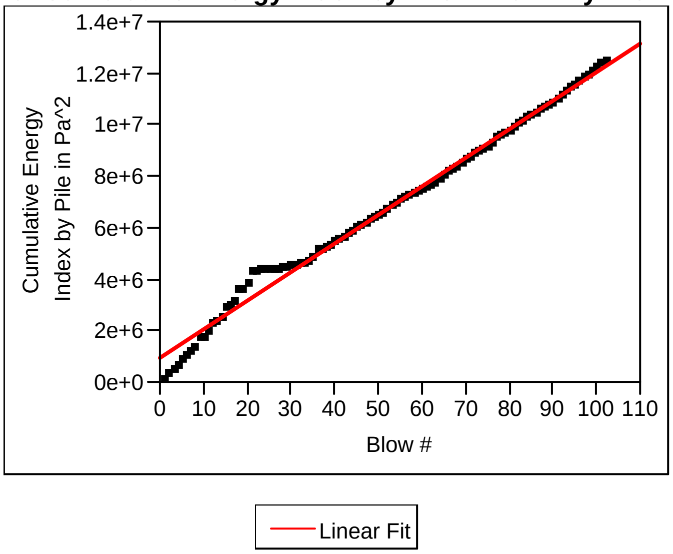

Linear Fit

Cumulative Energy Index by Pile in Pa^2 = 926248.22 + 111419.21 Blow #

Summary of Fit

RSquare	0.990317
RSquare Adj	0.99022
Root Mean Square Error	327619.8
Mean of Response	6664337
Observations (or Sum Wgts)	102

Analysis of Variance

Source	DF	Sum of Squares	Mean Square	F Ratio
Model	1	1.0977e+15	1.098e+15	10227.21
Error	100	1.0733e+13	1.073e+11	Prob > F
C. Total	101	1.1085e+15		<.0001

Parameter Estimates

Term	Estimate	Std Error	t Ratio	Prob>|t|
Intercept	926248.22	65358.39	14.17	<.0001
Blow #	111419.21	1101.746	101.13	<.0001

Bivariate Fit of Cumulative Energy Index by Pile in Pa^2 By Blow # Pile #=171

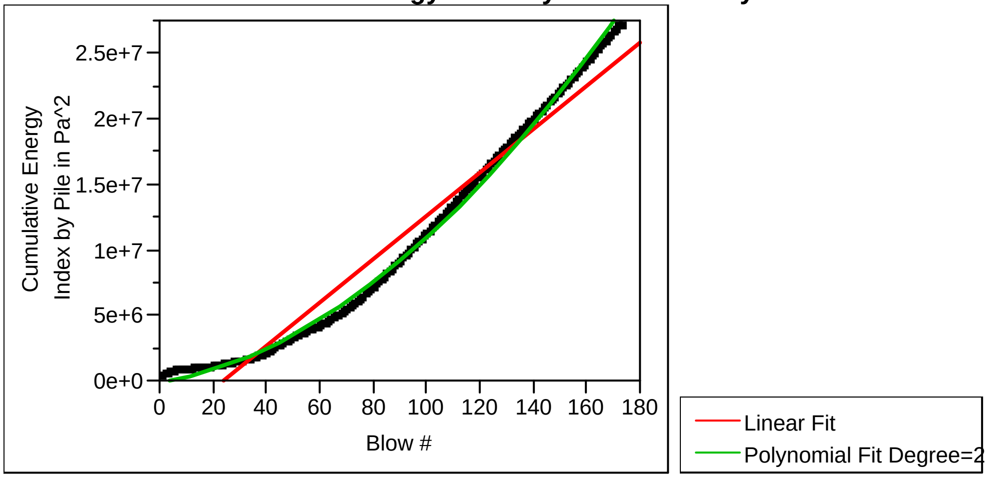

Linear Fit

Cumulative Energy Index by Pile in Pa^2 = -3942388 + 165519.36 Blow #

Summary of Fit

RSquare	0.958479
RSquare Adj	0.958236
Root Mean Square Error	1730471
Mean of Response	10457796
Observations (or Sum Wgts)	173

Analysis of Variance

Source	DF	Sum of Squares	Mean Square	F Ratio
Model	1	1.1821e+16	1.182e+16	3947.404
Error	171	5.1206e+14	2.995e+12	Prob > F
C. Total	172	1.2333e+16		<.0001

Parameter Estimates

Term	Estimate	Std Error	t Ratio	Prob>|t|
Intercept	-3942388	264275.4	-14.92	<.0001
Blow #	165519.36	2634.469	62.83	<.0001

Polynomial Fit Degree=2

Cumulative Energy Index by Pile in Pa^2 = -5789855 + 165519.36 Blow # + 740.76453 (Blow #-87)^2

Summary of Fit

RSquare	0.996778
RSquare Adj	0.99674
Root Mean Square Error	483457.3
Mean of Response	10457796
Observations (or Sum Wgts)	173

Analysis of Variance

Source	DF	Sum of Squares	Mean Square	F Ratio
Model	2	1.2293e+16	6.146e+15	26297.21
Error	170	3.9734e+13	2.337e+11	Prob > F
C. Total	172	1.2333e+16		<.0001

Parameter Estimates

Term	Estimate	Std Error	t Ratio	Prob>|t|
Intercept	-5789855	84500.24	-68.52	<.0001
Blow #	165519.36	736.0153	224.89	<.0001
(Blow #-87)^2	740.76453	16.47841	44.95	<.0001

Bivariate Fit of Cumulative Energy Index by Pile in Pa^2 By Blow # Pile #=172

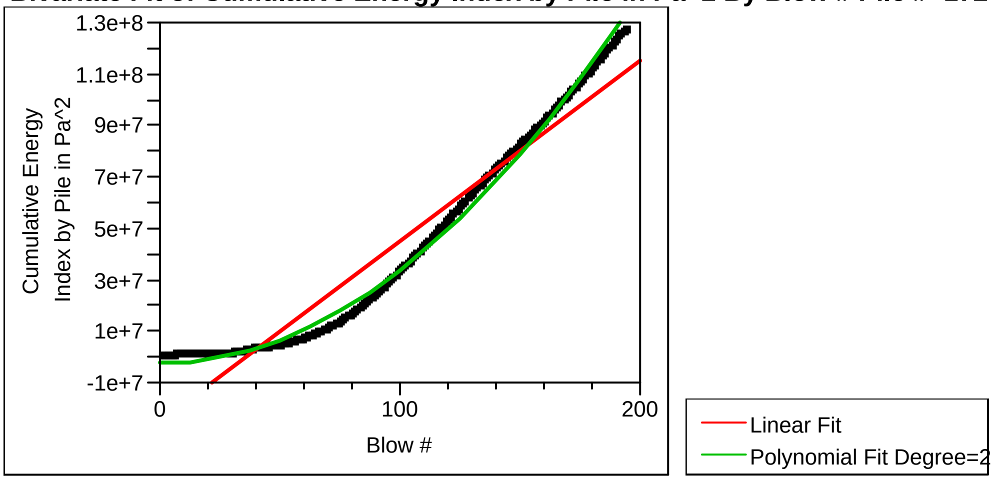

Linear Fit

Cumulative Energy Index by Pile in Pa^2 = -25390210 + 703834.13 Blow #

Summary of Fit

RSquare	0.932995
RSquare Adj	0.932646
Root Mean Square Error	10617919
Mean of Response	43233617
Observations (or Sum Wgts)	194

Analysis of Variance

Source	DF	Sum of Squares	Mean Square	F Ratio
Model	1	3.0141e+17	3.014e+17	2673.463
Error	192	2.1646e+16	1.127e+14	Prob > F
C. Total	193	3.2305e+17		<.0001

Parameter Estimates

Term	Estimate	Std Error	t Ratio	Prob>|t|
Intercept	-25390210	1530558	-16.59	<.0001
Blow #	703834.13	13612.35	51.71	<.0001

Polynomial Fit Degree=2

Cumulative Energy Index by Pile in Pa^2 = -36703690 + 703834.13 Blow # + 3607.3271 (Blow #-97.5)^2

Summary of Fit

RSquare	0.994481
RSquare Adj	0.994423
Root Mean Square Error	3055255
Mean of Response	43233617
Observations (or Sum Wgts)	194

Analysis of Variance

Source	DF	Sum of Squares	Mean Square	F Ratio
Model	2	3.2127e+17	1.606e+17	17208.59
Error	191	1.7829e+15	9.335e+12	Prob > F
C. Total	193	3.2305e+17		<.0001

Parameter Estimates

Term	Estimate	Std Error	t Ratio	Prob>|t|
Intercept	-36703690	504095	-72.81	<.0001
Blow #	703834.13	3916.889	179.69	<.0001
(Blow #-97.5)^2	3607.3271	78.20026	46.13	<.0001

Bivariate Fit of Cumulative Energy Index by Pile in Pa^2 By Blow # Pile #=174

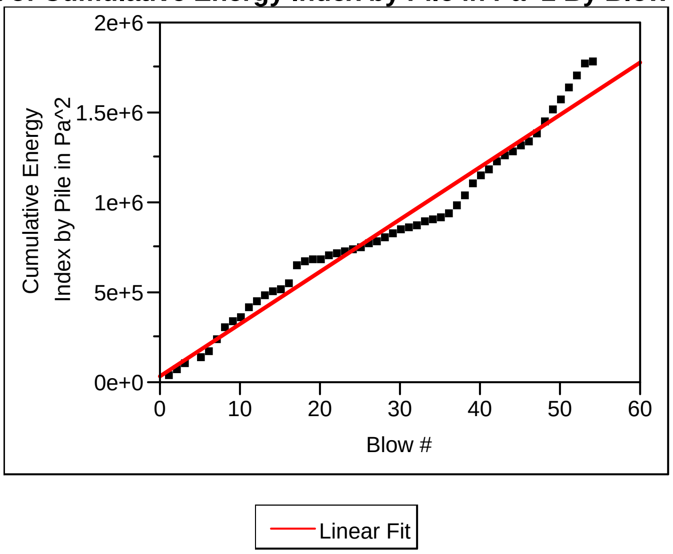

Linear Fit

Cumulative Energy Index by Pile in Pa^2 = 32969.503 + 29116.271 Blow #

Summary of Fit

RSquare	0.970951
RSquare Adj	0.970381
Root Mean Square Error	79017.86
Mean of Response	846577
Observations (or Sum Wgts)	53

Analysis of Variance

Source	DF	Sum of Squares	Mean Square	F Ratio
Model	1	1.0643e+13	1.064e+13	1704.637
Error	51	3.1843e+11	6.2438e+9	Prob > F
C. Total	52	1.0962e+13		<.0001

Parameter Estimates

Term	Estimate	Std Error	t Ratio	Prob>|t|
Intercept	32969.503	22497.45	1.47	0.1489
Blow #	29116.271	705.2122	41.29	<.0001

Bivariate Fit of Cumulative Energy Index by Pile in Pa^2 By Blow # Pile #=177

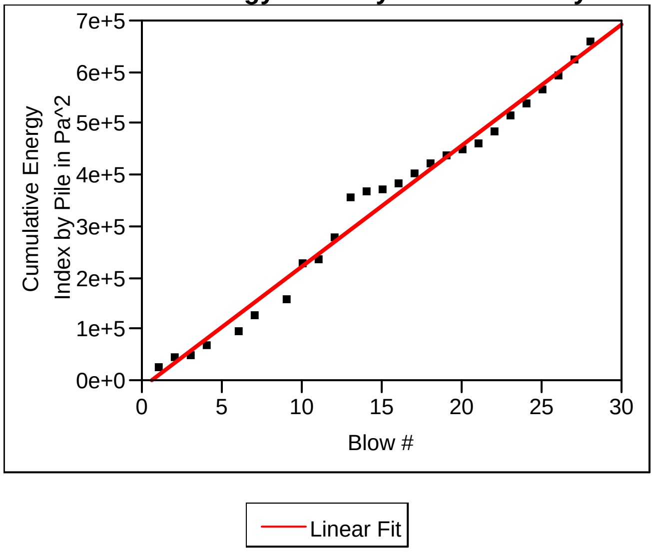

Linear Fit

Cumulative Energy Index by Pile in Pa^2 = -14292.82 + 23581.464 Blow #

Summary of Fit

RSquare	0.985261
RSquare Adj	0.984647
Root Mean Square Error	24164.41
Mean of Response	342150.1
Observations (or Sum Wgts)	26

Analysis of Variance

Source	DF	Sum of Squares	Mean Square	F Ratio
Model	1	9.3681e+11	9.368e+11	1604.352
Error	24	1.4014e+10	583918931	Prob > F
C. Total	25	9.5083e+11		<.0001

Parameter Estimates

Term	Estimate	Std Error	t Ratio	Prob>|t|
Intercept	-14292.82	10082.17	-1.42	0.1692
Blow #	23581.464	588.7365	40.05	<.0001

Bivariate Fit of Cumulative Energy Index by Pile in Pa^2 By Blow # Pile #=178

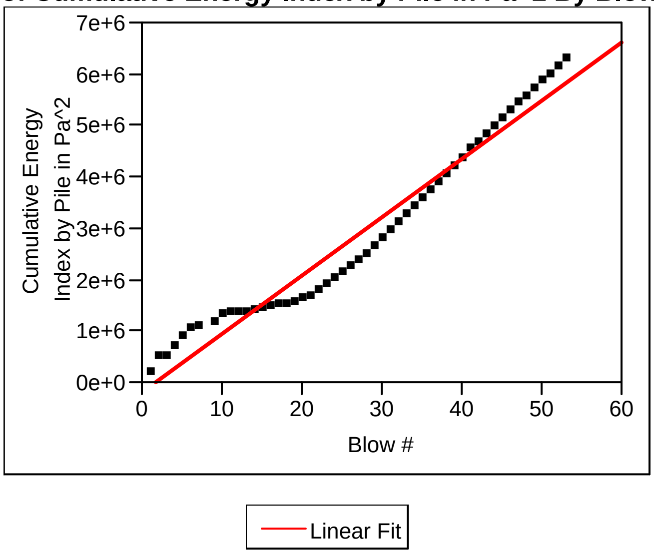

Linear Fit

Cumulative Energy Index by Pile in Pa^2 = -201301.5 + 113414.73 Blow #

Summary of Fit

RSquare	0.959963
RSquare Adj	0.959162
Root Mean Square Error	359331.2
Mean of Response	2902336
Observations (or Sum Wgts)	52

Analysis of Variance

Source	DF	Sum of Squares	Mean Square	F Ratio
Model	1	1.5479e+14	1.548e+14	1198.840
Error	50	6.4559e+12	1.291e+11	Prob > F
C. Total	51	1.6125e+14		<.0001

Parameter Estimates

Term	Estimate	Std Error	t Ratio	Prob>|t|
Intercept	-201301.5	102557.1	-1.96	0.0552
Blow #	113414.73	3275.585	34.62	<.0001

Bivariate Fit of Cumulative Energy Index by Pile in Pa^2 By Blow # Pile #=181

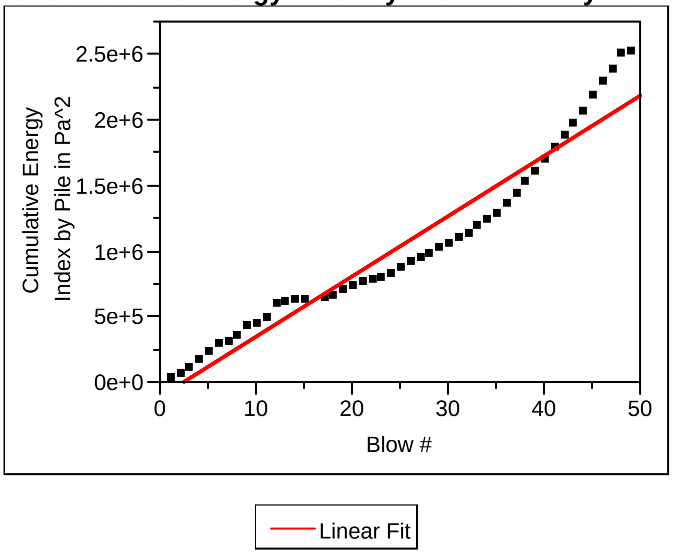

Linear Fit
Cumulative Energy Index by Pile in Pa^2 = -114797 + 46071.017 Blow #

Summary of Fit

RSquare	0.937537
RSquare Adj	0.936179
Root Mean Square Error	172837.5
Mean of Response	1045617
Observations (or Sum Wgts)	48

Analysis of Variance

Source	DF	Sum of Squares	Mean Square	F Ratio
Model	1	2.0625e+13	2.063e+13	690.4398
Error	46	1.3741e+12	2.987e+10	Prob > F
C. Total	47	2.2e+13		<.0001

Parameter Estimates

Term	Estimate	Std Error	t Ratio	Prob>|t|
Intercept	-114797	50721.23	-2.26	0.0284
Blow #	46071.017	1753.335	26.28	<.0001

Bivariate Fit of Cumulative Energy Index by Pile in Pa^2 By Blow # Pile #=182

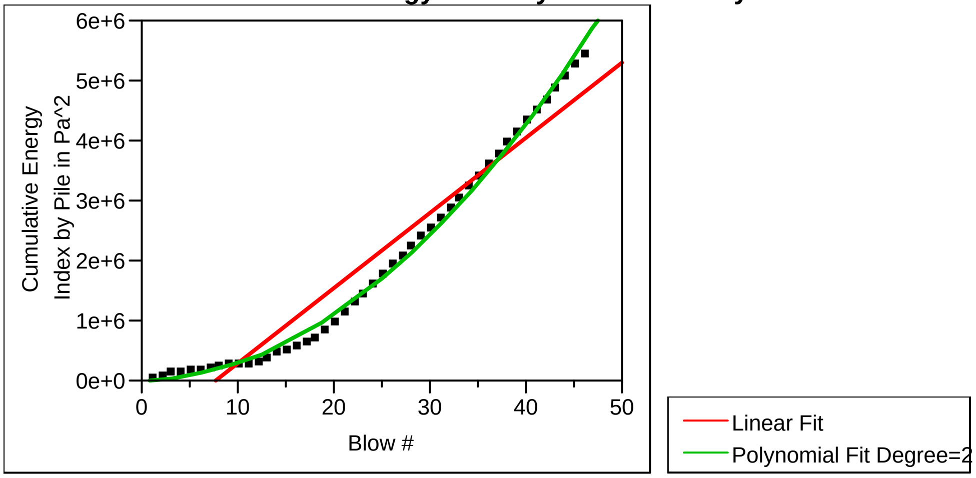

Linear Fit

Cumulative Energy Index by Pile in Pa^2 = -977025.3 + 125341.98 Blow #

Summary of Fit

RSquare	0.940806
RSquare Adj	0.939461
Root Mean Square Error	426777
Mean of Response	1968511
Observations (or Sum Wgts)	46

Analysis of Variance

Source	DF	Sum of Squares	Mean Square	F Ratio
Model	1	1.2737e+14	1.274e+14	699.3233
Error	44	8.0141e+12	1.821e+11	Prob > F
C. Total	45	1.3539e+14		<.0001

Parameter Estimates

Term	Estimate	Std Error	t Ratio	Prob>|t|
Intercept	-977025.3	127930	-7.64	<.0001
Blow #	125341.98	4739.773	26.44	<.0001

Polynomial Fit Degree=2

Cumulative Energy Index by Pile in Pa^2 = -1430498 + 125341.98 Blow # + 2572.8939 (Blow #-23.5)^2

Summary of Fit

RSquare	0.996622
RSquare Adj	0.996465
Root Mean Square Error	103134.5
Mean of Response	1968511
Observations (or Sum Wgts)	46

Analysis of Variance

Source	DF	Sum of Squares	Mean Square	F Ratio
Model	2	1.3493e+14	6.747e+13	6342.673
Error	43	4.5738e+11	1.064e+10	Prob > F
C. Total	45	1.3539e+14		<.0001

Parameter Estimates

Term	Estimate	Std Error	t Ratio	Prob>|t|
Intercept	-1430498	35287.61	-40.54	<.0001
Blow #	125341.98	1145.409	109.43	<.0001
(Blow #-23.5)^2	2572.8939	96.52929	26.65	<.0001

Bivariate Fit of Cumulative Energy Index by Pile in Pa^2 By Blow # Pile #=235

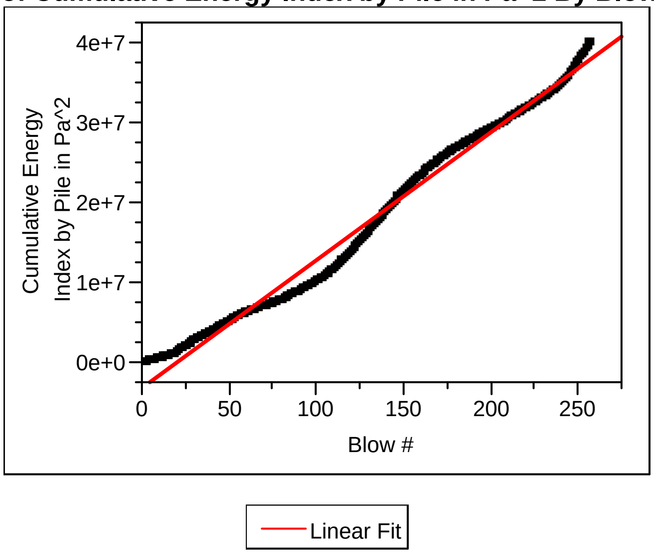

Linear Fit

Cumulative Energy Index by Pile in Pa^2 = -3150992 + 159659.54 Blow #

Summary of Fit

RSquare	0.986518
RSquare Adj	0.986465
Root Mean Square Error	1390120
Mean of Response	17445089
Observations (or Sum Wgts)	257

Analysis of Variance

Source	DF	Sum of Squares	Mean Square	F Ratio
Model	1	3.6058e+16	3.606e+16	18659.35
Error	255	4.9277e+14	1.932e+12	Prob > F
C. Total	256	3.6551e+16		<.0001

Parameter Estimates

Term	Estimate	Std Error	t Ratio	Prob>|t|
Intercept	-3150992	173934	-18.12	<.0001
Blow #	159659.54	1168.817	136.60	<.0001

Bivariate Fit of Cumulative Energy Index by Pile in Pa^2 By Blow # Pile #=237

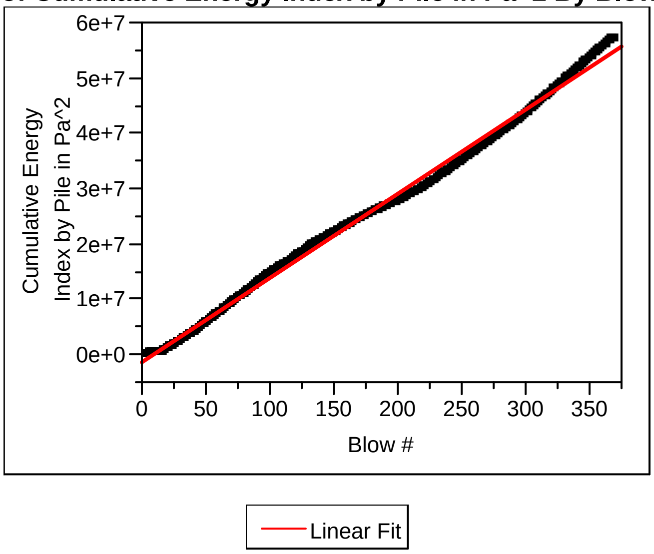

Linear Fit

Cumulative Energy Index by Pile in Pa^2 = -1459923 + 152461.13 Blow #

Summary of Fit

RSquare	0.99563
RSquare Adj	0.995618
Root Mean Square Error	1075908
Mean of Response	26669156
Observations (or Sum Wgts)	368

Analysis of Variance

Source	DF	Sum of Squares	Mean Square	F Ratio
Model	1	9.6533e+16	9.653e+16	83392.46
Error	366	4.2367e+14	1.158e+12	Prob > F
C. Total	367	9.6957e+16		0.0000

Parameter Estimates

Term	Estimate	Std Error	t Ratio	Prob>|t|
Intercept	-1459923	112400.2	-12.99	<.0001
Blow #	152461.13	527.9536	288.78	0.0000

Bivariate Fit of Cumulative Energy Index by Pile in Pa^2 By Blow # Pile #=238

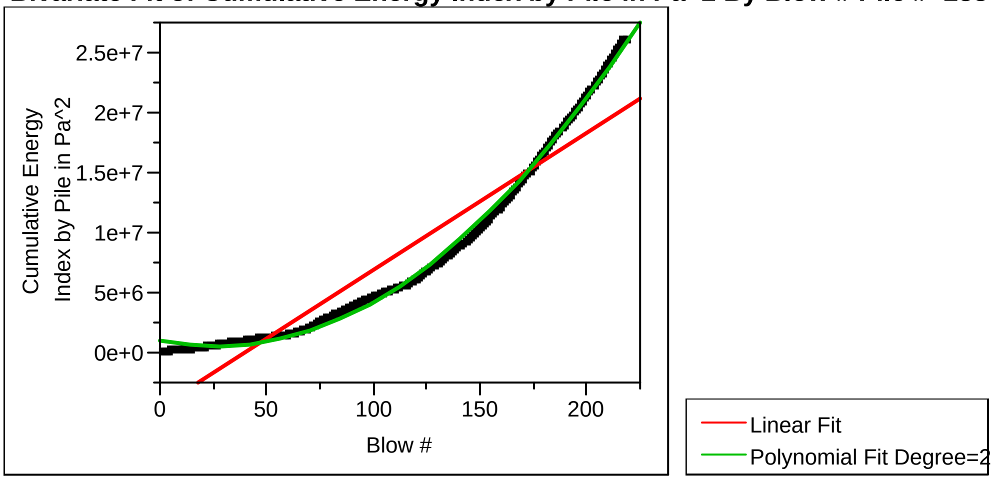

Linear Fit

Cumulative Energy Index by Pile in Pa^2 = -4550087 + 114011.08 Blow #

Summary of Fit

RSquare	0.893657
RSquare Adj	0.893164
Root Mean Square Error	2486449
Mean of Response	7934126
Observations (or Sum Wgts)	218

Analysis of Variance

Source	DF	Sum of Squares	Mean Square	F Ratio
Model	1	1.1222e+16	1.122e+16	1815.156
Error	216	1.3354e+15	6.182e+12	Prob > F
C. Total	217	1.2557e+16		<.0001

Parameter Estimates

Term	Estimate	Std Error	t Ratio	Prob>|t|
Intercept	-4550087	337969.3	-13.46	<.0001
Blow #	114011.08	2676.024	42.60	<.0001

Polynomial Fit Degree=2

Cumulative Energy Index by Pile in Pa^2 = -7282595 + 114011.08 Blow # + 689.98372 (Blow #-109.5)^2

Summary of Fit

RSquare	0.997347
RSquare Adj	0.997323
Root Mean Square Error	393624.4
Mean of Response	7934126
Observations (or Sum Wgts)	218

Analysis of Variance

Source	DF	Sum of Squares	Mean Square	F Ratio
Model	2	1.2524e+16	6.262e+15	40416.14
Error	215	3.3312e+13	1.549e+11	Prob > F
C. Total	217	1.2557e+16		<.0001

Parameter Estimates

Term	Estimate	Std Error	t Ratio	Prob>|t|
Intercept	-7282595	61245.95	-118.9	<.0001
Blow #	114011.08	423.6357	269.13	<.0001
(Blow #-109.5)^2	689.98372	7.526619	91.67	<.0001

Bivariate Fit of Cumulative Energy Index by Pile in Pa^2 By Blow # Pile #=240

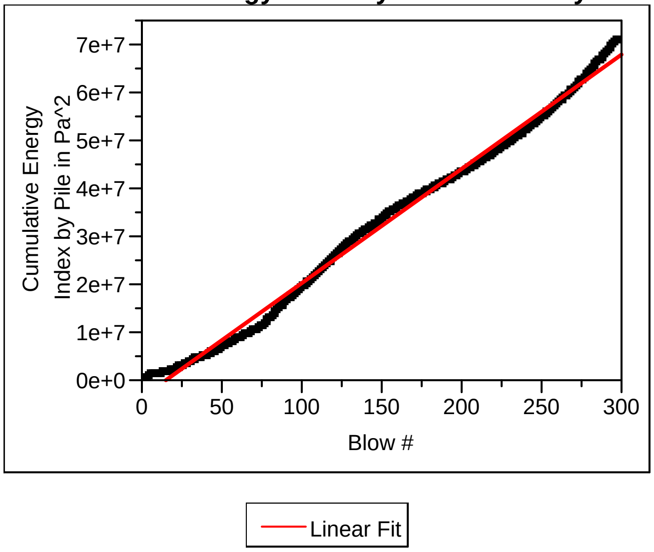

Linear Fit

Cumulative Energy Index by Pile in Pa^2 = -3737253 + 239383.29 Blow #

Summary of Fit

RSquare	0.994338
RSquare Adj	0.994319
Root Mean Square Error	1554003
Mean of Response	31930857
Observations (or Sum Wgts)	297

Analysis of Variance

Source	DF	Sum of Squares	Mean Square	F Ratio
Model	1	1.251e+17	1.251e+17	51804.44
Error	295	7.124e+14	2.415e+12	Prob > F
C. Total	296	1.2582e+17		0.0000

Parameter Estimates

Term	Estimate	Std Error	t Ratio	Prob>|t|
Intercept	-3737253	180801.2	-20.67	<.0001
Blow #	239383.29	1051.745	227.61	0.0000

Bivariate Fit of Cumulative Energy Index by Pile in Pa^2 By Blow # Pile #=244

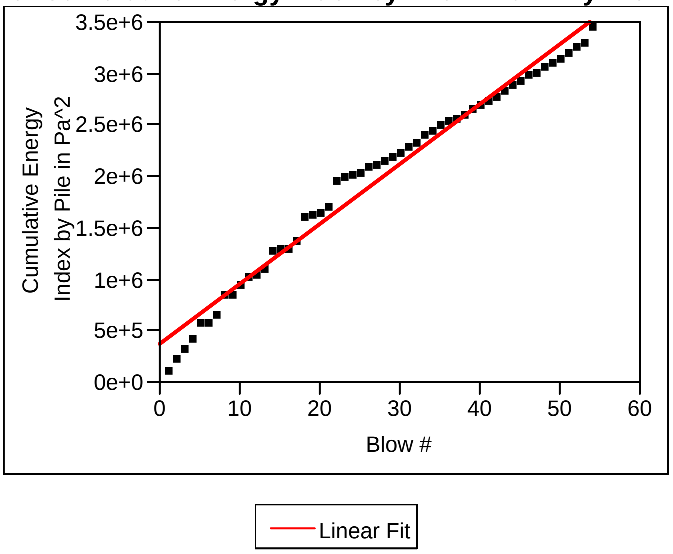

Linear Fit

Cumulative Energy Index by Pile in Pa^2 = 365738.42 + 58254.447 Blow #

Summary of Fit

RSquare	0.978304
RSquare Adj	0.977887
Root Mean Square Error	137784.9
Mean of Response	1967736
Observations (or Sum Wgts)	54

Analysis of Variance

Source	DF	Sum of Squares	Mean Square	F Ratio
Model	1	4.4515e+13	4.452e+13	2344.802
Error	52	9.872e+11	1.898e+10	Prob > F
C. Total	53	4.5502e+13		<.0001

Parameter Estimates

Term	Estimate	Std Error	t Ratio	Prob>|t|
Intercept	365738.42	38027.25	9.62	<.0001
Blow #	58254.447	1203.029	48.42	<.0001

Bivariate Fit of Cumulative Energy Index by Pile in Pa^2 By Blow # Pile #=249

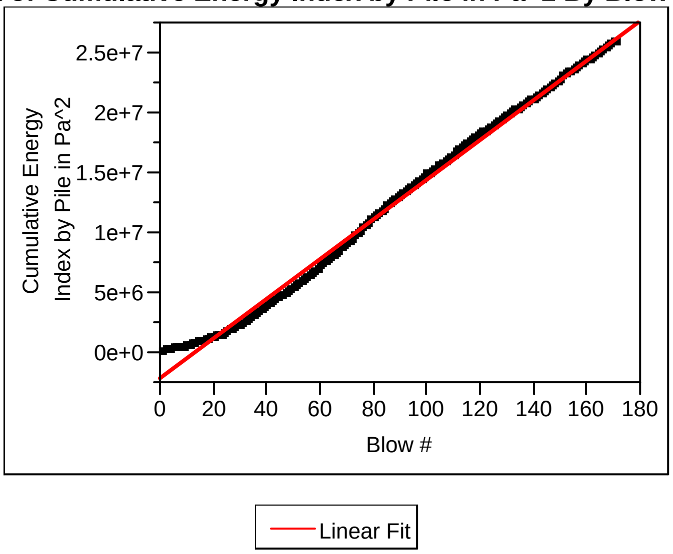

Linear Fit

Cumulative Energy Index by Pile in Pa^2 = -2124712 + 165411.14 Blow #

Summary of Fit

RSquare	0.995415
RSquare Adj	0.995388
Root Mean Square Error	557421.8
Mean of Response	12100646
Observations (or Sum Wgts)	171

Analysis of Variance

Source	DF	Sum of Squares	Mean Square	F Ratio
Model	1	1.14e+16	1.14e+16	36690.51
Error	169	5.2512e+13	3.107e+11	Prob > F
C. Total	170	1.1453e+16		<.0001

Parameter Estimates

Term	Estimate	Std Error	t Ratio	Prob>|t|
Intercept	-2124712	85629.52	-24.81	<.0001
Blow #	165411.14	863.5508	191.55	<.0001

Bivariate Fit of Cumulative Energy Index by Pile in Pa^2 By Blow # Pile #=252

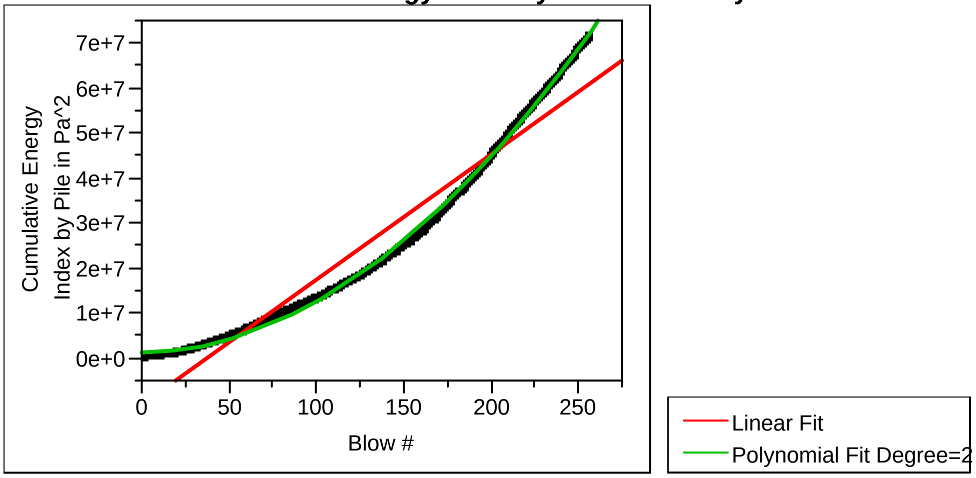

Linear Fit

Cumulative Energy Index by Pile in Pa^2 = -10295780 + 277428.42 Blow #

Summary of Fit

RSquare	0.941594
RSquare Adj	0.941365
Root Mean Square Error	5126195
Mean of Response	25353772
Observations (or Sum Wgts)	256

Analysis of Variance

Source	DF	Sum of Squares	Mean Square	F Ratio
Model	1	1.0761e+17	1.076e+17	4094.904
Error	254	6.6746e+15	2.628e+13	Prob > F
C. Total	255	1.1428e+17		<.0001

Parameter Estimates

Term	Estimate	Std Error	t Ratio	Prob>|t|
Intercept	-10295780	642656.2	-16.02	<.0001
Blow #	277428.42	4335.399	63.99	<.0001

Polynomial Fit Degree=2

Cumulative Energy Index by Pile in Pa^2 = -15943763 + 277428.42 Blow # + 1034.1925 (Blow #-128.5)^2

Summary of Fit

RSquare	0.998759
RSquare Adj	0.998749
Root Mean Square Error	748690
Mean of Response	25353772
Observations (or Sum Wgts)	256

Analysis of Variance

Source	DF	Sum of Squares	Mean Square	F Ratio
Model	2	1.1414e+17	5.707e+16	101811.5
Error	253	1.4182e+14	5.605e+11	Prob > F
C. Total	255	1.1428e+17		0.0000

Parameter Estimates

Term	Estimate	Std Error	t Ratio	Prob>|t|
Intercept	-15943763	107457.1	-148.4	<.0001
Blow #	277428.42	633.1929	438.14	0.0000
(Blow #-128.5)^2	1034.1925	9.579767	107.96	<.0001

Bivariate Fit of Cumulative Energy Index by Pile in Pa^2 By Blow # Pile #=255

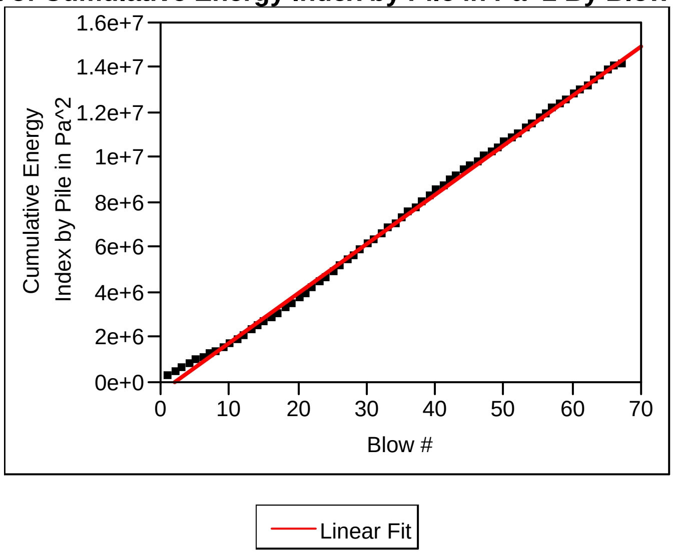

Linear Fit

Cumulative Energy Index by Pile in Pa^2 = -420937.9 + 219650.47 Blow #

Summary of Fit

RSquare	0.998482
RSquare Adj	0.998458
Root Mean Square Error	168184.4
Mean of Response	7047178
Observations (or Sum Wgts)	67

Analysis of Variance

Source	DF	Sum of Squares	Mean Square	F Ratio
Model	1	1.209e+15	1.209e+15	42740.49
Error	65	1.8386e+12	2.829e+10	Prob > F
C. Total	66	1.2108e+15		<.0001

Parameter Estimates

Term	Estimate	Std Error	t Ratio	Prob>|t|
Intercept	-420937.9	41558.33	-10.13	<.0001
Blow #	219650.47	1062.46	206.74	<.0001

Bivariate Fit of Cumulative Energy Index by Pile in Pa^2 By Blow # Pile #=50N

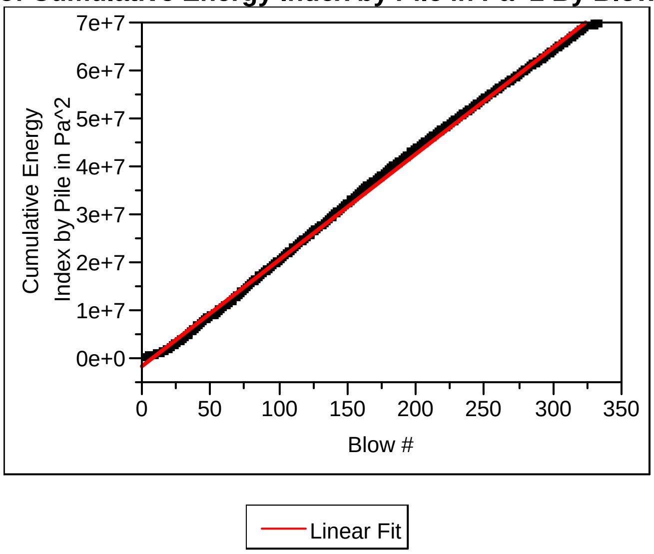

Linear Fit

Cumulative Energy Index by Pile in Pa^2 = -1669533 + 221520.91 Blow #

Summary of Fit

RSquare	0.998721
RSquare Adj	0.998717
Root Mean Square Error	764238.1
Mean of Response	35324460
Observations (or Sum Wgts)	333

Analysis of Variance

Source	DF	Sum of Squares	Mean Square	F Ratio
Model	1	1.51e+17	1.51e+17	258535.2
Error	331	1.9332e+14	5.841e+11	Prob > F
C. Total	332	1.5119e+17		0.0000

Parameter Estimates

Term	Estimate	Std Error	t Ratio	Prob>|t|
Intercept	-1669533	83948.98	-19.89	<.0001
Blow #	221520.91	435.6673	508.46	0.0000

Bivariate Fit of Cumulative Energy Index by Pile in Pa^2 By Blow # Pile #=52N

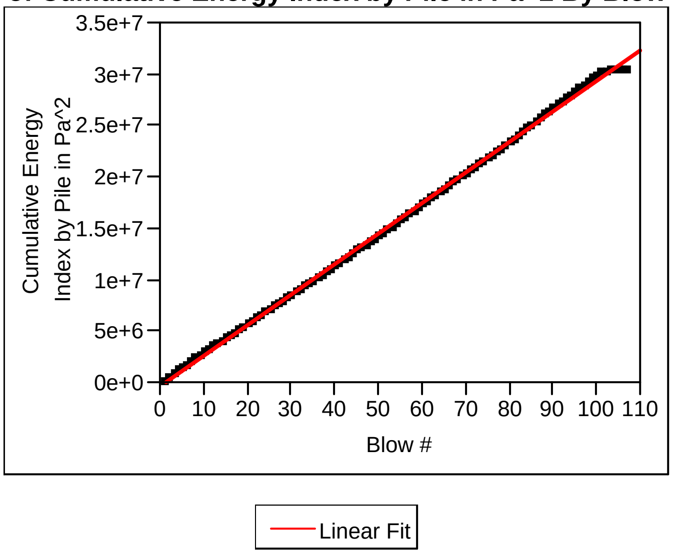

Linear Fit

Cumulative Energy Index by Pile in Pa^2 = -401418.9 + 296694.85 Blow #

Summary of Fit

RSquare	0.999204
RSquare Adj	0.999196
Root Mean Square Error	261155.8
Mean of Response	15620103
Observations (or Sum Wgts)	107

Analysis of Variance

Source	DF	Sum of Squares	Mean Square	F Ratio
Model	1	8.9857e+15	8.986e+15	131750.6
Error	105	7.1612e+12	6.82e+10	Prob > F
C. Total	106	8.9929e+15		<.0001

Parameter Estimates

Term	Estimate	Std Error	t Ratio	Prob>|t|
Intercept	-401418.9	50849.79	-7.89	<.0001
Blow #	296694.85	817.3982	362.97	<.0001